

# **Determination of a novel mine tracer gas and development of a methodology for sampling and analysis of multiple mine tracer gases for characterization of ventilation systems**

Rosemary Rita Patterson

Thesis submitted to the faculty of the Virginia Polytechnic Institute and State University  
in partial fulfillment of the requirements for the degree of

Master of Science  
In  
Mining Engineering

Kray D. Luxbacher  
Greg T. Adel  
Erik C. Westman

April 5, 2011  
Blacksburg, VA

Keywords: tracer gas; mine ventilation; sampling; gas chromatography

**Determination of a novel mine tracer gas and development of a methodology for sampling and analysis of multiple mine tracer gases for characterization of ventilation systems**

Rosemary Rita Patterson

**ABSTRACT**

Ventilation in underground mines is vital to creating a safe working environment. Though there have been numerous improvements in mine ventilation, it is still difficult to ascertain data on the state of the ventilation system following a disaster in which ventilation controls have been potentially damaged. This information is important when making the decision to send rescue personnel into the mine. By utilizing tracer gas techniques, which are powerful techniques for monitoring ventilation systems, especially in remote or inaccessible areas, analysis of the ventilation system immediately following a mine emergency can be more rapidly ascertained.

However, the success of this technique is largely dependent on the accuracy of release and sampling methods. Therefore, an analysis of sampling methods is crucial for rapid response and dependable results during emergencies. This research project involves evaluating and comparing four well-accepted sampling techniques currently utilized in the mining industry using sulfur hexafluoride, an industry standard, as the tracer gas. Additionally, Solid Phase Microextraction (SPME) fibers are introduced and evaluated as an alternative sampling means. Current sampling methods include plastic syringes, glass syringes, Tedlar bags, and vacutainers. SPME fibers have been successfully used in a variety of industries from forensics to environmental sampling and are a solvent-less method of sampling analytes. To analyze these sampling methods, samples were taken from a 0.01% standard mixture of SF<sub>6</sub> in nitrogen and analyzed using electron capture gas chromatography (GC). The technical and practical issues surrounding each sampling method were also observed and discussed.

Furthermore, the use of multiple tracer gases could allow for rapid assessment of the functionality of ventilation controls. This paper describes experimentation related to the determination of a novel mine tracer gas. Multiple tracer gases greatly increase the level of flexibility when conducting ventilation surveys to establish and monitor controls. A second tracer would substantially reduce the time it takes to administer multiple surveys since it is not necessary to wait for the first tracer to flush out of the mine which can take up to a few days. Additionally, it is possible to release different tracers at different points and follow their respective airflow paths, analyzing multiple or complex circuits. This

would be impossible to do simultaneously with only one tracer. Three different tracer gases, carbon tetrafluoride, octofluoropropane, and perfluoromethylcyclohexane, were selected and evaluated on various GC columns through utilizing different gas chromatographic protocols. Perfluoromethylcyclohexane was selected as the novel tracer, and a final protocol was established that ensured adequate separation of a mixture of SF<sub>6</sub> and perfluoromethylcyclohexane.

Since there is limited literature comparing sampling techniques in the mining industry, the findings and conclusions gained from the sampling comparison study provide a benchmark for establishing optimal sampling practices for tracer gas techniques. Additionally, the determination of a novel tracer gas that can be used with and separated from SF<sub>6</sub> using the same analytical method increases the practicality and robustness of multiple mine tracer gas techniques. This initial work will contribute to the larger project scope of determining a methodology for the remote characterization of mine ventilation systems through utilizing multiple mine tracer gases and computational fluid dynamics (CFD). This will be completed through several phases including initial laboratory testing of novel tracer gases in a model mine apparatus to develop a methodology for releasing, sampling, and modeling a mine ventilation plan and tracer gas dispersion in CFD and eventually completing field trials to validate and enhance the multiple tracer gas methodology.

## Acknowledgements

First and foremost, I would like to thank my advisor, Dr. Kray Luxbacher. Not only did she give me the opportunity to pursue a graduate degree related to ventilation, but has been a valuable asset both academically and professionally. Her advisement over the past two years has helped me immensely and has influenced where I am today. Dr. Luxbacher has not only been my advisor, but I consider her a great mentor and role model as there are few female engineering faculty members. Additionally, I sincerely appreciate the support of NIOSH, especially our program officer, Gerrit Goodman. This research project would not be possible without their funding.

I would also like to thank the other members of my committee, Dr. Erik Westman and Dr. Greg Adel. They have also provided guidance and support that is greatly appreciated. In addition, Dr. Adel has been there for me since I entered the department as a sophomore engineering student. For the past 6 years, he has not only been my professor, the department head, one of my committee members, but an advisor and sounding board for whenever I needed his guidance on decisions related to academics, summer internships, graduate school, and full time employment.

In addition, I would not have made it this far without the invaluable help and guidance from Dr. Harold McNair from the chemistry department. His expertise in gas chromatography was a great resource to have nearby. Furthermore, Kimberly Jackson, an undergraduate researcher from the chemistry department, was a great help with running experiments on the gas chromatograph.

Finally, I want to thank my family and friends for their love and support and always being there when I needed them.

This publication was developed under Contract No. 200-2009-31933, awarded by the National Institute for Occupational Safety and Health (NIOSH). The findings and conclusions in this report are those of the authors and do not reflect the official policies of the Department of Health and Human Services; nor does mention of trade names, commercial practices, or organizations imply endorsement by the U.S. Government.

# Table of Contents

<b>Chapter 1: Introduction.....</b>	<b>1</b>
<b>Chapter 2: Literature Review .....</b>	<b>4</b>
2.1 Introduction of Trace Element Analysis .....	4
2.2 Non-mining Applications of Tracer Gases .....	4
2.3 Mine Ventilation System Measurements .....	6
2.4 Mining Applications of Tracer Gases .....	8
2.4.1 Metal/Non-metal Applications .....	8
2.4.2 Coal Applications .....	9
2.5 Release, Sample and Analysis Methods .....	11
2.5.1 Releasing Techniques.....	11
2.5.2 Sampling Techniques .....	13
2.5.3 Methods of Analysis.....	14
2.6 Solid Phase Microextraction .....	15
2.7 Basic Gas Chromatography Theory .....	16
2.7.1 Gas Chromatography Mechanics.....	16
2.7.2 Column Efficiency.....	17
2.7.3 Solvent Efficiency .....	18
2.7.4 Selectivity .....	19
2.7.5 Column Selection .....	19
2.8 Summary .....	20
<b>Chapter 3: Comparison of Sampling Techniques .....</b>	<b>22</b>
3.1 Introduction of Sampling Techniques.....	22
3.2 Methods.....	24
3.3 Results.....	25
3.4 Discussion .....	29
3.5 Conclusion .....	30
<b>Chapter 4: Selecting Novel Tracer Gases.....</b>	<b>31</b>
4.1 Introduction of Tracer Gases.....	31
4.2 Standard Lab Experimentation Procedures.....	31
4.3 Calibration of Columns.....	32
4.4 Tracers Evaluated.....	32
4.4.1 Carbon Tetrafluoride .....	32

4.4.2 Octafluoropropane .....	32
4.4.3 Perfluoromethylcyclohexane .....	33
4.5 Methods Used to Evaluate Tracers .....	33
4.5.1 CF <sub>4</sub> & C <sub>3</sub> F <sub>8</sub> Experiments Using SBP-1 Sulfur Column .....	33
4.5.2 CF <sub>4</sub> & C <sub>3</sub> F <sub>8</sub> Experiments Using ZB-624 Column .....	34
4.5.3 CF <sub>4</sub> & C <sub>3</sub> F <sub>8</sub> Experiments Using TG Bond Q+ Column.....	35
4.5.4 CF <sub>4</sub> & C <sub>3</sub> F <sub>8</sub> Experiments Using TG Bond Q Column.....	36
4.5.5 PMCH Experiments Using HP-AL/S Column .....	37
4.6 Gas Chromatography Results of Evaluated Tracers .....	39
4.6.1 CF <sub>4</sub> & C <sub>3</sub> F <sub>8</sub> Experiments Using SBP-1 Sulfur Column .....	39
4.6.2 CF <sub>4</sub> & C <sub>3</sub> F <sub>8</sub> Experiments Using ZB-624 Column .....	42
4.6.3 CF <sub>4</sub> & C <sub>3</sub> F <sub>8</sub> Experiments Using TG Bond Q+ Column.....	45
4.6.4 CF <sub>4</sub> & C <sub>3</sub> F <sub>8</sub> Experiments Using TG Bond Q Column.....	49
4.6.5 PMCH Experiments Using HP-AL/S Column .....	52
4.7 Summary .....	58
<b>Chapter 5: Summary and Conclusion .....</b>	<b>59</b>
<b>References .....</b>	<b>62</b>
<b>Appendix A: Chromatograms of Sampling Technique Comparison.....</b>	<b>68</b>
<b>Appendix B: Chromatograms of Novel Tracer Gas Testing .....</b>	<b>71</b>

# List of Figures

## Main Text

Figure 3.1: Schematic of SPME Fiber Assembly.....	23
Figure 3.2: Chromatogram Showing Separation of O <sub>2</sub> & SF <sub>6</sub> .....	26
Figure 3.3: Sensitivity of Sampling Methods.....	27
Figure 3.4: Precision of Sampling Methods.....	28
Figure 3.5: Chromatogram of 5 SPME Sample Runs.....	28
Figure 3.6: Chromatogram of 5 Plastic Syringe Sample Runs.....	29
Figure 4.1: Comparison of Syringe Blank and 10µL Injection of Pure CF <sub>4</sub> .....	39
Figure 4.2: Comparison of Syringe Blank (black) and 10µL Injection of Pure C <sub>3</sub> F <sub>8</sub> @ 20°C (pink) .....	40
Figure 4.3: Comparison of Syringe Blank and 5µL Injection of Pure SF <sub>6</sub> .....	40
Figure 4.4: Comparison of Syringe Blank (Black) and 10µL injection of Pure CF <sub>4</sub> (pink) at 40°C .....	42
Figure 4.5: Comparison of Syringe Blank (Black) and 10µL Injection of Pure C <sub>3</sub> F <sub>8</sub> (pink) at 40°C .....	43
Figure 4.6: Overlay of Each Tracer Gas Sample Run.....	44
Figure 4.7: Comparison of Syringe Blank (black line) and 10µL Injection of Pure CF <sub>4</sub> (pink line) at 40°C.....	46
Figure 4.8: Comparison of Syringe Blank (black line) and 10µL Injection of Pure C <sub>3</sub> F <sub>8</sub> (pink line) at 40°C.....	46
Figure 4.9: Comparison of Syringe Blank (black line) and 0.5µL Injection of Pure SF <sub>6</sub> (pink line) at 20°C.....	47
Figure 4.10: Comparison of Syringe Blank (black line) and 10µL Injection of Pure C <sub>3</sub> F <sub>8</sub> (pink line) at 60°C.....	49
Figure 4.11: Comparison of Syringe Blank (black line) and 1µL Injection of 1% SF <sub>6</sub> in N <sub>2</sub> (pink line) at 60°C.....	50
Figure 4.12: Overlay of All Tracer Gases-Black=Syringe Blank; Pink=C <sub>3</sub> F <sub>8</sub> ; Blue=SF <sub>6</sub> .....	50
Figure 4.13: Comparison of Syringe Blank (pink) with 1mL Injection of 100ppm PMCH in N <sub>2</sub> (black).....	53
Figure 4.14: Zoomed-in Version of Figure 4.13.....	53
Figure 4.15: Comparison of Syringe Blank (Black) with 1mL Injection of 100ppm SF <sub>6</sub> in N <sub>2</sub> (pink).....	54
Figure 4.16: 100ppm Sample of SF <sub>6</sub> in N <sub>2</sub> (65°C initial column temp, hold 3 minutes, ramp 100°C to 175°C).....	54
Figure 4.17: 1mL Injection of a Sample of 100ppm SF <sub>6</sub> & PMCH in N <sub>2</sub> .....	55
Figure 4.18: 1mL Sample of 100ppm SF <sub>6</sub> & PMCH in N <sub>2</sub> Using Final GC Protocol.....	57
<b>Appendix A: Chromatograms of Sampling Technique Comparison</b>	
Figure A. 1: Overlay of 5 Glass Syringe Sample Runs.....	68
Figure A. 2: Overlay of 5 Plastic Syringe Sample Runs.....	68
Figure A. 3: Overlay of 5 SPME Sample Runs.....	68
Figure A. 4: Overlay of 5 Tedlar Bag/Glass Syringe Sample Runs.....	69
Figure A. 5: Overlay of 5 Tedlar Bag/Plastic Syringe Sample Runs.....	69
Figure A. 6: Overlay of 5 Vacutainer/Glass Syringe Sample Runs.....	69
Figure A. 7: Overlay of 5 Vacutainer/Plastic Syringe Sample Runs.....	70
<b>Appendix B : Chromatograms from Novel Tracer Gas Testing</b>	
Figure B. 1: Comparison of Oxygen Peak (black line) with 10µL Pure Injection of CF <sub>4</sub> (pink line) .....	71

Figure B. 2: Comparison of Oxygen Peak (black line) with 10 $\mu$ L Pure Injection of C <sub>3</sub> F <sub>8</sub> (pink line).....	71
Figure B. 3: Comparison of Oxygen Peak (black line) with 5 $\mu$ L Pure Injection of SF <sub>6</sub> (pink line) .....	71
Figure B. 4: Overlay of All Tracer Gases-Black=Syringe Blank;Pink=CF <sub>4</sub> ;Blue=C <sub>3</sub> F <sub>8</sub> ; Brown=SF <sub>6</sub> .....	72
Figure B. 5: Comparison of Oxygen Peak (black line) with 10 $\mu$ L Pure Injection of CF <sub>4</sub> (pink line) .....	72
Figure B. 6: Comparison of Oxygen Peak (black line) with 10 $\mu$ L Pure Injection of C <sub>3</sub> F <sub>8</sub> (pink line).....	72
Figure B. 7: Figure B.6 zoomed in uV x10,000.....	73
Figure B. 8: Magnified area of box in Figure B.7 .....	73
Figure B. 9: Comparison of Oxygen Peak (black line) with 1 $\mu$ L Pure Injection of SF <sub>6</sub> (pink line) .....	73
Figure B. 10: Zoomed-Out Version of Figure B.9 (uVx1,000,000); Indicates SF <sub>6</sub> is overloading column.....	74
Figure B. 11: Overlay of All Tracer Gases-Black=Syringe Blank;Pink=CF <sub>4</sub> ;Blue=C <sub>3</sub> F <sub>8</sub> ; Brown=SF <sub>6</sub> .....	74
Figure B. 12: Comparison of Oxygen Peak (black line) with 10 $\mu$ L Pure Injection of CF <sub>4</sub> (pink line).....	74
Figure B. 13: Zoomed-in version of Figure B.12 (uVx1,000); Shows potential CF <sub>4</sub> peak-very broad.....	75
Figure B. 14: Comparison of Oxygen Peak (black line) with 10 $\mu$ L Pure Injection of C <sub>3</sub> F <sub>8</sub> (pink line).....	75
Figure B. 15: Comparison of Oxygen Peak (black line) with 1 $\mu$ L Pure Injection of SF <sub>6</sub> (pink line) .....	75
Figure B. 16: Comparison of Oxygen Peak (black line) with 10 $\mu$ L Pure Injection of CF <sub>4</sub> (pink line).....	76
Figure B. 17: Comparison of Oxygen Peak (black line) with 10 $\mu$ L Pure Injection of C <sub>3</sub> F <sub>8</sub> (pink line).....	76
Figure B. 18: Magnified Area of Box in Figure B.17 .....	76
Figure B. 19: 1 $\mu$ L injections of pure SF <sub>6</sub> ; Variance demonstrates clogging of plastic syringe needle.....	77
Figure B. 20: Comparison of Oxygen Peak (black line) with 10 $\mu$ L Pure Injection of CF <sub>4</sub> (pink line).....	77
Figure B. 21: Comparison of Oxygen Peak (black line) with 10 $\mu$ L Pure Injection of C <sub>3</sub> F <sub>8</sub> (pink line).....	77
Figure B. 22: Magnified Area of Box in Figure B.21 .....	78
Figure B. 23: Comparison of Oxygen Peak (black line) with 10 $\mu$ L Pure Injection of CF <sub>4</sub> (pink line)-Repeat run.....	78
Figure B. 24: Comparison of Oxygen Peak (black line) with 10 $\mu$ L Pure Injection of C <sub>3</sub> F <sub>8</sub> (pink line)-Repeat run.....	78
Figure B. 25: Magnified Area of Box in Figure B.24 .....	79
Figure B. 26: Comparison of Oxygen Peak (black line) with 1 $\mu$ L Pure Injection of SF <sub>6</sub> (pink line) .....	79
Figure B. 27: Overlay of All Tracer Gases-Black=Syringe Blank;Pink=CF <sub>4</sub> ;Blue=C <sub>3</sub> F <sub>8</sub> ; Brown=SF <sub>6</sub> .....	79
Figure B. 28: Comparison of Oxygen Peak (black line) with 10 $\mu$ L Pure Injection of CF <sub>4</sub> (pink line).....	80
Figure B. 29: Comparison of Oxygen Peak (black line) with 10 $\mu$ L Pure Injection of C <sub>3</sub> F <sub>8</sub> (pink line).....	80



Figure B. 30: Comparison of Oxygen Peak (black line) with 10 $\mu$ L Pure Injection of CF <sub>4</sub> (pink line).....	81
Figure B. 31: Comparison of Oxygen Peak (black line) with 10 $\mu$ L Pure Injection of C <sub>3</sub> F <sub>8</sub> (pink line).....	81
Figure B. 32: Zoomed-in version of Figure B.31 Showing Broad C <sub>3</sub> F <sub>8</sub> Peak Eluting Around 5.2 Minutes.....	81
Figure B. 33: Comparison of Oxygen Peak (black line) with 1 $\mu$ L Pure Injection of SF <sub>6</sub> (pink line)--Flat Line Due to Column & Detector Overloaded with Sample .....	82
Figure B. 34: Comparison of Oxygen Peak (black line) with 0.5 $\mu$ L Pure Injection of SF <sub>6</sub> (pink line)--Very Broad Peak & Peak Tailing on Right Side until 7 Minutes.....	82
Figure B. 35: Comparison of Oxygen Peak (black line) with 10 $\mu$ L Pure Injection of CF <sub>4</sub> (pink line).....	83
Figure B. 36: Comparison of Oxygen Peak (black line) with 10 $\mu$ L Pure Injection of C <sub>3</sub> F <sub>8</sub> (pink line).....	83
Figure B. 37: Comparison of Oxygen Peak (black line) with 0.5 $\mu$ L Pure Injection of SF <sub>6</sub> (pink line).....	83
Figure B. 38: Overlay of all Gases (O <sub>2</sub> , CF <sub>4</sub> in box; C <sub>3</sub> F <sub>8</sub> too small on scale-under pink SF <sub>6</sub> peak), pink=SF <sub>6</sub> .....	84
Figure B. 39: Comparison of Oxygen Peak (black line) with 10 $\mu$ L Pure Injection of CF <sub>4</sub> (pink line).....	85
Figure B. 40: Comparison of Oxygen Peak (black line) with 10 $\mu$ L Pure Injection of C <sub>3</sub> F <sub>8</sub> (pink line).....	85
Figure B. 41: Comparison of Oxygen Peak (black line) with 1 $\mu$ L Injection of 1% standard SF <sub>6</sub> & N <sub>2</sub> (pink line) .....	85
Figure B. 42: Comparison of Oxygen Peak (black line) with 10 $\mu$ L Pure Injection of CF <sub>4</sub> (pink line).....	86
Figure B. 43: Comparison of Oxygen Peak (black line) with 10 $\mu$ L Pure Injection of C <sub>3</sub> F <sub>8</sub> (pink line).....	86
Figure B. 44: Comparison of Oxygen Peak (black line) with 1 $\mu$ L Injection of 1% standard SF <sub>6</sub> & N <sub>2</sub> (pink line) .....	86
Figure B. 45: Comparison of Oxygen Peak (black line) with 1 $\mu$ L Injection of 1% standard SF <sub>6</sub> & N <sub>2</sub> (pink line) .....	87
Figure B. 46: Extended view of Figure B.43 Showing Entire SF <sub>6</sub> Peak .....	87
Figure B. 47: Comparison of Oxygen Peak (black line) with 10 $\mu$ L Pure Injection of C <sub>3</sub> F <sub>8</sub> (pink line).....	88
Figure B. 48: Comparison of Oxygen Peak (black line) with 1 $\mu$ L Injection of 1% standard SF <sub>6</sub> & N <sub>2</sub> (pink line) .....	88
Figure B. 49: Zoomed-out View of Figure B.46 Showing Entire SF <sub>6</sub> Peak.....	88
Figure B. 50: Overlay of All Tracer Gases-Black=Syringe Blank; Pink=C <sub>3</sub> F <sub>8</sub> ; Blue=SF <sub>6</sub> .....	89
Figure B. 51: Zoomed-out version of Figure B.48 (uV 1,000,000).....	89
Figure B. 52: Zoomed-out version showing entire SF <sub>6</sub> peak.....	89
Figure B. 53: Comparison of Oxygen Peak (black line) with 10 $\mu$ L Pure Injection of C <sub>3</sub> F <sub>8</sub> (pink line).....	90
Figure B. 54: Comparison of Syringe Blank (pink) with 1mL Injection of 100ppm PMCH in N <sub>2</sub> (black).....	90
Figure B. 55: Zoomed-out version of Figure B. 52 above .....	91
Figure B. 56: Comparison of Syringe Blank (Black) with 1mL Injection of 100ppm SF <sub>6</sub> in N <sub>2</sub> (pink) .....	91
Figure B. 57: 100ppm Sample of SF <sub>6</sub> in N <sub>2</sub> (65 <sup>0</sup> C initial column temp, hold 3 minutes, ramp 100 <sup>0</sup> C to 175 <sup>0</sup> C).....	91

Figure B. 58: Establishing Protocol for Separation of SF <sub>6</sub> & PMCH; Initial Column Temperature of 70°C, Hold Time 8 Minutes.....	92
Figure B. 59: Establishing Protocol for Separation of SF <sub>6</sub> & PMCH; Initial Column Temperature of 70°C, Hold Time 15 Minutes.....	92
Figure B. 60: Separation of SF <sub>6</sub> & PMCH; Initial Column Temperature of 70°C, Hold Time 12:30 Minutes (Black=Syringe Blank; Pink=100ppm mix SF <sub>6</sub> & PMCH in N <sub>2</sub> ) .....	93
Figure B. 61: Zoomed-out version of Figure B. 58 showing entire SF <sub>6</sub> and PMCH peak .....	93
Figure B. 62: Separation of SF <sub>6</sub> & PMCH; Initial Column Temperature of 65°C, Hold Time 12:30 Minutes (Black=Syringe Blank; Pink=100ppm mix SF <sub>6</sub> & PMCH in N <sub>2</sub> ) .....	94
Figure B. 63: Separation of SF <sub>6</sub> & PMCH; Initial Column Temperature of 67°C, Hold Time 12:30 Minutes (Black=Syringe Blank; Pink=100ppm mix SF <sub>6</sub> & PMCH in N <sub>2</sub> ) .....	94
Figure B. 64: Zoomed-out version of Figure B. 61 showing entire SF <sub>6</sub> & PMCH peaks.....	95

## List of Tables

Table I: Summary of U.S. Underground Coal Incidents .....	1
Table II: Column Characteristics.....	24
Table III: Instrument Parameters for Sampling Comparison Study on Shimadzu GC-2014 .....	25
Table IV: Limit of Detection & Limit of Quantification.....	26
Table V: SBP-1 Sulfur Column Characteristics.....	33
Table VI: Standard GC Protocol for SBP-1 Sulfur Column .....	34
Table VII: ZB-624 Column Characteristics .....	35
Table VIII: Standard GC Protocol for ZB-624 Column.....	35
Table IX: TG Bond Q+ Column Characteristics.....	36
Table X: Standard GC Protocol for TG Bond Q+ Column .....	36
Table XI: TG Bond Q Column Characteristics .....	37
Table XII: Standard GC Protocol for TG Bond Q Column.....	37
Table XIII: HP-AL/S Column Characteristics .....	38
Table XIV: Standard GC Protocol for HP-AL/S Column.....	38
Table XV: Average Retention Time of Gases on SBP-1 Sulfur Column.....	41
Table XVI: Average Peak Area of Gases on SBP-1 Sulfur Column.....	41
Table XVII: Capacity Factor Values of Gases on SBP-1 Sulfur Column.....	41
Table XVIII: Selectivity Values of Gases on SBP-1 Sulfur Column.....	41
Table XIX: Average Retention Time of Gases on ZB-624 Column .....	43
Table XX: Average Peak Area of Gases on ZB-624 Column.....	44
Table XXI: Capacity Factor Values of Gases on ZB-624 Column .....	44
Table XXII: Selectivity Values of Gases on ZB-624 Column .....	45
Table XXIII: Average Retention Time of Gases on TG Bond Q+ Column.....	47
Table XXIV: Average Peak Area of Gases on TG Bond Q+ Column .....	47
Table XXV: Capacity Factor Values of Gases on TG Bond Q+.....	48
Table XXVI: Selectivity Values of Gases on TG Bond Q+ Column.....	48
Table XXVII: Average Retention Time of Gases on TG Bond Q Column.....	51
Table XXVIII: Average Peak Area of Gases on TG Bond Q Column.....	51
Table XXIX: Capacity Factor Values of Gases on TG Bond Q Column.....	51
Table XXX: Selectivity Values of Gases on TG Bond Q Column.....	52
Table XXXI: Average Retention Time of Gases on HP-AL/S Column.....	56
Table XXXII: Average Peak Area of Gases on HP-AL/S Column.....	56
Table XXXIII: Capacity Factor Values for Gases on HP-AL/S Column.....	56
Table XXXIV: Selectivity Values for Gases on HP-AL/S Column.....	56

## Chapter 1: Introduction

Ventilation in underground mines is vital to create a safe working environment. Ventilation helps to dilute dust, improve air quality, reduce exposure to harmful contaminants in the air such as diesel particulate matter (DPM) and arsenic, and to control methane levels for the prevention of mine explosions and ignitions.

Since the early 1900s, the number of fatalities in mines has been greatly reduced due to the implementation of government regulations and improved technology and control methods. Although there have been improvements, there are still a number of injuries and fatalities related to collapse or fall of roof and ribs, fire, and ignition or explosion of gas or dust. The Accident, Injury, Illness Database created by the Mine Safety and Health Administration (MSHA), shows that from 1983 to 2009, the number of fatalities, number of days lost, and non-fatal days lost is high as summarized in Table I below for U.S. underground coal only.

**Table I: Summary of U.S. Underground Coal Incidents**

<b>1983-2009</b>	<b>Fatal</b>	<b>NDL</b>	<b>NFDL</b>	<b>Total</b>
Fire	82	2,568	8,131	10,781
Ignition or Explosion of Gas or Dust	82	26	182	290
Total	164	2,594	8,313	11,071

There are several measures that can be taken to control methane levels, including methane drainage, preventing accumulation of combustible or explosive coal dust, eliminating ignition sources, monitoring methane-air mix pressures to ensure they do not reach the detonation pressure level, monitoring sealed areas, and designing and monitoring the ventilation system [1].

Focusing specifically on designing and monitoring the ventilation system, there have been numerous developments and technological advances that have improved ventilation controls and systems. The efficiency of the ventilation system can be measured by using various tools such as vane anemometers, smoke tubes, psychrometers, manometers, and barometers to determine air velocities, temperatures and pressures [2]. Calculating the product of the measured cross sectional area and averaged air velocity is a more traditional and less accurate method of determining air quantity through a section of a mine [2]. There have been numerous studies utilizing tracer gas techniques as a means to

evaluate ventilation controls in both metal/non-metal and coal mines. Tracer gas studies have been used extensively in areas related to: determining recirculation of air and airflow patterns in inactive workings, evaluating the effectiveness of seals and stoppings, and evaluating auxiliary fans. Typically, a single tracer gas is used for these mining applications. Although other tracer gases have been utilized in mining applications, sulfur hexafluoride is the industry standard and is the most often used tracer since the early 1970s.

Tracer gas methods are useful techniques for monitoring ventilation systems, especially in remote or inaccessible areas. Additionally, tracer gas surveys can be used to ascertain the state of ventilation controls in the event of a mine emergency such as an explosion or major ground event. The success of this technique is largely dependent on the accuracy of release and sampling methods. Analysis of sampling and release methods is crucial for rapid response and dependable results during emergencies. There is limited information on the literature comparing sampling techniques, therefore it is necessary to evaluate and establish optimal sampling practices.

Furthermore, the use of multiple tracer gases can add to the flexibility of ventilation surveys by decreasing the time needed between surveys and allowing for different tracers to be released at different points simultaneously and determining their respective airflow paths. However, there have been limited studies on the use of multiple tracer gases. Some of these tracers include various Freon's and a radioactive isotope of xenon. The practicality of these other tracers is limited due to either pre-existing background concentration levels or the need for specialized detectors to analyze samples. To maintain practicality of utilizing multiple tracer gases for purposes of characterizing ventilation systems, it is important for not only release and sampling methods to be accurate and easy to implement, but for samples to be easily, conveniently, and accurately analyzed.

There are many characteristics that aid in the selection of an appropriate tracer gas for mining applications which include being chemically and thermally stable, safe, non-toxic, non-corrosive, readily attainable and easily transportable, inexpensive, odorless, and not naturally occurring in the environment. Therefore, there were several measures taken when determining a novel tracer gas. In addition to meeting the above criteria, it was necessary that the novel tracer gas could be used with SF<sub>6</sub> since SF<sub>6</sub> has been implemented successfully in industry. Second, the novel tracer gas needed to be as sensitive as SF<sub>6</sub> so that a SF<sub>6</sub> signal in an electron capture detector (ECD) would be comparable to a signal from the novel tracer gas. Additionally, it is vital that to ensure

that the novel tracer could be separated from SF<sub>6</sub> by using a gas chromatograph equipped with an electron capture detector and be separated on a single column. It is also important that all tracers can be separated using one established gas chromatographic protocol and that protocol be optimized to achieve the best possible peak shape and separation while minimizing sample analysis time.

The establishment of optimal sampling practices and determination of a novel tracer gas contribute to the larger project scope of determination of a methodology for the remote characterization of mine ventilation systems. This methodology will include optimal and rapid sampling and release practices, robust analytical methods, multiple mine tracer gases, and modeling gas dispersion in computational fluid dynamics (CFD).

## Chapter 2: Literature Review

### *2.1 Introduction of Trace Element Analysis*

Due to advances in analytical chemistry, tracer gas techniques have been introduced and used across various industries where characterization of airflow is required. The general concept of tracer gases is to introduce a gas at a very low concentration into the environment to be tested. Depending on the application, the attributes of the tracer gas will vary. A standard requirement of a tracer gas across most industries is that the tracer gas should not already be present in the environment. However, it should be noted that there is inherent error associated with trace element analysis, and there is a need to further improve the reliability and power of detection while reducing the cost of analysis [3]. Tracer gases have been used to test the state of controls, ventilation systems of mines and buildings, and pathways of gas and water for environmental testing.

### *2.2 Non-mining Applications of Tracer Gases*

Liquid and gaseous tracers have been utilized extensively for environmental monitoring in oceans, underground reservoirs, and the atmosphere. Dating back to the early 1900s, carbon tetrachloride ( $\text{CCl}_4$ ), a volatile liquid, was used as an oceanic tracer which allowed waters to be “dated” to determine how subsurface water is composed of different ages [4]. Huhn *et al.* also report that the stability of  $\text{CCl}_4$  is sufficient for use in the South Atlantic to observe transfer into the Central Water and Antarctic Intermediate Water however, the stability of  $\text{CCl}_4$  decreases in waters with warmer temperatures and oceanic studies progressed to include chlorofluorocarbons as tracer gases [4]. Since it is important to have accurate greenhouse gas inventories of livestock methane emissions, the Emissions from Ruminants Using a Calibrated Tracer (ERUCT) technique was developed and currently utilizes sulfur hexafluoride ( $\text{SF}_6$ ) as the tracer though other tracers are being evaluated as  $\text{SF}_6$  is itself a greenhouse gas [5].  $\text{SF}_6$  was also used to determine the potential for gas exchange between wetland plants during each season [6]. Waste degradation is influenced by the amount of water present in a landfill, and thus the partitioning gas tracer test was utilized to measure seasonal variations of landfill moisture [7]. Organic wastes in streams require substantial oxygen demands and therefore, methyl chloride was utilized as a gas tracer to determine the reaeration coefficients in streams [8]. Stable isotopes and chemical tracers were used to quantify the injected steam in vapor-dominated areas such as the Geysers in northern California [9]. Tritium was initially used at the Geysers; then chlorofluorocarbons were used for about seven years, and more recently hydrofluorocarbons since they can be developed for use as a vapor-phase tracer and possess many of the characteristics of chlorofluorocarbons without contributing to

ozone depletion [9]. Clark *et al.* utilized multiple tracers, including dissolved noble gases, to determine ground water residence times, local and intermediate flow system mixing, and recharge sources in the Dakota aquifer [10]. A method of tagging methane in underground storage fields as well as other forms using two tracers, sulfur hexafluoride and chloropentafluoroethane, was developed and patented [11]. Multiple perfluorocarbon tracers and sulfur hexafluoride were injected into gas reservoirs and an analysis of samples was conducted to further describe the off-shore reservoir [12]. Perfluorocarbon tracers were also utilized by McCallum *et al.* to monitor breakthrough and transport times of geologically sequestered CO<sub>2</sub> [13].

There have been several studies utilizing tracer gases to study airflow patterns in homes, office buildings, hospitals, and factories. The effectiveness of a building's ventilation system was tested through a comparative study using SF<sub>6</sub> and nitrous oxide (N<sub>2</sub>O) utilizing continuous injection of the tracer gas and both cold-air and hot-air trials [14]. Another study determined the accuracy of the decay and constant concentration methods for using tracer gases to quantify air flows in buildings to be approximately 10% [15]. Freon 12, Freon 14, and bromochlorodifluoromethane (BCF) were all utilized in respective zones in a house to determine internal airflow paths which could ultimately lead to energy savings [16]. A statistical analysis was conducted on another multi-zonal building study that utilized multiple perfluorocarbon tracers [17]. Tracer gas simulations were conducted by Lim, Cho, and Kim to analyze airflow patterns in high rise hospitals to predict if certain airborne viruses could be transmitted vertically from infected patients to non-infected patients [18].

Overall, tracer gases have been used in a variety of industries. Applications of single and multiple tracer gases have been tested as well as different release rates. Though the preceding discussion is not an exhaustive list of other industries aside from mining utilizing tracer gases to study various patterns and flows, it demonstrates the extensive use of tracer gases. Studying tracer gas applications in other industries can help highlight the deficiencies associated with the technique, improvements and developments of the technique that could be ahead of the mining industry, and provide insight into difficulties that could be incurred when using the technique in underground ventilation systems. In addition, applications of tracer gases related to measuring airflows and ventilation in a multitude of industries help to provide a benchmark from which to study, evaluate, and compare tracer gas techniques utilized in the mining industry.



### 2.3 Mine Ventilation System Measurements

Underground mines are dynamic environments making it difficult to always know and understand the state of ventilation controls. Daily advancement and retreat, major development or introduction of new ventilation shafts or raises, declines, and mine disasters all affect mine ventilation. Fans, ventilation ducts, and ventilation raises/shafts can all be utilized to control underground airflows. Modeling software helps to understand complex airflows, but validation data is necessary to calibrate and verify ventilation systems. Ventilation surveys are routinely conducted underground to evaluate the efficiency of a ventilation system as well as the quality of air. By obtaining the frictional pressure drop and corresponding airflow a number of parameters can be calculated which include friction factors, branch resistances, natural ventilation effects, distribution of airflows, airpower losses and associated costs, and overall volumetric efficiency of the system [19]. Instruments that have been used for underground measurements to determine air velocities, temperatures, and pressures include smoke tubes, vane anemometers, psychrometers, manometers and barometers [2]. Air quantity,  $Q$ , is calculated utilizing measured air velocities and the cross-sectional area of the working area as indicated in Equation (1) below.

$$Q = u \times A \quad (1)$$

where  $u$  is the mean velocity (m/s) and  $A$  is the cross-sectional area ( $m^2$ ) [19]. Furthermore, a density correction can be applied to obtain the corrected velocity value,  $u$ , shown below in Equation (2).

$$u = u_i + C_c \sqrt{\frac{\rho_c}{\rho_m}} \quad (2)$$

where  $u_i$  is the indicated velocity,  $C_c$  is the correction from the instrument calibration curve,  $\rho_c$  is the air density at time of calibration, and  $\rho_m$  is the actual air density at the time of measurement [19]. Air velocity measurements can be taken several ways including smoke tubes, swinging vane anemometers, vortex-shedding anemometers, and pitot tubes [19]. For pitot tubes, the velocity pressure,  $p_v$ , can be determined by the following equation.

$$p_v = p_t - p_s \quad (3)$$

where  $p_t$  is the total pressure of the moving airstream (Pa) and  $p_s$  is the static pressure (Pa) [19]. This velocity head can then be related to the velocity of air,  $u$ , as indicated below in Equation (4).

$$u = \sqrt{\frac{2p_v}{\rho}} \quad (4)$$

However, the accuracy of using the above methods and respective calculations is limited due to presence of turbulence, obstructions, or inaccessibility of certain areas [2], and the repeatability of this method might not suffice for obtaining reliable airflow measurements [20]. Additionally, these methods rely on point measurement, while utilization of tracer gas techniques are a more global approach, eliminating the need to measure cross-sectional areas and reducing inaccuracies of calculated air quantities associated with irregular areas and flows [2] and allowing the quantity of airflow to be measured directly [20].

Early tracer gas studies in mining date back to 1958 when Higgins and Shuttleworth utilized nitrous oxide to measure airflow in headings, and when coupled with an infrared analyser, concentrations could be determined to 100ppm [20]. Preliminary tracer studies in the United States date back to the 1970s and many were conducted in a limestone mine in Pennsylvania as well as the Bureau of Mines research coal mine in Bruceton, PA [21]. There are several characteristics that define an appropriate mining tracer gas. Due to the nature of underground mines, tracer gases must not only be detected easily at low concentrations, but must also be chemically and thermally stable, odorless, safe, non-explosive, and alien to the current environment [21]. Furthermore, tracers should be inexpensive, easily transportable, readily attainable, non-toxic, non-corrosive, and non-radioactive [22]. Mining tracer gas studies have ranged from measuring potential leakages in sealed areas, effectiveness of permanent stoppings and bleeder systems [23] to monitoring methane levels in gob areas [24] to studying the complexity of airflows in non-coal mines [21]. Kennedy *et al.* explored the use of multiple tracer gases at the Cape Breton Coal Research Laboratory (CBCRL) through using sulfur hexafluoride in conjunction with Freon-13B1 and Freon-12 [22]. Preliminary tests showed that although the Freon gases are not as sensitive as SF<sub>6</sub>, similar mixing and adsorption characteristics were observed, however, it was noted that background samples should be taken to determine if Freon-12 is present in the area since it is commonly used in aerosols [22]. Klinowsky and Kennedy highlight several applications of tracer gas techniques which include pressure-volume surveys, fan testing, auxiliary ventilation system tests,

volumetric surveys, shaft and ventilation raise surveys, air leakage and recirculation control, and mine fire simulations [25].

## 2.4 Mining Applications of Tracer Gases

### 2.4.1 Metal/Non-metal Applications

An operating limestone mine utilizing a simple ventilation scheme that included a main drift intake and single vertical hole for exhaust housed some of the earlier testing of SF<sub>6</sub> [21]. The low velocities that were a direct result of the large cross sectional areas present in the limestone mine made it difficult to utilize many conventional methods of airflow quantity determination [21]. Several different tests were run using SF<sub>6</sub> and compared with conventional methods to evaluate auxiliary fans, the vertical exhaust hole, the natural draft vertical intake hole, air exchange on a working face at the end of a room, air flow in non-working areas, and airflow in main intake airways [21].

Thimons *et al.* continued to use SF<sub>6</sub> in a vein-type metal mine to determine how much air was recirculating through old stopes [21]. A narrow vein underground gold mine near Lae, Papua New Guinea utilized SF<sub>6</sub> and the MIVENA mine ventilation simulator to monitor and model airflow patterns through operating shrinkage stopes [26]. It was reported that the measured and simulated curves of the flow in the shrinkage stopes were comparable; however deviation exists at the tail end of the curves due to the delayed arrival of the tracer [26]. Residence times in non-active stopes in a uranium mine were studied to help determine relationships between radon gas and daughter concentrations [27].

The White Pine Copper mine hosted SF<sub>6</sub> studies pertaining to the effectiveness of different jet fans and their ability to redistribute fresh air as well as the usefulness of their location in a dead heading [28]. The Yucca Mountain Exploratory Studies Facility, which is a tunnel designed to house nuclear waste, utilized SF<sub>6</sub> to determine if ventilation duct was carrying silica dust [29].

Total mill ventilation systems were developed to reduce respirable dust concentrations at various processing sites which included a clay mill and a silica/sand mill [30]. Tracer gas techniques were used at the silica/sand mill to determine the effectiveness of the total mill ventilation system [30].

## 2.4.2 Coal Applications

There have been several applications of tracer gas techniques in coal mines, with many related to determining leakage across stoppings and seals. Air leakages across stoppings, doors, and air-crossings pose potential hazards as well as create a need for increased fan circulation to provide adequate airflow to the face and therefore, an understanding of the leakage in mines is invaluable [31]. Since it is often difficult to provide adequate fresh air to the working face, tracer gas studies along with decay curves were used to evaluate mixing and determine eddy zones [32]. Auxiliary ventilation in three headings of a coal mine along with the dilution rate of methane in development headings were analyzed utilizing SF<sub>6</sub> as the tracer gas [2]. SF<sub>6</sub> tests were conducted under a mucking scenario in a dead heading to determine if fan systems were providing uniform mixing [33]. In 1976, Vinson and Kissel used SF<sub>6</sub> tracer gas techniques to study air movement in a sealed area, stopping leakage, and a ventilated gob area [23]. The SF<sub>6</sub> technique for measuring leakage in stoppings was developed in 1978 to allow even smaller leakages to be detected to within 10% of known leakage values which is more accurate than the brattice window measurement method [34]. Stoppings are often damaged with mine convergence and therefore, the SF<sub>6</sub> tracer gas technique was used to test leakage characteristics across squeeze stoppings which were designed to combat damages associated with floor heave and roof/rib convergence [35]. Leakage measurements of various stoppings including damage-resistant brattice, brattice and wire mesh, pipe and sheeting, transformable stoppings, muckpile and brattice, and muckpile stoppings were made using both SF<sub>6</sub> tracer gas and brattice window measurements [36]. Both methods were effective, with the tracer gas method useful for low leakage rates and the brattice window method useful for high leakage rates [36]. These tests were conducted at a large opening room-and-pillar oil shale mine in Colorado [37]. Singh *et al.* used tracer gas techniques to determine leakage characteristics through a remote filled cement concrete plug in a coal mine in central India [31].

Extensive tracer gas studies involving inactive workings and gob areas have been conducted. Due to the potential for spontaneous heating and combustion of coal in abandoned workings and gob areas, it is important to understand the flow of gases and mine air through these areas [24,38]. Timko *et al.* used SF<sub>6</sub> to evaluate three different gob areas at a longwall operation and two different room-and-pillar operations [24]. Since seals only restrict rather than eliminate the flow of gases, it is necessary to study the gas exchange between active and inactive workings [39]. Therefore, five different abandoned workings and respective seals were evaluated by releasing SF<sub>6</sub> and measuring the rate of diffusion from the seals in the Orchard Valley Coal mine [39]. Sulfur hexafluoride was

utilized by Buchwald and Jaskolski in two case studies to understand the air flows in sealed areas of a longwall mine in Poland [38]. Too much vacuum on gob wells can also dilute methane with mine air and render ventilation less effective [40]. Mucho *et al.* studied a longwall mine in the Pittsburgh Coalbed in Greene County to determine the interactions between the bleeder ventilation system and the gob gas venthole system through seven injections of SF<sub>6</sub> underground [40]. Tracer gas techniques in conjunction with computational fluid dynamics (CFD) were used to gain a better understanding of gob gas flow in an underground Australian coal mine [41]. Kennedy *et al.* highlighted the flexibility multiple tracer gases could bring to field surveys and tested the Freons along with SF<sub>6</sub> in the CBCRL [22]. Xenon was tested in a lab and experimental coal mine and found to be an effective radioactive tracer that could be used to evaluate flows in abandoned underground workings because it does not deposit in the airways, has an appropriate half-life, and is even more sensitive than SF<sub>6</sub> [42].

Different studies were conducted to test effectiveness of scrubbers and spray systems. SF<sub>6</sub> was injected directly into a scrubber in a laboratory to calculate the necessary variables to determine air-methane recirculation associated with dust scrubbers and further tests utilized a full-scale plywood model of a working face in a coal mine [43]. Vinson *et al.* conducted extensive SF<sub>6</sub> studies in a full-scale mine entry model to see the effects of different curtain setbacks, air volumes, and box cuts on the face ventilation measurements [44]. As the ability to make longer mining cuts progresses, so does the demand for increased ventilation, resulting in a study utilizing SF<sub>6</sub> to determine jet fans' ability to provide ventilation to the face [45]. The "extended-cut system" was a modification of the original "sprayfan" on a continuous mining machine used to maintain ventilation to the mine face [46]. This system was evaluated in a Utah coal mine by releasing SF<sub>6</sub> on the off-curtain corner of the continuous miner boom to simulate methane [46]. A study conducted at the National Institute for Occupational Health and Safety (NIOSH) Pittsburgh Research Laboratory (PRL) introduced coal dust and SF<sub>6</sub> in front of and alongside the cutting drum of a full-scale continuous miner gallery to simulate the pulverized coal dust and methane that would emanate from the use of a continuous miner to test and optimize various spray considerations [47].

The tracer gas technique was used to monitor the natural ventilation as well as fan effectiveness of a reclaiming area of a double silo and feeder ventilation, respectively [48]. Different mine fire scenarios were simulated by releasing SF<sub>6</sub> at various locations to determine how safe fire escapeways actually were in a drift mine [49]. MSHA evaluated six different bleeder ventilation systems throughout fourteen room-and-pillar gob areas

by using the SF<sub>6</sub> tracer gas technique [50]. Since respirable dust can be an issue with overburden drilling at surface coal operations, SF<sub>6</sub> was used to determine how much dust flowed to downwind locations [51].

Tracer gas techniques are important in mining since they can be used successfully in inaccessible areas, areas where adequate point measurement is not possible, and areas where the summation of small losses is important such as leakages across stoppings.

## *2.5 Release, Sample and Analysis Methods*

### **2.5.1 Releasing Techniques**

With extensive applications of tracer gases in mining, there have been numerous variations of releasing techniques. Releasing techniques are important for several reasons. Release quantities and rates of the tracer need to be known in order to determine and compare how much is circulating through the mine air. It is also necessary to ensure adequate mixing and dispersion of the tracer gas, especially in areas that might not have fully developed turbulent flow. If the tracer is not mixed throughout the cross-sectional area of the airway, sampling could be biased. Higgins and Shuttleworth discuss the “Steady Release Method” and the “Pulse Release Method” of introducing SF<sub>6</sub> into the underground mine environment [20]. The steady release method continuously releases the tracer at a constant known volume rate ultimately allowing the tracer concentration in the airstream to plateau [20]. When the tracer has built up to the constant value, the airflow quantity, Q, can be determined by Equation (5) assuming there is no loss of tracer [20].

$$Q = \frac{q}{c} \quad (5)$$

Where q is the constant known volume rate and c is the concentration of tracer. The pulse release method does not require a constant release rate, but instead requires a known mass of the tracer to be continuously released [20]. Utilizing this method requires a concentration-time curve to be developed in order to calculate the area under the curve [20].

At the Bureau of Mines Safety Research coal mine, SF<sub>6</sub> was first introduced by utilizing a water displacement method and the results indicated that there was variation between samples based on the airway sample location [21]. Past research conducted by the Bureau of Mines indicated that a mixing problem is present when there are low velocities in mine

airways which resulted in the technique developed in 1974, detailing release of SF<sub>6</sub> from a pressurized lecture bottle [21]. A small 0.006 inch hole in the cap of the lecture bottle allowed SF<sub>6</sub> to be released as a jet spray, and moving the bottle around the cross section of the airway during release helped to improve mixing in the airway [21]. When SF<sub>6</sub> is released through highly pressurized bottles holding a determined amount of the tracer, the BOM determined that the volume of gas released can be calculated from Equation (6) below.

$$V = nR \quad (6)$$

where V is the volume of SF<sub>6</sub> released, n is the moles of SF<sub>6</sub> released, and R is the volume per mole. This equation was adapted from the ideal gas law [52].

For initial underground tests of leakage characteristics, a known volume of SF<sub>6</sub> was released from a syringe and a board was waved to ensure mixing in the test area [28]. Steady state and unsteady state experiments were conducted by either releasing SF<sub>6</sub> at a constant rate followed by measurements at various locations or releasing SF<sub>6</sub> at a constant rate for a fixed period of time and measuring changes in concentration [32]. For face ventilation measurement studies in the lab, a syringe with SF<sub>6</sub> was connected to a 0.25" diameter plastic tube with an air pump [44]. In the underground copper mine study of jet fan effectiveness, SF<sub>6</sub> was released uniformly from a lecture bottle with a 0.006 inch hole and then the weight loss of the lecture bottle was used to calculate the amount of SF<sub>6</sub> released [28]. The CBCRL typically uses the constant steady flow release method from a lecture bottle with a regulator and varies the pressure to change the flow rate of the tracer gas [22]. Klinowsky and Kennedy also varied stainless steel tube diameter and length to change the release rate while measuring the rate with a soap bubble flowmeter [53]. Similarly, SF<sub>6</sub> was released from a gas bottle through a laboratory-calibrated flowmeter [51]. SF<sub>6</sub> was introduced to the continuous miner gallery at the PRL at a flow of 6 milliliters/sec using a multipoint gas doser provided by California Analytical Instruments [47]. SF<sub>6</sub> was injected into an inactive gob gas venthole, into the gob, and released into underground ventilation airflow utilizing either the "fast" or "slow" tracer gas release methods [54]. The fast method was utilized in areas with a minimum determined airflow and the 0.04m<sup>3</sup> lecture bottle would be emptied in 30 seconds [54]. The slow release method took about 20 minutes to empty the standard size lecture bottle and was best for locations that had low airflows [54]. Wala *et al.* designed a tracer-gas release system that included a tank and pressure gage, flow meter, and control valves that would enable the pulse-dilution tracer release method to be executed [42]. Arpa *et al.*

reported utilizing a pulse injection technique through releasing and popping of balloons containing a known mass of SF<sub>6</sub> [26]. Pulse injection was also utilized at Yucca Mountain [29].

Various release systems are necessary to provide the most flexibility in mine ventilation applications. Steady release methods are best when employed in areas with known turbulent flow as the tracer concentration plateaus in a shorter period of time. Pulse methods are useful in areas with lower velocities or when sampling at a larger distance from the release point. Regardless of the release method, it is important to be able to accurately determine the quantity of tracer being released in the test environment to obtain the most reliable results.

### **2.5.2 Sampling Techniques**

Sampling techniques are a vital component of tracer gas applications. It is necessary to find sampling containers that do not leak and have reasonable storage periods to provide the most accurate results. The SF<sub>6</sub> technique developed by the U.S. Bureau of Mines, used 10mL glass syringe bottles with rubber stoppers to create an airtight environment [21]. This technique was also used in further studies [28],[54]. The Bureau also employed vacutainers as a popular sampling method after conducting a study which studied gas concentrations and leakage over time and determined that vacutainers had the best performance when evacuated completely before use [55]; this method was also adopted by Timko and Lincoln [49] and used in other studies [44], [50].

Tygon tube and plastic syringe systems were used to collect samples at fixed time intervals in early SF<sub>6</sub> studies underground [34]. The U.S. Bureau of Mines also designed a sequential sampler which adds more flexibility to tracer gas studies and reduces manpower required for sampling in multiple locations [56]. The sampler is based on the Archimedes screw principle and is described in detail by Vinson and Kissell [56]. Diamond *et al.* used 20mL glass sample tubes to manually collect periodic samples and an automated gas sampling (AGS) system for gathering samples at more critical time periods [54].

Arpa *et al.* measured the SF<sub>6</sub> concentration underground using a photo-acoustic gas monitor that had a sampling rate of 40 seconds and a high resolution [26]. A photo-acoustic gas monitor was also utilized at PRL to measure the SF<sub>6</sub> at the off-curtain side, the curtain side, and the return air path in the continuous miner gallery [47]. The



respirable dust surface test utilized gas bag samplers equipped with a constant flow pump [51].

Disposable plastic syringes are also often used [22], [30], [32]. Grab samples are collected with plastic syringes and Tedlar bags in most CBCRL applications [22]. However, Kennedy *et al.* determined that the plastic syringe sampling system was not suitable for the Freon-12 tracer due to significant sample loss [22]. A special radioactive detector system was designed to both collect, analyze, and record samples on-site of a radioactive isotope of the xenon gas [42].

Sampling techniques vary not only with the medium used to physically take a sample, but also with the time a sample is taken. Under the “Steady Release Method” discussed previously, Higgins and Shuttleworth discuss taking two or three samples at the sampling point after the concentration of the tracer reaches the buildup value while the “Pulse Release Method” calls for samples to be taken immediately and as frequently as possible in order to have enough samples to develop the concentration-time curve [20].

Furthermore, sampling position can influence the accuracy of the results. A non-mining related study on sampling position highlighted the inaccuracies of the tracer gas method as a means of monitoring ventilation rates due to the large variations associated with non-perfect mixing [57], and emphasizes the importance of well-planned sampling locations and methods.

Overall, the methods employed above have been successful to varying degrees. However, with improving technology it is important to continue to evaluate current methods as well as develop newer sampling techniques to achieve the most accurate sample analysis.

### **2.5.3 Methods of Analysis**

Chromatographic methods are common for analyzing tracer gas samples. Electron capture detectors (ECD) are extremely sensitive to electronegative atoms, including halogens and oxygen, sulfur and nitrogen. This makes it a commonly used detector, ideal for sulfur hexafluoride. Many of the mining applications above reported using a gas chromatograph often equipped with an ECD to aid in sample analysis [34], [38], [44], [54]. The Bureau of Mines technique developed in 1974 used a portable electron capture detector (ECD) equipped with a stainless steel packed column which was packed with Chromosorb 102 [21]. The carrier gas used in this method was argon with five percent methane [21]. Portable ECDs were also used in other studies [28], [30]. Kennedy *et al.*

analyzed multiple tracer gas samples with an ECD and both a molecular sieve column for SF<sub>6</sub> and Freon-13B1 and a Porapak Type P column for Freon-12 [22].

Other analysis methods not as common as the ECD have included the Bruel & Kjaer Model 1302 photo-acoustic gas monitor which had a resolution of 10 ppb with an absolute accuracy of +/- 50ppb used by Arpa *et al.* [26], the infrared gas analyzer used to determine nitrous oxide concentrations [20], and specially designed radioactive detector for measuring xenon in studies conducted by Wala *et al.*[42]. The radioactive detector was designed by EG&G ORTEC and included a large-area proportional counter, high detection efficiency for low-energy gamma rays while maintaining a low detection efficiency for the background noise, and is completely portable [42]. Essentials of gas chromatography are discussed further in section 2.7.

## 2.6 Solid Phase Microextraction

Solid-Phase Microextraction (SPME) fibers were developed in 1990 by Pawlizyn and group at the University of Waterloo. This technique has nearly eliminated the need for sample preparation through use of a coated silica fiber which can adsorb and absorb target analytes [58]. There have been several successful reports of SPME applications in other industries including forensics, polymers and coating, natural products, pharmaceuticals, food and beverages [59], toxicology, biomedical analysis, and various environmental-type sampling [60]. Several studies have also been conducted with SPME to analyze volatile organic compounds (VOCs) in buildings [61] and formaldehyde in indoor air [60] and other various field scenarios where the indoor air quality needed to be tested as outlined by Koziel and Novak [62]. Furthermore, work has been done to create and validate a portable dynamic air sampling device for rapid field air sampling [63].

There are many positive attributes of SPME fiber technology that could make it a viable sampling method in mining applications. SPME fibers are small and convenient to carry and since analytes adsorb onto the fiber coating, samples do not desorb until heated, eliminating issues related to sample loss. However, preliminary laboratory testing utilizing SPME fibers indicated that it was not as sensitive as other sampling methods when testing sulfur hexafluoride [64] which is an issue since sensitivity is an important characteristic as samples may be in the ppb or ppt range in the underground mining environment. The fiber coating used in the preliminary studies was a non-polar Divinylbenzene (DVB)/Carboxen/Polydimethylsiloxane (PDMS) [64]. As reported, the SPME fibers did have the lowest error during preliminary testing and further evaluation of SPME fibers is necessary to determine if sensitivity can be improved [64].

## *2.7 Basic Gas Chromatography Theory*

Chromatography dates back to 1905, when Ramsey used active adsorption on or active desorption from solid adsorbents to separate mixtures of gases [65]. Since then it has continually developed to include both gas and liquid chromatography and there are continual advancements to improve the sensitivity, speed, and accuracy of chromatographic methods for separation and identification of volatile compounds [65].

### **2.7.1 Gas Chromatography Mechanics**

A standard gas chromatograph contains seven different elements which include: a cylinder of a carrier gas, flow controller and pressure regulator, injector port or sample inlet, column (packed or capillary), detector and associated electronics, recorder, and thermostats to set and monitor the injector, column, and detector temperatures [65].

When a sample is injected into the injector port of a gas chromatograph, it is carried through the column by the carrier gas, which is an inert gas. Typical carrier gases are helium, nitrogen, and hydrogen [65]. Separation is determined by partitioning of the sample mixture between the carrier gas and the stationary phase of the column, which is a non volatile liquid [65]. The distribution coefficient of the sample components affects the selectivity of the solvent and determines when the sample elutes from the column and is carried out by the inert gas [65]. This is called the elution technique and it has several advantages and disadvantages. The advantages of this technique are that there is continual restoration of the column by the inert gas phase, collection and quantitative determination of sample components is relatively simple because sample components are completely separated, and typically analysis time is short [65]. The main disadvantage of this technique occurs when a sample component is strongly retained on the column and therefore travels very slowly throughout the column resulting in a long analysis time, or the sample component does not move from the column [65].

Gas chromatography has several advantages including quick analysis time, good resolution, high sensitivity, simplistic methodology, and can provide both qualitative and quantitative analysis [65]. Sensitivity of gas chromatography methods varies not only with the compound being tested, but also with the detector installed in the gas chromatograph. There are four main classes of detectors: bulk versus specific property, selective versus universal, destructive versus non-destructive, and mass flow rate versus concentration dependent. Bulk detectors measure the property of both the mobile phase and the analyte and include refractive index, thermal conductivity, electron capture, and conductivity detectors [66]. Specific property detectors receive more signal from the

analyte than the mobile phase and include flame ionization, photoionization, UV/VIS, and Fluorescence detectors [66]. These detectors are also more sensitive than bulk detectors. Universal detectors measure all analytes, while selective detectors measure only certain analytes. Detector characteristics include noise, time constant, sensitivity, detectivity, and linearity. Noise is the background fluctuation in the signal and the signal to noise ratio must be at least three for detection of an analyte. Each detector has associated strengths and weaknesses. This research project utilizes an electron capture detector (ECD). ECDs are well known for their exceptional sensitivity for detection of molecules containing electronegative atoms such as halogens (F, Cl, Br, I) and oxygen and sulfur [66]. This detector is non-destructive and concentration dependent [66]. Despite its exceptional sensitivity for certain compounds a limiting factor of the ECD is its poor linearity [66].

With gas chromatography, good peak resolution means two things: a sharp peak with Gaussian distribution and adequate or baseline separation between peaks. The resolution of the peaks is related to column efficiency and solvent efficiency [65].

### 2.7.2 Column Efficiency

Column efficiency is associated with peak broadening which is a result of the operating conditions and column design [65]. This efficiency can be quantified by determining the number of theoretical plates (N) which is a unit less value. Efficiency can be calculated using Equation (7) below. The larger N is, the more efficient the column.

$$N = 16 \left( \frac{t_r}{W_B} \right)^2 \quad (7)$$

where  $t_r$  is the analyte's retention time and  $W_B$  is the width of the peak at the baseline. Additionally, height equivalent to a theoretical plate (HETP), which is the necessary length of the column for solute equilibrium to occur between the stationary liquid phase and mobile gas phase, is another indicator of a good or bad column [65]. This value can be calculated using Equation (8) below and the smaller the HETP, the better the column.

$$HETP = \frac{L}{N} \quad (8)$$

where L is the length of the column, typically in given in meters. HETP can vary greatly depending on a number of factors including: the linear velocity ( $\mu$ ) through the column, temperature settings, sample size, type of liquid phase, particle diameter, column

diameter, pressure, and thickness of the liquid phase [65]. These parameters can all be adjusted to optimize HETP. Additionally, the simplified Van Deemter Equation below summarizes the major factors affecting HETP.

$$HETP = A + \frac{B}{\mu} + C\mu \quad (9)$$

where A is the eddy diffusion or multipath effect, B is molecular diffusion, and C is resistance to mass transfer [65]. The linear velocity ( $\mu$ ) is calculated using Equation (10) below.

$$\mu = \frac{\text{length of column, cm}}{\text{retention time of air, s}} \quad (10)$$

Parameters A, B, and C all contribute to peak broadening in various ways, and thus influence HETP and are discussed in more detail by McNair and Bonelli [65].

### 2.7.3 Solvent Efficiency

Solvent efficiency is associated with the solvent used in the column's liquid phase. There are various considerations to make when selecting the appropriate stationary liquid phase including interaction forces and partition coefficients [65]. These various interaction forces include orientation forces, induced dipole forces, non-polar forces, and specific interaction forces which are discussed by McNair and Bonelli [65]. Since these forces determine the solubility of the sample in the solvent, they also determine the separation achieved. The partition coefficient, also known as the capacity factor, is a unit less value that numerically describes how well a substance is retained on the column (e.g. in the liquid phase) and is determined using Equation (11) below.

$$k = \frac{t'_{R, s}}{t_o, s} \quad (11)$$

where  $t'_R$  is the adjusted retention time given by Equation (12) below and  $t_o$  is the dead time given by Equation (13) below which is the time it takes for an unretained analyte or the mobile phase to pass through the column.

$$t'_R = t_R - t_o \quad (12)$$

$$t_o \text{ (or } t_m) = \frac{L}{\mu} \quad (13)$$

where  $t_r$  is the analyte's retention time,  $\mu$  is the linear velocity or flow rate (cm/s), and  $L$  is the column length (cm). A higher capacity factor,  $k$ , indicates that the substance is well retained and spends more time in the stationary phase, and therefore, will have a longer retention time. Compounds in a sample can be separated if their partition coefficients are different and additionally, the larger the difference between compounds'  $k$  value indicates that a shorter column length is required for separation [65]. Furthermore, the capacity factor decreases with an increasing temperature since the analyte will elute faster [65].

#### 2.7.4 Selectivity

Selectivity is an indicator of the difficulty of separating analytes and is measured by alpha which a unit less value and is calculated using Equation (14) below and the calculation for adjusted retention time is shown above in Equation (12).

$$\alpha = \frac{\text{adjusted retention time of analyte B, min}}{\text{adjusted retention time of analyte A, min}} \quad (14)$$

If alpha equals one, then the two substances cannot be separated. If alpha equals two, then the two substances can be separated easily [66]. Additionally, use of retention times as a means to determine the capacity factor, distribution of analytes, and the selectivity is the ideal measure as it is difficult to measure masses and volumes of analytes [66]. Alpha is also temperature dependant [65], and through modification of column temperatures, or temperature programming it may be possible to improve separation. Since the elution time is decreased with an increase in temperature, typically lower temperatures will help achieve better separation [65].

#### 2.7.5 Column Selection

The column of a gas chromatograph is where actual separation of a compound is achieved [65]. Therefore, choice of a column is indicative of the success or failure of any given separation. Analytes are able to be separated in gas chromatography due to the varying amounts of time they spend in the stationary phase. There are two distinct types of columns: packed and capillary. Packed columns contain solid, inert material while capillary columns have a smaller diameter and are open tubes with a thin liquid coating on the walls [65]. Packed columns are less expensive than capillary columns and can handle larger samples. However, packed columns can only handle fixed gases while capillary columns can handle complex mixtures. Capillary columns also have a higher efficiency and are more inert.

Liquid phases (e.g. stationary phases) should have low viscosity, low vapor pressure, and be chemically and thermally stable [65]. There are four liquid phase classifications and five solute classifications ranging from high to low polarity [65]. Common stationary phases include silicone polymers, carbowaxes, dexsil, diethyleneglycol succinate, squalene, and poropak Q [66]. Some helpful generalizations to consider when selecting a column are matching the polarity of the stationary phase with the polarity of the analyte, using the least polar phase that would provide adequate separation. Gas-solid columns such as molecular sieves and alumina are good for light hydrocarbons and sulfur gases, and DB-5 is the best column for general purpose use [66].

When choosing the column and the liquid phase, it is beneficial to review manuals, example chromatogram catalogs, technical support and past experiments as useful guidelines. Selecting a column can be tedious as it often is based on trial and error [65].

## *2.8 Summary*

There have been extensive uses of tracer gases, primarily sulfur hexafluoride, in various mining applications. Only a few researchers have examined use of multiple tracer gases. The use of multiple tracer gases enhances experiment flexibility by allowing for new experiments to be conducted before background levels of previous tracers are sufficiently reduced, and also enables rapid analysis of complex and interrelated circuits.

Collection and analysis of samples can be tedious and time consuming. Additionally storage and transportation of samples make it necessary to evaluate the shelf life of samples. New technology, including SPME, could greatly enhance the ease and speed of the method making it more accessible to mining operations, but also to other industries including earth atmospheric sciences and indoor air quality control. SPME, in particular, is highly portable and accurate, if appropriate protocols and optimum fiber coatings can be determined.

Tracer gases are an invaluable tool in examining underground mine air flows, and through continued research and development of this technique from type of tracer gas used to releasing, sampling and analyzing methods, it can become more flexible, precise, sensitive, cost-effective, user friendly, and robust.

Overall, tracer gas techniques have been effective in various industries and have thus far been useful in mining for evaluating ventilation systems in underground mines. Through establishing standard protocol and best practices, this technique is practical for large-

scale implementation and helps combat error associated with atypical cross-sectional areas, sporadic or inconsistent flow, and repeatability in measurements from. It allows for a more global evaluation of the system through greater flexibility over conventional methods since this technique can be used in both low and high velocity areas.



## Chapter 3: Comparison of Sampling Techniques

### *3.1 Introduction of Sampling Techniques*

Tracer gases have been utilized successfully in a variety of industries, each with specific releasing, sampling, and detection methods. The various attributes of tracer gases are dependent on the industry the tracers are utilized in. The review summarized in Chapter 2 discusses the various characteristics of underground tracer gases, highlights the multiple applications of tracer gas studies, as well as different sampling and releasing techniques. Though the sampling techniques discussed previously have become well-accepted in the industry, there are few, if any, studies comparing the relative strengths and weaknesses of the various sampling techniques.

The various sampling techniques utilized in the mining industry include glass syringe bottles with tight-fitting rubber stoppers, disposable plastic syringes, Tedlar bags, and non-adsorbing stainless steel cylinders. Since comparative studies are limited, this chapter will evaluate four of the current sampling techniques and introduce a fifth technique not currently utilized in industry. Six primary characteristics are discussed in a later section for which to evaluate the sampling techniques.

In an effort to improve the sampling methods, Solid-Phase Microextraction (SPME) fibers are being introduced and evaluated as an alternative method to sampling tracer gases in underground mining applications. SPME fibers are a unique and solvent less method of sampling developed in the early 1990s. Chai and Pawlizyn found that SPME fibers are suitable for on-site analysis and air monitoring due to their simplicity and minimal sample preparation time. SPME fibers have been successfully used in various applications. Similar to a capillary GC column, SPME fibers are coated with a stationary phase or sorbent and are made of fused silica. Fiber coatings typically range from 7 $\mu$ m to 85 $\mu$ m. As depicted in Figure 3.1 below, these thin fibers are housed in a holder assembly, similar to that of a syringe, for protection during transportation and storage and to allow for piercing of rubber septum when injecting into a gas chromatograph or other vessel. The plunger is pushed down to expose the SPME fiber, and the z-slot is present to limit the extension of the fiber from the casing. While the fiber is exposed from its metal sheath directly into the air, analytes can either adsorb or absorb onto the fiber coating. When sampling is complete, the plunger is pulled up to retract the fiber back into the protective casing. Air does not need to be drawn through the fiber, simple exposure is adequate. A septa can be placed on the septum piercing needle for an additional seal from

the surrounding atmosphere. The analytes then desorb from the fiber when injected into the gas chromatograph for analysis.

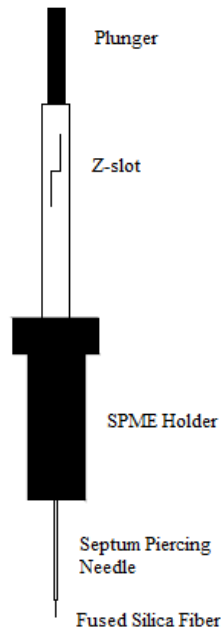


**Figure 3.1: Schematic of SPME Fiber Assembly**

Six primary characteristics to evaluate the various sampling techniques have been determined when considering mining applications. These include precision, convenience, sensitivity, storage and transportation, cost, and robustness. Precision is based on exactness and is more difficult to obtain using the current industry sampling techniques because it is influenced by user technique. It is imperative for the sampling method to be convenient and easy to use so that mine personnel do not require time-intensive training on sample collection. Sensitivity of the sampling method is significant because there will be very low concentrations of the tracer gases in the mine. Storage and transportation is another vital component in using tracer gases to evaluate underground mine ventilation systems. Since it can be several hours or days before a sample is analyzed and samples may need to be carried off-site for analysis, it is important that there is minimal sample leakage. Sampling methods should be cost-effective and robust so that there is negligible impact on the sample from the underground environment. Each sampling method introduced was evaluated with regard to the above characteristics to determine the most effective and efficient technique to use.

### 3.2 Methods

Four well-accepted sampling techniques currently used in the mining industry were evaluated. These techniques are plastic syringes, glass syringes, Tedlar bags, and vacutainers. In addition, the use of Solid-Phase Microextraction (SPME) fibers was introduced as an alternative sampling method that is not currently employed in the mining industry.

A 0.01% standard mixture of SF<sub>6</sub> and nitrogen was made inside a 275 ml glass bulb. Samples were taken from this bulb with a 3 ml plastic syringe, a 2.5 ml glass, gas-tight syringe, and a SPME fiber with a Divinylbenzene (DVB)/ Carboxen/ Polydimethylsiloxane (PDMS) coating which is non-polar. The SPME fiber was exposed inside the standard for five minutes. A separate 0.01% standard was made inside a Tedlar bag with a volume of 0.5 liters. Samples were then taken from the Tedlar bag with a plastic syringe and a glass syringe. Standards were made by injecting a known volume of pure SF<sub>6</sub> into a known volume of nitrogen. Finally, the vacutainer was evacuated with a small laboratory vacuum pump. The vacutainer was then checked by allowing water to infiltrate it. A 10 ml vacutainer can hold approximately 12 ml of water. Repeated tests indicated that the vacutainer would take 11 ml of water. The 0.01% standard was transferred to the vacutainer from the Tedlar bag and samples were pulled using plastic and glass syringes. There were two different users performing each of the above tests in order to compare how much variance in the results could occur person to person. After making the standards, samples were not extracted for several minutes to ensure dilution of SF<sub>6</sub> throughout the vessel.

All of the samples were analyzed using a Shimadzu GC-2014 electron capture detector (ECD). The column in the ECD was a TG-Bond Q+ supplied from Thermo Scientific with the properties listed in Table II below.

**Table II:** Column Characteristics

Column Name	TG Bond Q+
Column Type	Capillary
Column Length	30 m
Column Inner Diameter	0.32 mm
Film Thickness	10 μm

The following gas chromatograph protocol listed in Table III below was set for the purpose of this study. Temperature programming was utilized in the method of analysis

and optimized in order to obtain the best separation in the shortest amount of time. The protocol, specifically initial column temperature and split ratio, was adjusted for the SPME fiber samples in order to achieve Gaussian distribution of the peak shape and greater sensitivity.

**Table III:** Instrument Parameters for Sampling Comparison Study on Shimadzu GC-2014

<b><i>STANDARD GC PROTOCOL</i></b>	<i>Syringes/Tedlar Bags/Vacutainers</i>	<i>SPME Fibers</i>
<i>Split Injector Temperature</i>	250°C	250°C
<i>Split Ratio</i>	200:1	20:1
<i>Pressure</i>	9.7 psi	10.6 psi
<i>Carrier Gas</i>	He	He
<i>Total Flow</i>	327.5 mL/min	32.6 mL/min
<i>Column Flow</i>	1.64 mL/min	1.64 mL/min
<i>Linear Velocity</i>	30.0 cm/sec	30.0 cm/sec
<i>Purge Flow</i>	2.0 mL/min	2.0 mL/min
<i>Detector Temperature</i>	250°C	250°C
<i>Initial Column Temperature</i>	45°C hold 1 min	90°C hold 3 min
<i>Ramp</i>	40°C until 120°C	40°C until 150°C
<i>Final Temperature</i>	120°C hold 1.20 min	150°C hold 1.00 min
<i>Total Program Time</i>	4.07 min	5.50 min

Data analysis included calculating the relative standard error for each sampling technique. This calculation was based on the peak area. The retention time was also tracked to evaluate precision.

### 3.3 Results

Adequate separation of oxygen and SF<sub>6</sub> was the initial concern. As shown in Figure 3.2 below, it is clear that there are two well resolved peaks. This is important for quantifying the peak area.

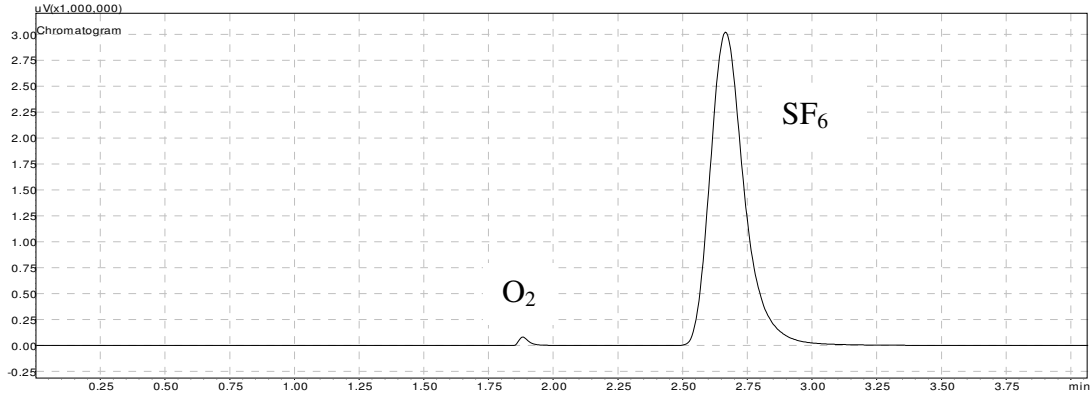


**Figure 3.2: Chromatogram Showing Separation of O<sub>2</sub> & SF<sub>6</sub>**

Since both adequate separation and sensitivity were obtained, the current GC protocol (column, detector, and settings) will be used for future experiments. Sensitivity is best expressed by the signal (peak area) to noise ratio. The signal to noise ratio was calculated using the signal of the peak area for each sampling method and the associated noise on the chromatograph that was present before the oxygen peak. From this ratio, the limit of detection (LOD) and the limit of quantification (LOQ) were calculated for each method. It is standard EPA practice that LOD is three times the signal to noise and LOQ is 10 times this ratio. Table IV below shows the LOD and LOQ for each sampling method in parts per million. As apparent in this chart, the sensitivity for all sampling methods, with the exception of SPME, is comparable. Higher concentration levels are required for the limit of detection utilizing SPME fibers.

**Table IV: Limit of Detection & Limit of Quantification**

<b>Sensitivity</b>	<i>LOD (ppm)</i>	<i>LOQ (ppm)</i>
<i>Glass Syringes</i>	0.01	0.04
<i>Plastic Syringes</i>	0.01	0.03
<i>SPME</i>	0.44	1.47
<i>Tedlar/Glass</i>	0.02	0.05
<i>Tedlar/Plastic</i>	0.01	0.04
<i>Vacutainer/Glass</i>	0.02	0.07
<i>Vacutainer/Plastic</i>	0.02	0.05

Figure 3.3 below compares sensitivity of all methods based solely on peak area and assuming the noise is the same for all sample runs. Disregarding the SPME technique, the comparable sensitivity between all methods with varying materials, would suggest that a representative sample is being collected. Also, the sampling bulb has a small volume of 275 ml relative to the sampler. At room temperature dilution of SF<sub>6</sub> occurs quickly in the

bulb, but as a precaution the bulb is not sampled for at least 10 minutes after mixing to insure proper dilution. There is no evidence that segregation of SF<sub>6</sub> occurs inside the bulb.

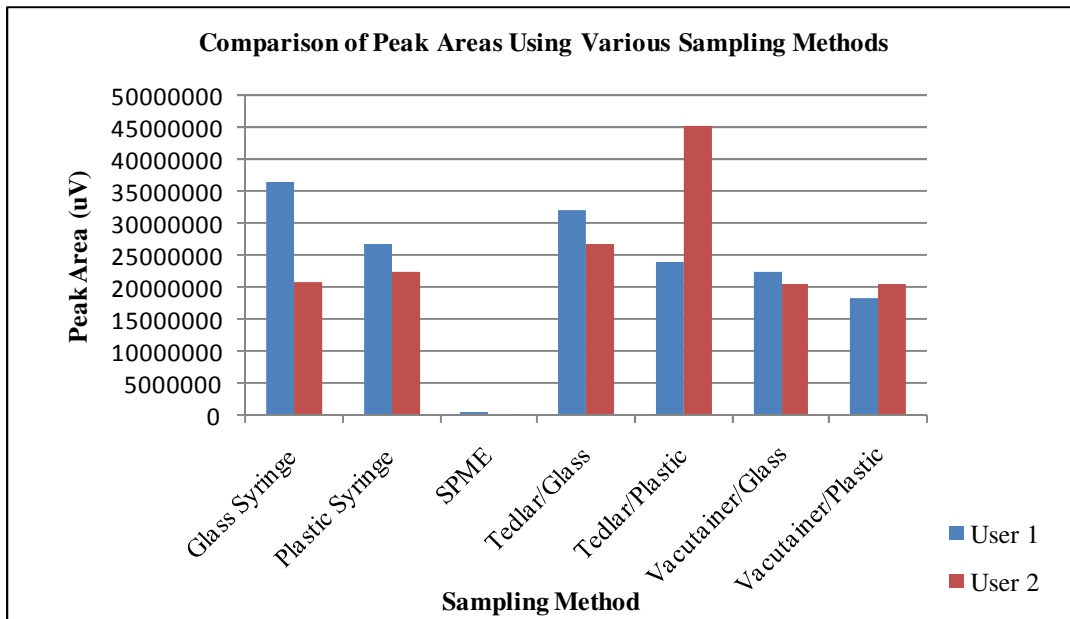


Figure 3.3: Sensitivity of Sampling Methods

Precision data was collected for all the sampling methods. Precision is also comparable for methods as depicted in Figure 3.4 below, with SPME again being the exception. The SPME technique is able to maintain a lower level of error over the traditional methods despite its decreased sensitivity because the method is not influenced by user technique. Since analytes absorb onto the fiber, and then desorb when placed into the injector of the GC, error associated with syringe clogging or user technique when sampling and injecting is eliminated. The error associated with all sampling methods is less than 20% with the exception of user 2 utilizing the vacutainer/plastic syringe sampling method. This large error is associated with persistent clogging of the needle utilized with the plastic syringe. As a result, side bore needles are recommended.

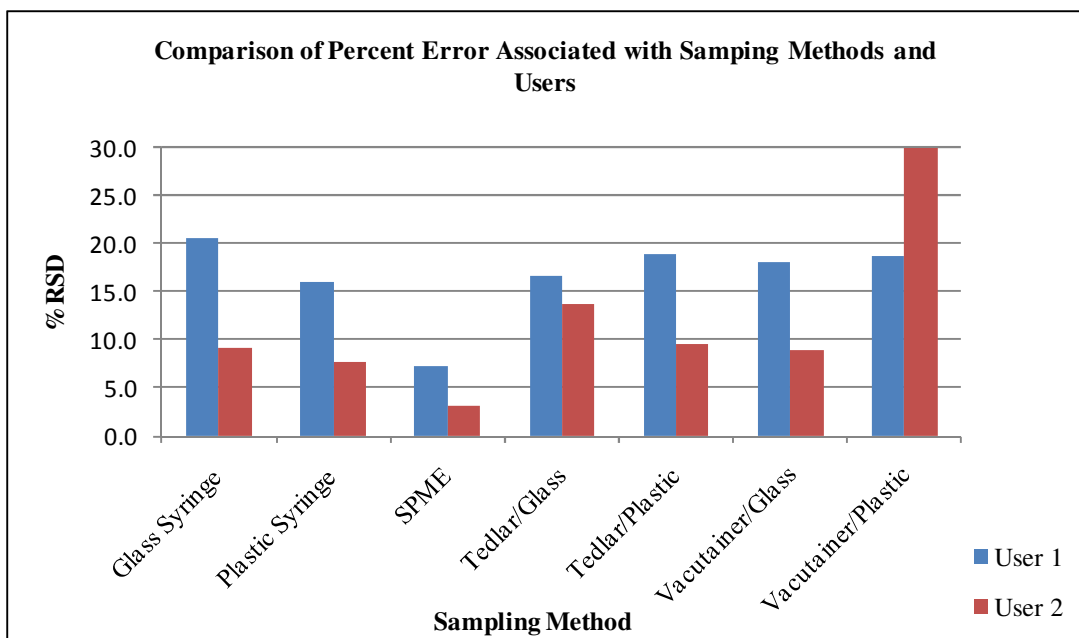


Figure 3.4: Precision of Sampling Methods

SPME had the lowest error for both users and the overlay of the five samples in Figure 3.5 shows that as a sampling method SPME is extremely precise. Most of the error associated with SPME sampling is probably due to the peak tailing.

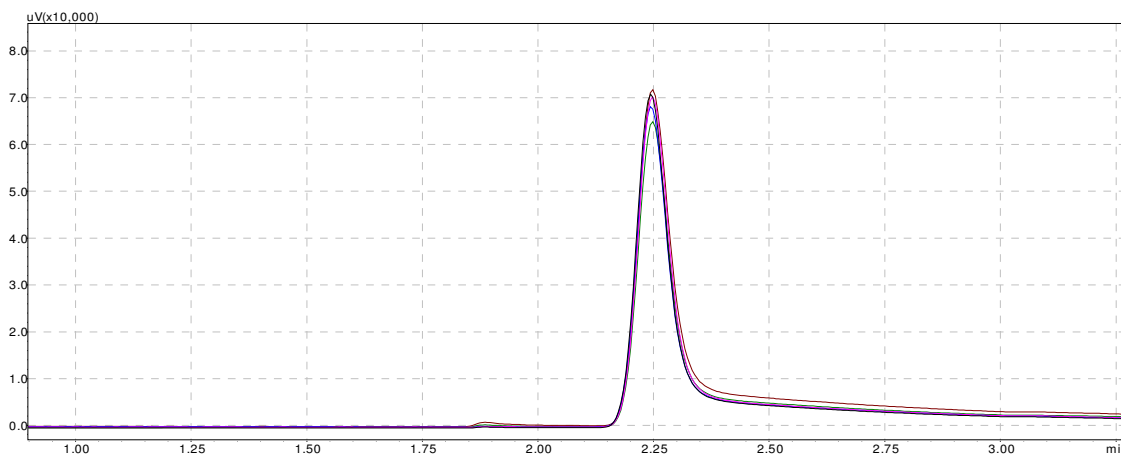
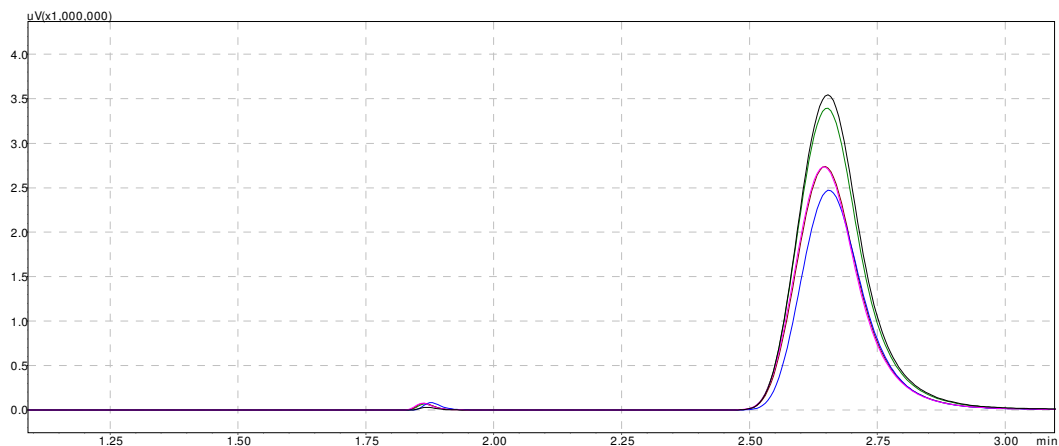


Figure 3.5: Chromatogram of 5 SPME Sample Runs

For comparison purposes, Figure 3.6 shows an overlay of five sample runs using the plastic syringes. Though plastic syringes have the better sensitivity over SPME, it is clear here that this method is less precise as there is obvious variance in peak area. The plastic syringe samples do have better Gaussian peak shape, opposed to the peak tailing presented in Figure 3.5 above. Other chromatogram comparisons of sampling methods can be found in Appendix A.



**Figure 3.6: Chromatogram of 5 Plastic Syringe Sample Runs**

### *3.4 Discussion*

Of the six characteristics used to evaluate sampling methods, the GC analysis focused on precision and sensitivity. Precision and sensitivity can vary greatly between users. There is inherent human error associated with manual injections which is apparent in Figure 3.3 and Figure 3.4. Human error along with the variability between users could make it difficult to obtain the accurate results needed to evaluate the mine's ventilation controls. Additionally, it was not possible to obtain fully evacuated vacutainers which is another source of error. Furthermore, there are inherent sources of error when making standards. When a standard is made, there are multiple transfers of the pure tracer gas into the glass bulb. As a result, the 100ppm standard is not exactly 100ppm. Figure 3.4 shows that plastic syringes and SPME fibers have the lowest error of the seven sampling techniques. Sampling via SPME fibers has the lowest error and varies only 4% between users compared to the 8% between users of plastic syringes. The benefit of using SPME, despite having lower sensitivity than the other sampling methods, is that there is less room for user error resulting in more consistent results between users. It is likely that the main source of error with the SPME sampling method is associated with the tailing of the peaks due to slow desorption from the fiber.

Another important consideration in choosing the most appropriate sampling method is cost. Plastic syringes have the lowest cost. A pack of 100 Luer Lock plastic syringes can typically be purchased for under US \$25.00 with reusable needles costing approximately US \$50.00 per pack of six. Additional benefits of plastic syringes are that they do not need to be primed or cleaned using solvents prior to use and they are disposable. Glass syringes are more expensive and are not considered disposable. Since glass syringes are reused, it is important to flush solvents such as hexane through the syringe and needle



after use to remove any remaining tracers. The glass syringe used in this experiment was also less inert than the plastic syringe, which could be a cause of the larger error of glass syringes. Tedlar bags are on the higher end of cost, running about US \$100 for a pack of ten 0.5L bags. A pack of 100 BD vacutainer 10 ml glass serum tubes cost approximately US \$40 and an additional US \$10 for 100 BD vacutainer passive safety needles. A SPME fiber assembly will cost around US \$100 for a fiber and US \$300 for a holder. Although this is a much higher cost, the fiber can be reused up to 100 times and creates less waste than the plastic syringes, tedlar bags, and vacutainers.

### *3.5 Conclusion*

Overall, utilizing plastic syringes for sampling is a good method, and is currently the best in terms of sensitivity, lower user error, ease of use, lower cost, and convenience. However, it is yet to be determined how plastics syringes will perform over time when storage and transportation from the mine to the lab are considered. Therefore, a time dependent study will need to be conducted to evaluate the robustness of the various sampling methods. Additionally, an auto sampler can significantly reduce the error.

Sensitivity of sampling methods is of the utmost importance in this application because gases will be at trace levels. SPME fibers have the lowest sensitivity, but SPME fibers have better precision. It will be beneficial to further evaluate different types of fiber coatings to maximize the fiber's sensitivity. It is also important to consider that multiple tracers will be used and the optimal sampling method could change.

## Chapter 4: Selecting Novel Tracer Gases

### *4.1 Introduction of Tracer Gases*

For a tracer gas to be suitable for mining applications it must meet several criteria which include: being chemically and thermally stable, non-toxic, easily transportable, readily attainable, non-radioactive, inexpensive, odorless, safe, and detectable at low concentrations. Therefore, careful consideration of these characteristics was made when selecting novel tracer gases to test.

While the new tracer gases must satisfy the above conditions, there are other considerations to make when choosing the best second tracer. Sulfur hexafluoride ( $\text{SF}_6$ ) has become the industry standard, and therefore, it is important that a second or even third tracer gas can be used in tandem with  $\text{SF}_6$ .  $\text{SF}_6$  has been found to be extremely sensitive using the electron capture detector and its strong signal can diminish the signal of other tracer gases. This results in a need for the other tracers to have a sensitivity similar to that of  $\text{SF}_6$  as well as have a dissimilar retention time on any particular column. In addition, it is vital that the tracers separate not only from each other but also from the oxygen peak.

The tracers that were tested include carbon tetrafluoride, octafluoropropane, and perfluoromethylcyclohexane which were all tested using different columns and temperatures. These tracers were first analyzed separately and then compared with the observed retention time of  $\text{SF}_6$  to determine if adequate separation could be achieved. The main indicators of a viable tracer are selectivity and separation which are indicated by the capacity factor and alpha value, respectively. Additionally, percent relative standard error was monitored during experimentation to confirm that it was below 15%RSD to ensure good sample technique.

### *4.2 Standard Lab Experimentation Procedures*

In order to ensure the most accurate results, standard procedures were followed when using the gas chromatograph to evaluate samples. Before any samples are run, the oven of the ECD was baked out for thirty minutes. This ensures any residue from previous experiments or build up in the column from long idle periods is removed by raising the column temperatures just below the maximum column temperature indicated by the column manufacturer. After the column is cleared out, the parameters are set to protocol for the specific experiment and a column blank is run to confirm that the resulting baseline is free of high noise. Depending on the sampling method, syringe blanks may be

run before drawing in any sample to make sure there are no contaminants in the syringe. This is primarily for glass syringes as plastic syringes are disposed of after use. The syringe blank, which is a sample of the laboratory air, is also a good indicator of when oxygen elutes from the column or the retention time of air. It is also an indicator of needle clogging, which would prevent any sample from actually being drawn and injected into the gas chromatograph. Finally, at least three samples are always run of a given tracer to obtain average values and percent relative standard deviation (%RSD).

### *4.3 Calibration of Columns*

Since columns vary greatly between each other depending on their polarity and liquid phase, it is necessary to calibrate each column for the gas that is being tested if concentration levels are desired. For the purpose of this study, calibration curves were made by gradually increasing the concentration of the specific gas in known amounts. For example, a 275 mL glass bulb is flushed out and then filled with nitrogen. Then, in 1 $\mu$ L increments, the tracer being tested is added to the bulb. After adding 1 $\mu$ L of the tracer, five samples are drawn from the bulb and run through the gas chromatograph to determine an average. This is repeated for 2 $\mu$ L, 3 $\mu$ L, 4 $\mu$ L, and 5 $\mu$ L. From this data, a calibration curve can be made utilizing the average peak areas associated with the concentration in the glass bulb. It is important to note that the linearity of electron capture detectors is limited and therefore, if testing outside the range of the calibration curve, a second curve needs to be made to account for concentrations that are much higher or lower than the bounds.

### *4.4 Tracers Evaluated*

#### **4.4.1 Carbon Tetrafluoride**

Carbon tetrafluoride (CF<sub>4</sub>) also known as Halocarbon 14 or Freon 14 was selected because it is not a known carcinogen, teratogen, or mutagen and also has molecular weight of 88.01 which differs from that of sulfur hexafluoride which is 146.05. In addition, the fluorine compounds should make it easily detectable by the electron capture detector. CF<sub>4</sub> is not expected in the mine atmosphere and is readily available in compressed gas cylinders.

#### **4.4.2 Octafluoropropane**

Octafluoropropane (C<sub>3</sub>F<sub>8</sub>) also known as Halocarbon 218 was selected because the fluorine compound should make it easily detectable by the ECD. C<sub>3</sub>F<sub>8</sub> is also not a known carcinogen and has a molecular weight of 188.02 which also differs substantially from

that of SF<sub>6</sub>. C<sub>3</sub>F<sub>8</sub> is also not expected in the mine atmosphere and is readily attainable in compressed gas cylinders.

#### 4.4.3 Perfluoromethylcyclohexane

Perfluoromethylcyclohexane also referred to as PMCH or C<sub>7</sub>F<sub>14</sub> or cyclohexane was chosen due to its high molecular weight of 350.05 which differs substantially from SF<sub>6</sub> which is 146.06. Despite PMCH being supplied as a liquid, this compound has been successfully used in past studies as a tracer gas as it is extremely volatile.

#### 4.5 Methods Used to Evaluate Tracers

A Shimadzu GC-2014 electron capture detector was the gas chromatograph used in testing of the potential tracers. Sulfur hexafluoride was also tested on each column that the novel tracers that were being evaluated. This was to ensure that SF<sub>6</sub> could be detected on a particular column and separated from the tracer of interest.

##### 4.5.1 CF<sub>4</sub> & C<sub>3</sub>F<sub>8</sub> Experiments Using SBP-1 Sulfur Column

Initial testing of CF<sub>4</sub> and C<sub>3</sub>F<sub>8</sub> on the gas chromatograph (GC)/electron capture detector (ECD) system in the mining ventilation laboratory was conducted with a SBP-1 Sulfur column installed. This column was supplied from Supelco and its properties are listed below in Table V.

**Table V: SBP-1 Sulfur Column Characteristics**

Column Name	SBP-1 Sulfur
Column Type	Capillary
Column Length	30 m
Column Inner Diameter	0.32 mm
Film Thickness	4.0 μm

Though much of the GC protocol remained the same throughout sample runs, the protocol was adjusted to achieve better peak shapes and/or separation of peaks by changing the temperature of the column. The initial standard protocol used for much of the early testing stages is listed below in Table VI.

**Table VI: Standard GC Protocol for SBP-1 Sulfur Column**

<b><i>STANDARD GC PROTOCOL</i></b>	
<i>Split Injector Temperature</i>	120°C
<i>Split Ratio</i>	10 to 1
<i>Pressure</i>	15.1 psi
<i>Carrier Gas</i>	He
<i>Total Flow</i>	38.3 mL/min
<i>Column Flow</i>	3.43 mL/min
<i>Linear Velocity</i>	50.0 cm/sec
<i>Purge Flow</i>	0.5 mL/min
<i>Detector Temperature</i>	150°C
<i>Initial Column Temperature</i>	40°C
<i>Ramp</i>	none
<i>Final Temperature</i>	40°C
<i>Total Program Time</i>	5 minutes

The above protocol was varied to also run samples using a column temperature of 20°C. The lower temperature was possible after setting up a cryogenic method which utilized carbon dioxide as the carrier gas. The lower temperatures were believed to be a good idea since initial testing indicated poor separation of peaks. Typically, lower temperatures increase separation because the lower temperatures increase the amount of time an analyte spends in the stationary phase, allowing more time for separation.

To test CF<sub>4</sub> and C<sub>3</sub>F<sub>8</sub> using the above protocol and different temperatures, manual syringe injections were made. For each temperature, at least three 10µL samples of pure tracer were injected into the gas chromatograph. In addition, a sample of 5µL of pure SF<sub>6</sub> was run on the column to compare retention times with that of CF<sub>4</sub> and C<sub>3</sub>F<sub>8</sub>. 5µL samples of pure SF<sub>6</sub> overloaded the column and subsequently, 1µL injections of SF<sub>6</sub> were then made. Since SF<sub>6</sub> is extremely sensitive to the ECD, even 1µL was too much sample.

#### **4.5.2 CF<sub>4</sub> & C<sub>3</sub>F<sub>8</sub> Experiments Using ZB-624 Column**

CF<sub>4</sub> and C<sub>3</sub>F<sub>8</sub> were also evaluated using a ZB-624 column supplied by Zebron with the properties listed below in Table VII. The column is composed of 6% cyanopropylphenyl and 94% methylpolysiloxane and replaces the well known DB-624 column.

**Table VII: ZB-624 Column Characteristics**

Column Name	ZB-624
Column Type	Capillary
Column Length	60 m
Column Inner Diameter	0.32 mm
Film Thickness	1.8 $\mu$ m

Testing of the tracer gases on the ZB-624 column was similar to the protocol established with the SBP-1 Sulfur column installed. The protocol used is listed below in Table VIII.

**Table VIII: Standard GC Protocol for ZB-624 Column**

<b><i>STANDARD GC PROTOCOL</i></b>	
<i>Split Injector Temperature</i>	250°C
<i>Split Ratio</i>	10 to 1
<i>Pressure</i>	9.6 psi
<i>Carrier Gas</i>	He
<i>Total Flow</i>	18.6 mL/min
<i>Column Flow</i>	1.64 mL/min
<i>Linear Velocity</i>	50.0 cm/sec
<i>Purge Flow</i>	0.5 mL/min
<i>Detector Temperature</i>	250°C
<i>Initial Column Temperature</i>	40°C
<i>Total Program Time</i>	4 minutes

Changes to the above protocol included again using the cryogenic method and conducting sample runs with a column temperature of 20°C and 0°C. Again, three 10 $\mu$ L samples of pure CF<sub>4</sub> and C<sub>3</sub>F<sub>8</sub> were injected into the GC for qualitative analysis of each unique retention time. 1 $\mu$ L samples of SF<sub>6</sub> were also run on this column to compare retention times to the other tracers being tested.

#### **4.5.3 CF<sub>4</sub> & C<sub>3</sub>F<sub>8</sub> Experiments Using TG Bond Q+ Column**

A TG Bond Q+ column was used next for the evaluation of CF<sub>4</sub> and C<sub>3</sub>F<sub>8</sub>. This column was supplied by Thermo Scientific and has the properties listed below in Table IX.

**Table IX: TG Bond Q+ Column Characteristics**

Column Name	TG Bond Q+
Column Type	Capillary
Column Length	30 m
Column Inner Diameter	0.32 mm
Film Thickness	10 $\mu$ m

Testing of the tracer gases on the TG Bond Q+ column was very similar to the protocol established with previous two columns installed. The protocol used is listed below in Table X.

**Table X: Standard GC Protocol for TG Bond Q+ Column**

<b><i>STANDARD GC PROTOCOL</i></b>	
<i>Split Injector Temperature</i>	250°C
<i>Split Ratio</i>	10 to 1
<i>Pressure</i>	9.6 psi
<i>Carrier Gas</i>	He
<i>Total Flow</i>	18.6 mL/min
<i>Column Flow</i>	1.64 mL/min
<i>Linear Velocity</i>	30.0 cm/sec
<i>Purge Flow</i>	0.5 mL/min
<i>Detector Temperature</i>	250°C
<i>Initial Column Temperature</i>	40°C
<i>Total Program Time</i>	4.50 min

The same method used to test CF<sub>4</sub> and C<sub>3</sub>F<sub>8</sub> on the SBP-1 Sulfur and ZB-624 columns was utilized in conjunction with the above protocol set for the TG Bond Q+ column. Again manual syringe injections were made. For each temperature, at least three 10 $\mu$ L samples of pure tracer were injected into the gas chromatograph. Since in previous experiments 5 $\mu$ L and 1 $\mu$ L pure injections of SF<sub>6</sub> overloaded the column, injections of 0.5 $\mu$ L were used. The protocol above was adjusted to conduct sample runs under the cryogenic method setting column temperatures to 20°C and 0°C.

#### **4.5.4 CF<sub>4</sub> & C<sub>3</sub>F<sub>8</sub> Experiments Using TG Bond Q Column**

Final testing of CF<sub>4</sub> and C<sub>3</sub>F<sub>8</sub> was conducted with a TG Bond Q column installed in the gas chromatograph. The properties of this column are listed below in Table XI and it was supplied by Thermo Scientific.

**Table XI: TG Bond Q Column Characteristics**

Column Name	TG Bond Q
Column Type	Capillary
Column Length	30 m
Column Inner Diameter	0.32 mm
Film Thickness	10 $\mu$ m

Similar protocol was established with the TG Bond Q column installed as was run with the previous tests on the TG Bond Q+ column. The protocol used is listed below in Table XII.

**Table XII: Standard GC Protocol for TG Bond Q Column**

<b><i>STANDARD GC PROTOCOL</i></b>	
<i>Split Injector Temperature</i>	250°C
<i>Split Ratio</i>	10 to 1
<i>Pressure</i>	9.6 psi
<i>Carrier Gas</i>	He
<i>Total Flow</i>	18.6 mL/min
<i>Column Flow</i>	1.64 mL/min
<i>Linear Velocity</i>	30.0 cm/sec
<i>Purge Flow</i>	0.5 mL/min
<i>Detector Temperature</i>	250°C
<i>Initial Column Temperature</i>	40°C
<i>Total Program Time</i>	5 minutes

The above protocol was modified to utilize the cryogenic method and to conduct sample runs with a column temperature of 20°C and 0°C. As well as utilizing the same method above samples were run with increased column temperatures of 50°C and 60°C to observe the effects of a higher temperature. Again three 10 $\mu$ L samples of pure CF<sub>4</sub> and C<sub>3</sub>F<sub>8</sub> were injected into the GC for qualitative analysis of each retention time and peak shape. Samples of SF<sub>6</sub> were also run on this column by injecting 1 $\mu$ L of a 1% standard of SF<sub>6</sub> in nitrogen to compare retention times to the other tracers being tested.

#### 4.5.5 PMCH Experiments Using HP-AL/S Column

PMCH was evaluated with an HP-AL/S column installed. This column is an aluminum oxide column and was chosen because it was used in a previous perfluorocarbon tracer study [67]. This column was purchased from Agilent Technologies and has the characteristics listed below in Table XIII.



**Table XIII: HP-AL/S Column Characteristics**

Column Name	HP-AL/S
Column Type	Capillary
Column Length	30 m
Column Inner Diameter	0.250 mm
Film Thickness	5 $\mu$ m

Protocol varied throughout testing of this tracer, but the final protocol that was established is listed below in Table XIV. The main variations were in initial column temperature, hold times, and the temperature programming rate. These variations are discussed with their individual results. This final protocol was established as it provided the best separation while allowing enough time for all material to elute from the column which is discussed later.

**Table XIV: Standard GC Protocol for HP-AL/S Column**

<b><u>STANDARD GC PROTOCOL</u></b>	
<i>Split Injector Temperature</i>	150 <sup>0</sup> C
<i>Split Ratio</i>	50 to 1
<i>Pressure</i>	16.2 psi
<i>Carrier Gas</i>	He
<i>Total Flow</i>	60.8 ml/min
<i>Column Flow</i>	1.15 ml/min
<i>Linear Velocity</i>	30 cm/s
<i>Purge Flow</i>	2.0 ml/min
<i>Detector Temperature</i>	200 <sup>0</sup> C
<i>Initial Column Temperature</i>	67 <sup>0</sup> C hold 2.75 min
<i>Ramp</i>	120 <sup>0</sup> C/min
<i>Final Temperature</i>	180 <sup>0</sup> C hold 12.30 min
<i>Total Program Time</i>	15.99 min

Initial experimentation of PMCH showed many impurities associated with the PMCH. In order to remove these impurities from the column, or the SPME fiber if that is the chosen sampling method, it is necessary to hold the column at a high temperature for a set period of time that would allow for all trace impurities to elute. Initial column temperatures and various hold times were tested to determine the above protocol and are discussed in detail in section 4.6.5.

In addition, since PMCH is a volatile liquid, the 100ppm standard was made through calculating the volume of liquid necessary to inject to obtain 100ppm of vapor utilizing assumptions based on the ideal gas law. By using the molecular weight (350 g/mol) and density of PMCH (1.788 g/L), various ratios and conversions, and the approximation that 1 $\mu$ L of liquid is equivalent to 500 $\mu$ L of gas the volume was calculated to be 0.49 $\mu$ L of liquid PMCH. This was injected using a liquid syringe into the 275mL glass bulb filled with nitrogen.

## 4.6 Gas Chromatography Results of Evaluated Tracers

### 4.6.1 CF<sub>4</sub> & C<sub>3</sub>F<sub>8</sub> Experiments Using SBP-1 Sulfur Column

Three samples of pure CF<sub>4</sub> were injected into the GC with a column temperature of 40°C and a resulting chromatogram is shown below in Figure 4.1. In the figure, the black line is the chromatogram of the syringe blank, showing that the oxygen peak elutes around 1.1 minutes while the pink line is the result of the 10 $\mu$ L injection of pure CF<sub>4</sub>. The pink line shows that the oxygen peak is much smaller, but a CF<sub>4</sub> peak is not apparent. The same procedure was followed with a column temperature of 20°C and still a peak for the CF<sub>4</sub> tracer did not elute.

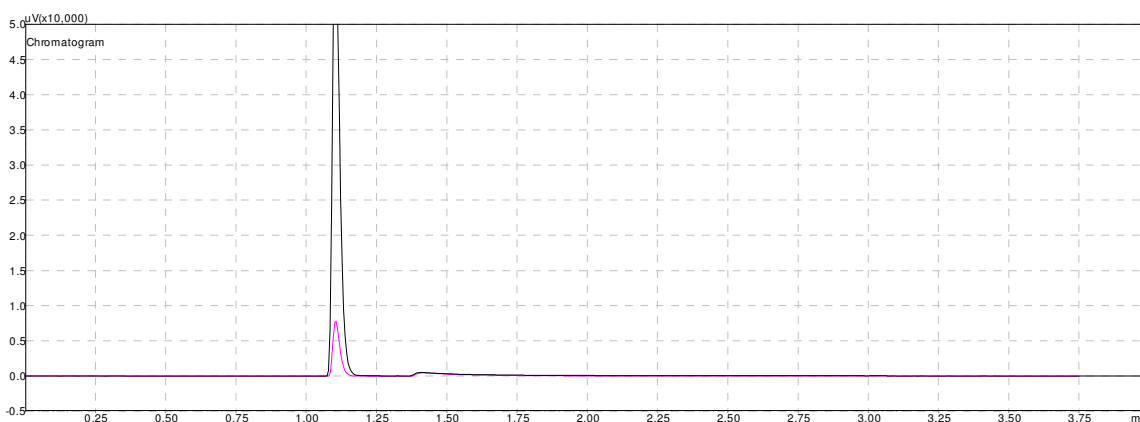
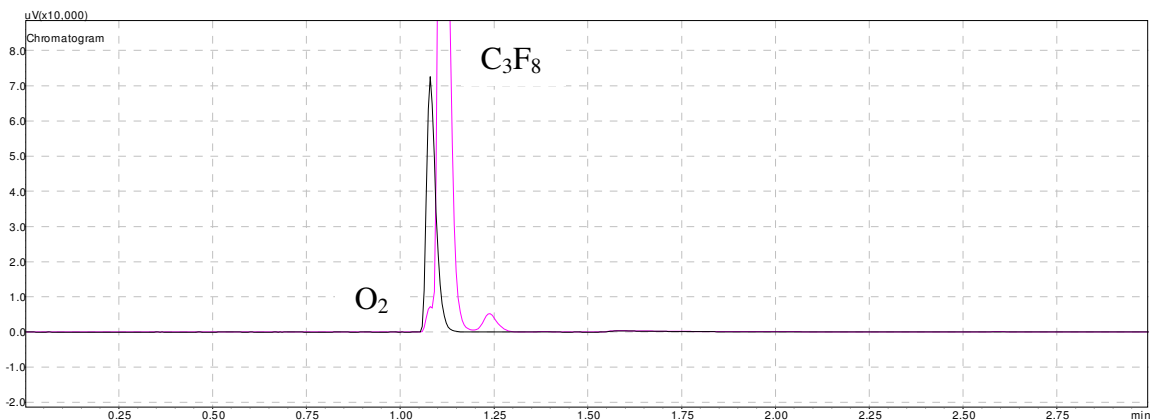


Figure 4.1: Comparison of Syringe Blank and 10 $\mu$ L Injection of Pure CF<sub>4</sub>

Sample runs of C<sub>3</sub>F<sub>8</sub> were also conducted with the SBP-1 Sulfur column installed. For a column temperature of 40°C a small peak eluted immediately after the oxygen peak. Slight separation of C<sub>3</sub>F<sub>8</sub> from oxygen can be seen in Figure 4.2 below as indicated by the slight elbow on the left portion of the C<sub>3</sub>F<sub>8</sub> peak. The small peak to the right is a trace impurity.



**Figure 4.2: Comparison of Syringe Blank (black) and 10µL Injection of Pure C<sub>3</sub>F<sub>8</sub> @ 20°C (pink)**

For comparison, 5µL samples of SF<sub>6</sub> were injected and run under the same conditions that CF<sub>4</sub> and C<sub>3</sub>F<sub>8</sub> were tested. As apparent in Figure 4.3, SF<sub>6</sub> is substantially more sensitive than the other tracers due to the wide peak, and also overlaps with the oxygen peak. The chromatogram shown below is from a sample run utilizing the 40°C column temperature; however the other column temperatures produce similar results.

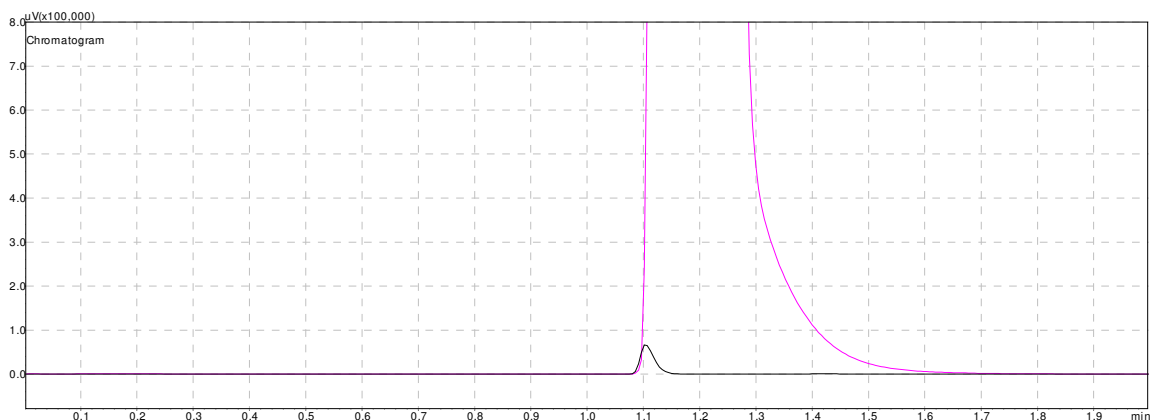


**Figure 4.3: Comparison of Syringe Blank and 5µL Injection of Pure SF<sub>6</sub>**

Each tracer gas was tested three times under each condition. Table XV below is a summary of the average retention times and Table XVI is a summary of the average peak area. Chromatograms of all runs with the SBP-1 Sulfur column installed in the gas chromatograph are located in Appendix B.

**Table XV: Average Retention Time of Gases on SBP-1 Sulfur Column**

Method		Average Retention Time ( $t_R$ )			
Name	Column Temperature	O <sub>2</sub>	SF <sub>6</sub>	CF <sub>4</sub>	C <sub>3</sub> F <sub>8</sub>
gas_sf6.gcm	40°C	1.10	1.22	1.10	1.20
cryo_method.gcm	20°C	1.08	1.19	1.10	1.24

**Table XVI: Average Peak Area of Gases on SBP-1 Sulfur Column**

Method		Average Peak Area		
Name	Column Temperature	SF <sub>6</sub>	CF <sub>4</sub>	C <sub>3</sub> F <sub>8</sub>
gas_sf6.gcm	40°C	89,100,000	14,300	14,400
cryo_method.gcm	20°C	76,900,000	15,600	13,000

Aside from observing the peak shapes in resulting chromatograms and noting retention times and peak areas, quantifiable results indicated that all gases are poorly retained, CF<sub>4</sub> cannot be separated from the oxygen peak and C<sub>3</sub>F<sub>8</sub> and SF<sub>6</sub> cannot be separated from each other as apparent from the low capacity factor ( $k$ ) and selectivity ( $\alpha$ ) values in Table XVII and Table XVIII respectively.

**Table XVII: Capacity Factor Values of Gases on SBP-1 Sulfur Column**

Method		k-values			
Name	Column Temperature	O <sub>2</sub>	SF <sub>6</sub>	CF <sub>4</sub>	C <sub>3</sub> F <sub>8</sub>
gas_sf6.gcm	40°C	0.100	0.227	0.105	0.209
cryo_method.gcm	20°C	0.080	0.190	0.105	0.240

**Table XVIII: Selectivity Values of Gases on SBP-1 Sulfur Column**

Method		$\alpha$ values				
Name	Column Temperature	SF <sub>6</sub> & O <sub>2</sub>	CF <sub>4</sub> & O <sub>2</sub>	C <sub>3</sub> F <sub>8</sub> & O <sub>2</sub>	SF <sub>6</sub> & CF <sub>4</sub>	SF <sub>6</sub> & C <sub>3</sub> F <sub>8</sub>
gas_sf6.gcm	40°C	2.27	1.05	2.09	2.16	1.09
cryo_method.gcm	20°C	2.37	1.31	3.00	1.81	1.26

The low  $k$  and  $\alpha$  values indicate that the SBP-1 Sulfur column is not sufficient for separating the novel tracer gases from SF<sub>6</sub> or from oxygen in some cases. The low capacity factors indicate that little time is spent in the stationary phase, resulting in the analyte being poorly retained on the column. Due to the poor selectivity and separation of the gases from each other and oxygen this column was eliminated from future experimentation.

#### 4.6.2 CF<sub>4</sub> & C<sub>3</sub>F<sub>8</sub> Experiments Using ZB-624 Column

CF<sub>4</sub> and C<sub>3</sub>F<sub>8</sub> were also evaluated with a ZB-624 column installed in the gas chromatograph. Similar to the experiments run with the SBP-1 Sulfur column installed, these tracers were evaluated with column temperatures set at 40°C, 20°C, and 0°C. Three sample injections were made of pure CF<sub>4</sub> and qualitative observations were made for peak shape and retention time. As depicted in Figure 4.4 below, CF<sub>4</sub> does not appear to elute on this column. The sample of laboratory air (black line) demonstrates when oxygen elutes and is much larger than in the case where a pure sample of CF<sub>4</sub> is injected (pink line). Therefore, it can be concluded that CF<sub>4</sub> either has the same elution time as oxygen or cannot be separated on this particular column. Similar results occur at temperatures of 20°C and 0°C.

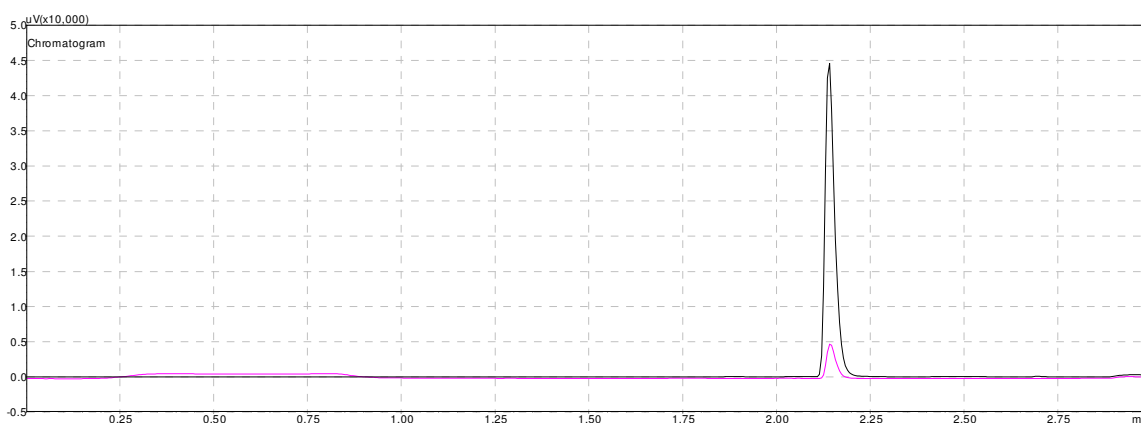


**Figure 4.4: Comparison of Syringe Blank (Black) and 10µL injection of Pure CF<sub>4</sub> (pink) at 40°C**

Results of pure injections of C<sub>3</sub>F<sub>8</sub> with the ZB-624 column installed were similar to the experiments run on the previous column. Below, in Figure 4.5, the pink line is the resulting chromatogram of a 10µL injection of pure C<sub>3</sub>F<sub>8</sub>. Again, it is apparent that the peak has a close retention time to that of oxygen, and the smaller peak is to the right is a trace impurity.

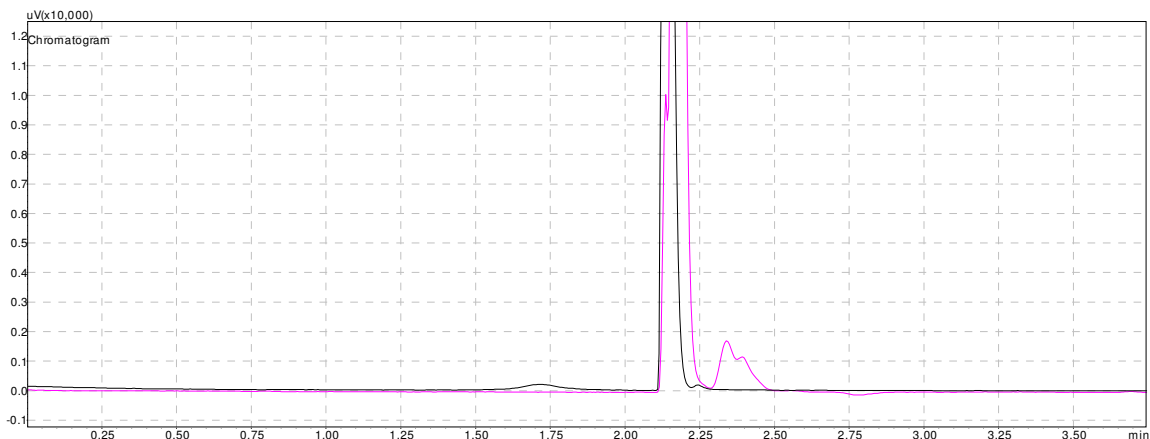


**Figure 4.5: Comparison of Syringe Blank (Black) and 10µL Injection of Pure C<sub>3</sub>F<sub>8</sub> (pink) at 40°C**

As apparent in the above chromatograms, the retention times are similar. Table XIX below is a summary of the average retention time from the three injections made of each tracer gas.

**Table XIX: Average Retention Time of Gases on ZB-624 Column**

Method		Average Retention Time (t <sub>R</sub> )			
Name	Column Temperature	O <sub>2</sub>	SF <sub>6</sub>	CF <sub>4</sub>	C <sub>3</sub> F <sub>8</sub>
gas_sf6.gcm	40°C	2.14	2.22	no peak	2.23
cryo_method.gcm	20°C	2.14	2.22	no peak	2.27
cryo_method.gcm	0°C	2.14	2.24	no peak	2.17

SF<sub>6</sub> was also run on the ZB-624 column for comparison and is much more sensitive than the other tracers and unfortunately it also overlaps with the oxygen peak as depicted in Figure 4.6 which would make separation difficult, if not impossible. In the figure below, the black line shows oxygen only, the pink line is from a pure injection of CF<sub>4</sub>, the blue line is from a pure injection of C<sub>3</sub>F<sub>8</sub> and the brown line is from a pure injection of SF<sub>6</sub>. The chromatograms are overlaid to show how close each peak is to each other and how much larger the SF<sub>6</sub> peak is in comparison.

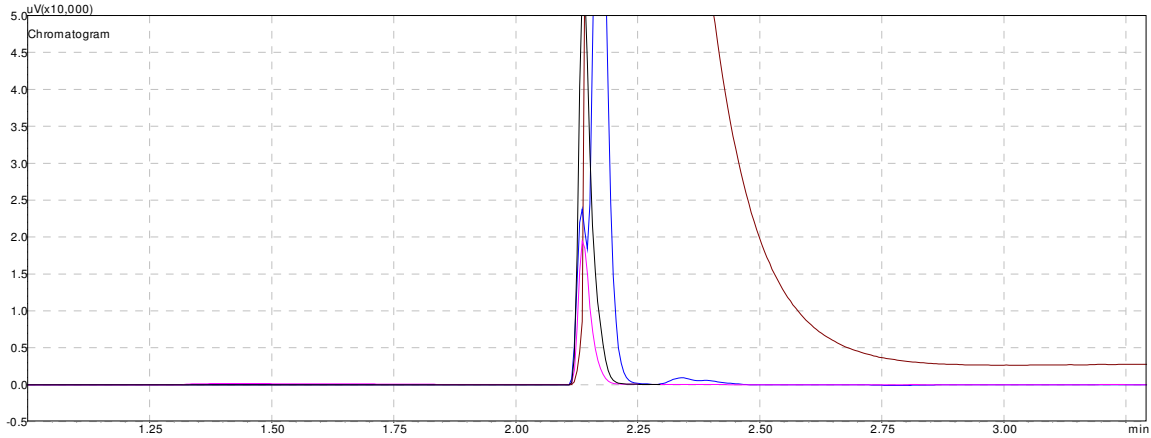


**Figure 4.6: Overlay of Each Tracer Gas Sample Run**

The average peak area of each gas is shown below in Table XX and indicates the difference in magnitude of the GC signal of each tracer.

**Table XX: Average Peak Area of Gases on ZB-624 Column**

Method		Average Peak Area		
Name	Column Temperature	SF <sub>6</sub>	CF <sub>4</sub>	C <sub>3</sub> F <sub>8</sub>
gas_sf6.gcm	40°C	59,300,000	2,066	10,200
cryo_method.gcm	20°C	61,200,000	no peak	8,630
cryo_method.gcm	0°C	65,650,000	no peak	220,000

In addition to peak area and retention time, the low  $k$  and  $\alpha$  values summarized below in Table XXI and Table XXII respectively are also good indicators that this column is not sufficient for the novel tracer gases.

**Table XXI: Capacity Factor Values of Gases on ZB-624 Column**

Method		k-values			
Name	Column Temperature	O <sub>2</sub>	SF <sub>6</sub>	CF <sub>4</sub>	C <sub>3</sub> F <sub>8</sub>
gas_sf6.gcm	40°C	0.070	0.111	no peak	0.115
cryo_method.gcm	20°C	0.070	0.112	no peak	0.134
cryo_method.gcm	0°C	0.070	0.118	no peak	0.086

**Table XXII: Selectivity Values of Gases on ZB-624 Column**

Method		$\alpha$ values				
Name	Column Temperature	SF <sub>6</sub> & O <sub>2</sub>	CF <sub>4</sub> & O <sub>2</sub>	C <sub>3</sub> F <sub>8</sub> & O <sub>2</sub>	SF <sub>6</sub> & CF <sub>4</sub>	SF <sub>6</sub> & C <sub>3</sub> F <sub>8</sub>
gas_sf6.gcm	40°C	1.59	no peak	1.64	no peak	1.03
cryo_method.gcm	20°C	1.60	no peak	1.91	no peak	1.20
cryo_method.gcm	0°C	1.68	no peak	1.22	no peak	1.03

Overall, the tracer gases were not well retained as indicated by the capacity factor values, especially CF<sub>4</sub> since there were no resulting peaks. In addition, the low alpha values for SF<sub>6</sub> and C<sub>3</sub>F<sub>8</sub> indicate that adequate separation of the two tracers from each other would be difficult, if not impossible. Inadequate separation makes it difficult to accurately and consistently quantify peak area. Therefore, this column was eliminated from future experimentation with these tracer gases. Additional chromatograms showing results on this column can be found in Appendix B (Figure B. 12-Figure B. 27).

#### **4.6.3 CF<sub>4</sub> & C<sub>3</sub>F<sub>8</sub> Experiments Using TG Bond Q+ Column**

CF<sub>4</sub> and C<sub>3</sub>F<sub>8</sub> again produced similar results to the samples run with the previous two columns installed in the GC. Similar to the experiments run with the previous columns installed, these tracers were evaluated with column temperatures set at 40°C, 20°C, and 0°C.

Three sample injections were made of pure CF<sub>4</sub> at each temperature and qualitative observations were made for peak shape and retention time. As illustrated in Figure 4.7 below for samples run with a 40°C column temperature, there is a small peak (pink line) which is larger than the oxygen peak from the syringe blank (black line). This indicates that CF<sub>4</sub> elutes around the same time as oxygen, but that it might not be possible to achieve better separation. Samples were also run at lower temperatures which did not produce any peaks. These chromatograms can be found in Appendix B (Figure B. 28-Figure B. 38).



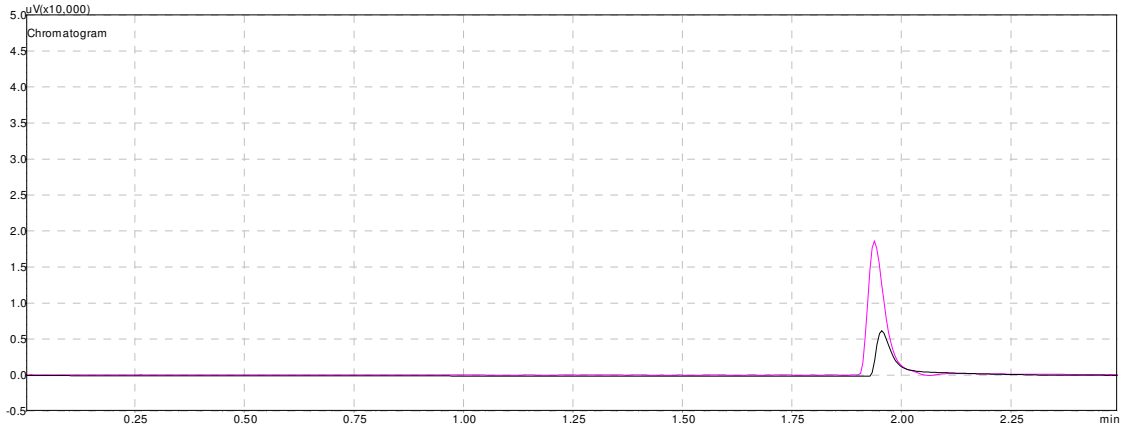


**Figure 4.7: Comparison of Syringe Blank (black line) and 10µL Injection of Pure CF<sub>4</sub> (pink line) at 40°C**

Below in Figure 4.8, the pink line is the resulting chromatogram of a 10µL injection of pure C<sub>3</sub>F<sub>8</sub>. The sample of laboratory air (black line) shows when oxygen elutes and is much larger than the injection of pure C<sub>3</sub>F<sub>8</sub> (pink line). When the runtime is extended, a small, broad C<sub>3</sub>F<sub>8</sub> peak elutes around 5.2 minutes. Similar results occur at column temperatures of 20°C and 0°C which can be found in Appendix B.

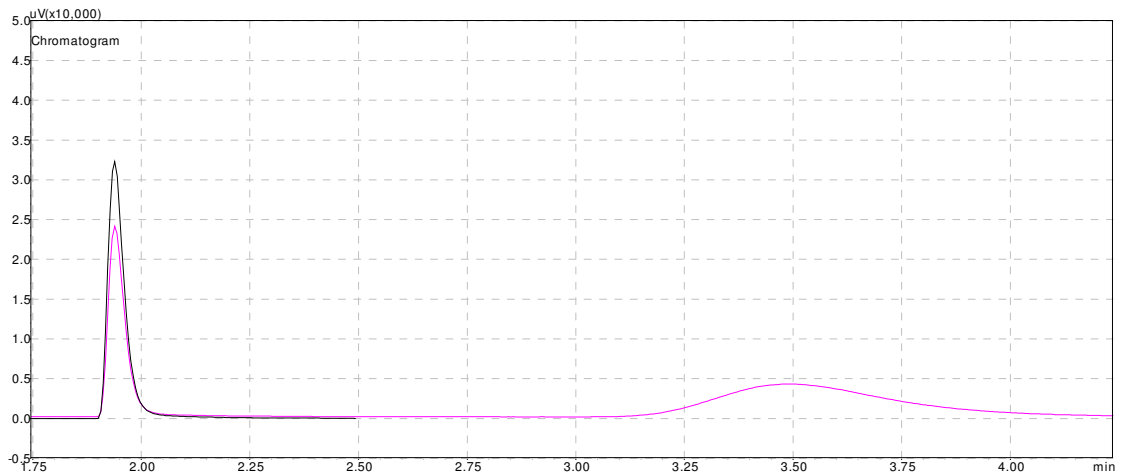


**Figure 4.8: Comparison of Syringe Blank (black line) and 10µL Injection of Pure C<sub>3</sub>F<sub>8</sub> (pink line) at 40°C**

Injections of pure SF<sub>6</sub> under the set protocol described previously, produced poor results. In Figure 4.9 below, the pink line is the result of the SF<sub>6</sub> injections and the peak is broad with tailing on the right side which continues until about 7 minutes. This indicates that the method utilized for the previous two tracers is not suitable for SF<sub>6</sub>.

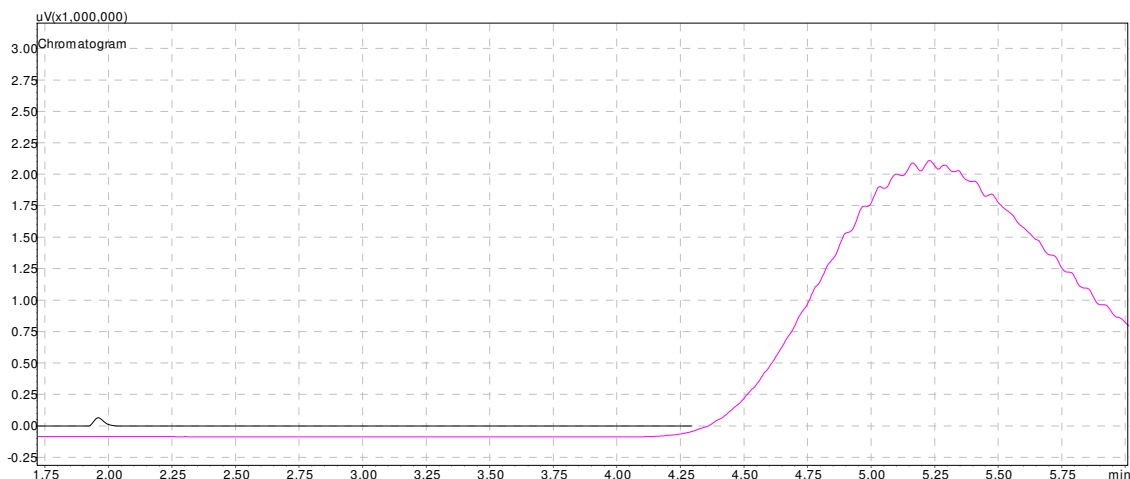


**Figure 4.9: Comparison of Syringe Blank (black line) and 0.5µL Injection of Pure SF<sub>6</sub>(pink line) at 20°C**

The average retention times for the different gases are given below in Table XXIII. From this data, it is apparent that SF<sub>6</sub> and C<sub>3</sub>F<sub>8</sub> have similar retention times, particularly at the lower column temperatures.

**Table XXIII: Average Retention Time of Gases on TG Bond Q+ Column**

Method		Average Retention Time (t <sub>R</sub> )			
Name	Column Temperature	O <sub>2</sub>	SF <sub>6</sub>	CF <sub>4</sub>	C <sub>3</sub> F <sub>8</sub>
gas_sf6.gcm	40°C	1.94	2.22	2.12	3.49
cryo_method.gcm	20°C	1.96	5.22	no peak	5.22
cryo_method.gcm	0°C	1.99	9.65	no peak	9.84

Although C<sub>3</sub>F<sub>8</sub> and SF<sub>6</sub> have different retention times at a column temperature of 40°C, Table XXIV below shows the average peak area showing the relative magnitude of the GC signal. These numbers indicate that C<sub>3</sub>F<sub>8</sub> is far less sensitive than SF<sub>6</sub> even when 10 times the sample amount is injected. This would make quantification difficult especially at the low concentration ranges that would be found in the underground mining environment.

**Table XXIV: Average Peak Area of Gases on TG Bond Q+ Column**

Method		Average Peak Area		
Name	Column Temperature	SF <sub>6</sub>	CF <sub>4</sub>	C <sub>3</sub> F <sub>8</sub>
gas_sf6.gcm	40°C	59,300,000	2,790	115,000
cryo_method.gcm	20°C	109,100,000	no peak	61,500
cryo_method.gcm	0°C	1,100,000	no peak	41,300

The larger k-values below in Table XXV for SF<sub>6</sub> and C<sub>3</sub>F<sub>8</sub> at the lower column temperatures indicate that the lower temperatures result in the analytes being better retained on the column.

**Table XXV: Capacity Factor Values of Gases on TG Bond Q+**

Method		k-values			
Name	Column Temperature	O <sub>2</sub>	SF <sub>6</sub>	CF <sub>4</sub>	C <sub>3</sub> F <sub>8</sub>
gas_sf6.gcm	40°C	0.163	0.333	0.27	1.10
cryo_method.gcm	20°C	0.176	2.13	no peak	2.13
cryo_method.gcm	0°C	0.194	4.79	no peak	4.90

The low  $\alpha$  values, specifically for C<sub>3</sub>F<sub>8</sub> and SF<sub>6</sub> at the lower column temperatures, summarized below in Table XXVI show that this column is not sufficient for the novel tracer gases. Despite C<sub>3</sub>F<sub>8</sub> and SF<sub>6</sub> having an alpha value of 3.28 at a column temperature of 40°C which indicates baseline separation can be achieved, the sensitivity of C<sub>3</sub>F<sub>8</sub> is too low as previously discussed. Additionally, the k values at a temperature of 40°C are substantially lower.

**Table XXVI: Selectivity Values of Gases on TG Bond Q+ Column**

Method		$\alpha$ values				
Name	Column Temperature	SF <sub>6</sub> & O <sub>2</sub>	CF <sub>4</sub> & O <sub>2</sub>	C <sub>3</sub> F <sub>8</sub> & O <sub>2</sub>	SF <sub>6</sub> & CF <sub>4</sub>	C <sub>3</sub> F <sub>8</sub> & SF <sub>6</sub>
gas_sf6.gcm	40°C	2.04	1.67	6.70	1.22	3.28
cryo_method.gcm	20°C	12.1	no peak	12.1	no peak	1.00
cryo_method.gcm	0°C	24.7	no peak	25.3	no peak	1.02

Again, CF<sub>4</sub> was not retained on this column as indicated by the lack of a peak on resulting chromatograms. When tested at 40°C, there was a small peak that had the lowest capacity factor relative to the other tracers indicating poor retainement. Furthermore, C<sub>3</sub>F<sub>8</sub> and SF<sub>6</sub> had the best separation from each other at the higher column temperature, however, the separation from oxygen at the higher temperature was poor for SF<sub>6</sub> as evidenced by the low alpha values. Lower column temperatures resulted in better separation of SF<sub>6</sub> from oxygen and C<sub>3</sub>F<sub>8</sub> from oxygen, but separation of C<sub>3</sub>F<sub>8</sub> and SF<sub>6</sub> was worse. Due to the poor results, this column was eliminated from future experimentation.

#### 4.6.4 CF<sub>4</sub> & C<sub>3</sub>F<sub>8</sub> Experiments Using TG Bond Q Column

Sample runs of pure CF<sub>4</sub> did not produce any peaks, and therefore qualitative and quantitative analysis could not be performed on this tracer. Resulting chromatograms are shown in Appendix B (Figure B. 39-Figure B. 57). Sample analysis was conducted following the previous procedures and while poor results were obtained with the lower temperatures, column temperatures of 50°C and 60°C produced a C<sub>3</sub>F<sub>8</sub> peak as illustrated in Figure 4.10 below.

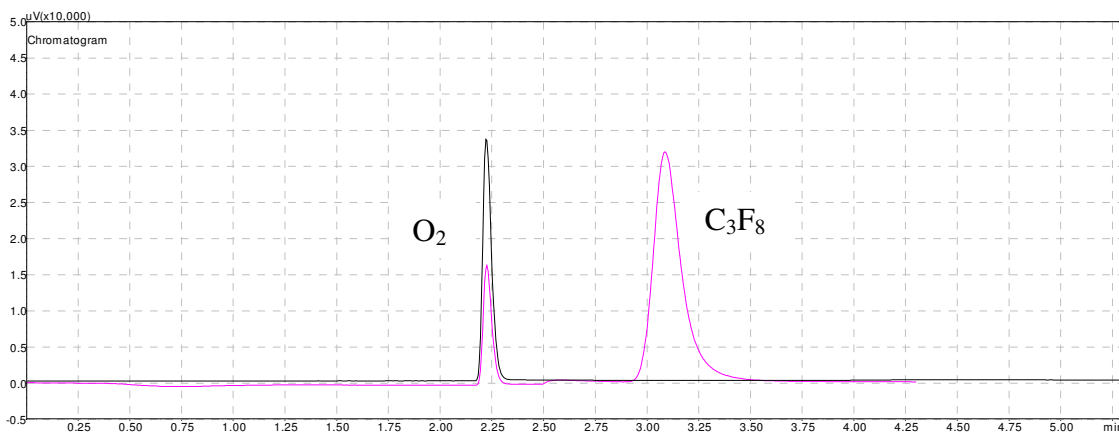


**Figure 4.10: Comparison of Syringe Blank (black line) and 10μL Injection of Pure C<sub>3</sub>F<sub>8</sub> (pink line) at 60°C**

1μL samples were taken from a 1% standard of SF<sub>6</sub> in nitrogen that was made inside of a 275mL glass bulb. These samples produced a large peak, but with better peak shape than previous experiments as indicated by Figure 4.11 below. The oxygen peak is very small in this figure, demonstrating the sensitivity of SF<sub>6</sub>. There is some minor peak tailing on the right side, which is another indicator that the sample could be too concentrated for the column.

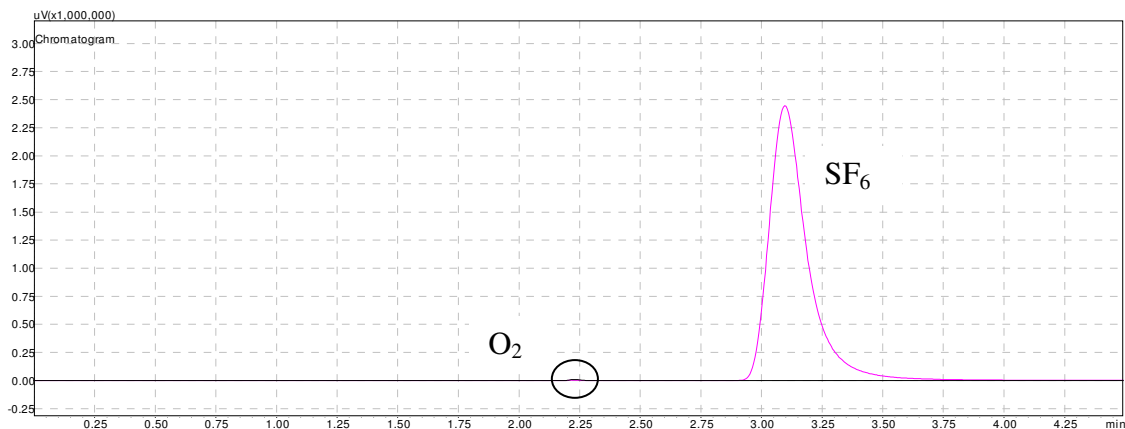


**Figure 4.11: Comparison of Syringe Blank (black line) and 1µL Injection of 1% SF<sub>6</sub> in N<sub>2</sub> (pink line) at 60°C**

Even though C<sub>3</sub>F<sub>8</sub> elutes with a Gaussian distribution on this column and has adequate separation from oxygen, it does not have adequate separation from SF<sub>6</sub> as pictured below in Figure 4.12. Since the C<sub>3</sub>F<sub>8</sub> peak lies below the SF<sub>6</sub> peak (blue peak), if a mixture of SF<sub>6</sub> and C<sub>3</sub>F<sub>8</sub> were injected, the two would not separate. Also, SF<sub>6</sub>, being highly sensitive, would overshadow the C<sub>3</sub>F<sub>8</sub> peak.

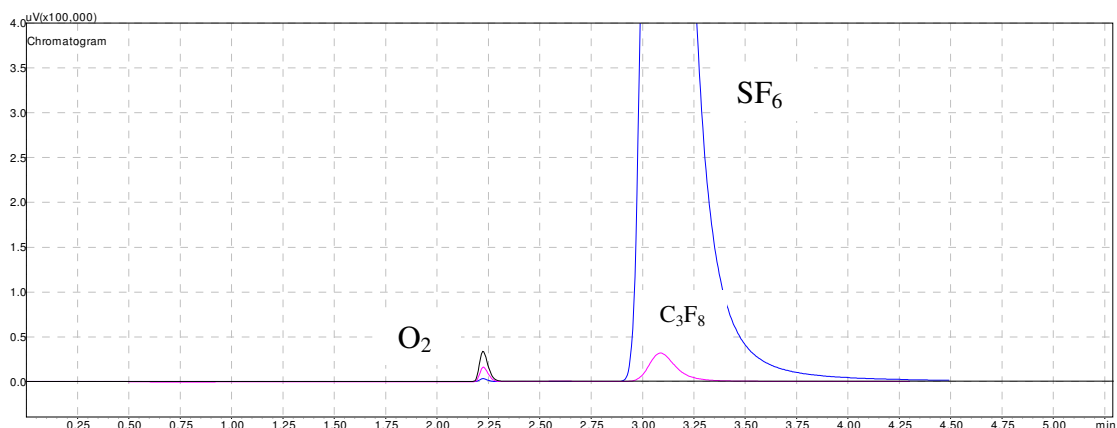


**Figure 4.12: Overlay of All Tracer Gases-Black=Syringe Blank; Pink=C3F8; Blue=SF6**

Furthermore, Table XXVII and Table XXVIII below summarize the average retention times and peak areas at various temperatures respectively. Noted here are again the similar retention times, and the difference in sensitivity between the two gases.

**Table XXVII: Average Retention Time of Gases on TG Bond Q Column**

Method		Average Retention Time ( $t_R$ )		
Name	Column Temperature	O <sub>2</sub>	SF <sub>6</sub>	C <sub>3</sub> F <sub>8</sub>
gas_sf6.gcm	40°C	2.24	3.88	3.88
gas_sf6.gcm	50°C	2.33	3.42	3.41
gas_sf6.gcm	60°C	2.30	3.10	3.09
cryo_method.gcm	20°C	2.27	5.74	5.70
cryo_method.gcm	0°C	2.27	10.6	no peak

**Table XXVIII: Average Peak Area of Gases on TG Bond Q Column**

Method		Average Peak Area	
Name	Column Temperature	SF <sub>6</sub>	C <sub>3</sub> F <sub>8</sub>
gas_sf6.gcm	40°C	7,260,000	3,880
gas_sf6.gcm	50°C	26,000,000	418,000
gas_sf6.gcm	60°C	25,600,000	334,000
cryo_method.gcm	20°C	4,500,000	1,960
cryo_method.gcm	0°C	3,700,000	no peak

Capacity factor ( $k$ ) values are given below in Table XXIX. When  $k$  is above one it indicates that the gases are well retained in the stationary phase (e.g. liquid phase of the column).

**Table XXIX: Capacity Factor Values of Gases on TG Bond Q Column**

Method		k-values		
Name	Column Temperature	O <sub>2</sub>	SF <sub>6</sub>	C <sub>3</sub> F <sub>8</sub>
gas_sf6.gcm	40°C	0.34	1.33	1.33
gas_sf6.gcm	50°C	0.40	1.05	1.04
gas_sf6.gcm	60°C	0.38	0.86	0.85
cryo_method.gcm	20°C	0.40	2.45	2.42
cryo_method.gcm	0°C	0.38	5.35	no peak

However, since the alpha values for SF<sub>6</sub> and C<sub>3</sub>F<sub>8</sub>, given in Table XXX below, are equal to one, the two cannot be separated.

**Table XXX: Selectivity Values of Gases on TG Bond Q Column**

Method		$\alpha$ values		
Name	Column Temperature	SF <sub>6</sub> & O <sub>2</sub>	C <sub>3</sub> F <sub>8</sub> & O <sub>2</sub>	SF <sub>6</sub> & C <sub>3</sub> F <sub>8</sub>
gas_sf6.gcm	40°C	3.86	3.87	1.00
gas_sf6.gcm	50°C	2.64	2.62	1.01
gas_sf6.gcm	60°C	2.26	2.24	1.01
cryo_method.gcm	20°C	6.81	6.74	1.01
cryo_method.gcm	0°C	14.9	no peak	no peak

Overall, the GC results improved with this column over the TG Bond Q+ column; however, C<sub>3</sub>F<sub>8</sub> and SF<sub>6</sub> have the same alpha value, indicating that separation of the two compounds is impossible under these conditions. Different syringes were used for injections so that it could be confirmed there wasn't SF<sub>6</sub> residue on syringes sampling C<sub>3</sub>F<sub>8</sub>. Syringe blanks were also run to ensure that syringes were clean prior to sampling, and therefore it can be confirmed that SF<sub>6</sub> and C<sub>3</sub>F<sub>8</sub> do have the same retention time, and it is not residue of the other tracer gas. Future experimentation was not conducted on this column, and CF<sub>4</sub> and C<sub>3</sub>F<sub>8</sub> were eliminated as potential tracer gases due to the consistently poor results obtained.

#### 4.6.5 PMCH Experiments Using HP-AL/S Column

Initial testing of PMCH indicated that a high column temperature was needed for the tracer to elute from the column. Early protocol called for an initial column temperature of 80°C, which was held for one minute, and then the column temperature was set to increase at a rate of 30°C per minute to 190°C, which was held for five minutes. Figure 4.13 below shows the results of the PMCH sample run under the above conditions. In this case, the pink line is the syringe blank, and the black line is a sample of 100ppm PMCH mixed in nitrogen.

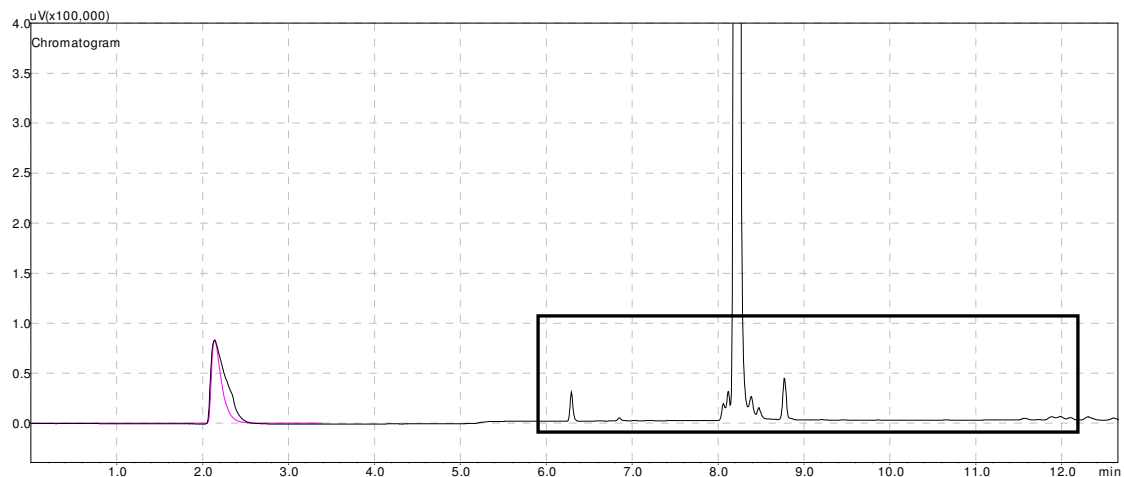


**Figure 4.13: Comparison of Syringe Blank (pink) with 1mL Injection of 100ppm PMCH in N<sub>2</sub> (black)**

Additionally, Figure 4.14 below shows the zoomed in area of the box in Figure 4.13 above. Though these peaks are small relative to the PMCH peak, it is necessary to adjust protocol to allow enough time for all of these components to elute from the column so that they do not remain in the column for subsequent runs. The components are a case of organic synthesis, increasing isomers with increasing molecular weight.

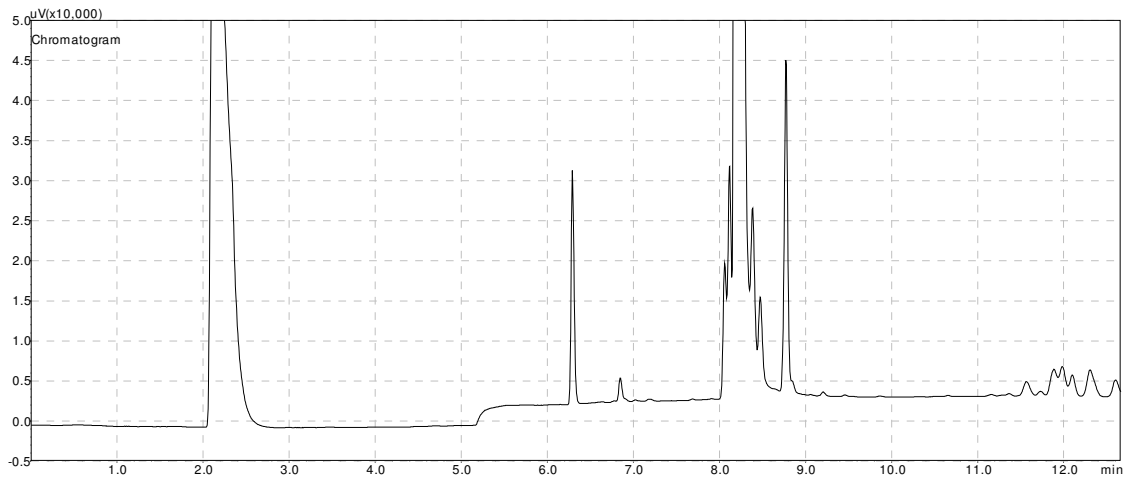


**Figure 4.14: Zoomed-in Version of Figure 4.13**

When SF<sub>6</sub> was run under the above conditions, baseline separation of SF<sub>6</sub> and oxygen was not achieved as shown below in Figure 4.15. Despite SF<sub>6</sub> having poor separation from oxygen, it has an entirely different retention time than that of PMCH. SF<sub>6</sub> has a retention time of approximately 2.4 minutes while the retention time of PMCH is above eight minutes.



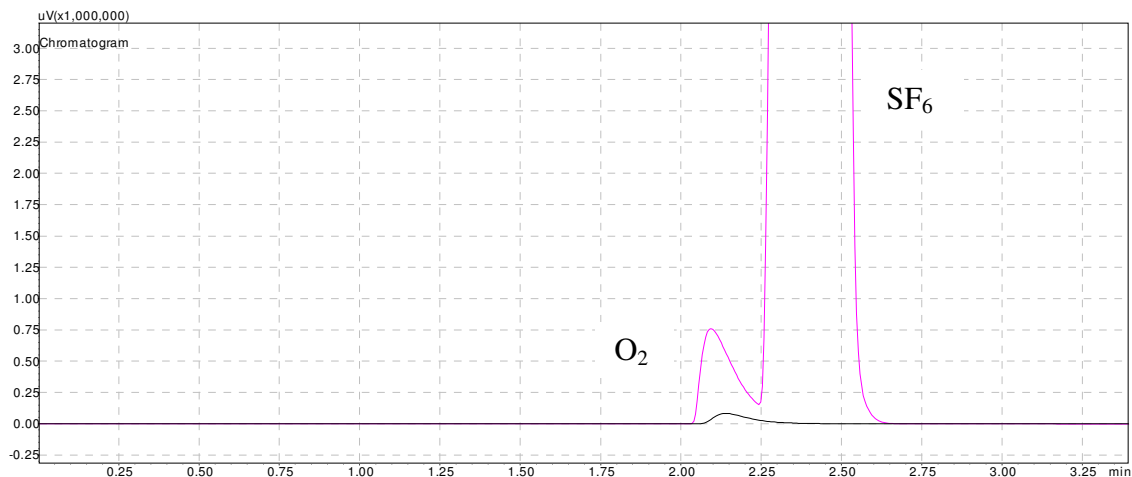


**Figure 4.15: Comparison of Syringe Blank (Black) with 1mL Injection of 100ppm SF<sub>6</sub> in N<sub>2</sub> (pink)**

Since PMCH and SF<sub>6</sub> have significantly different retention times, samples were run under different conditions to develop the final protocol that would be used to evaluate a mixture of the two tracers. The primary concern was to achieve baseline separation of oxygen and SF<sub>6</sub>. In an effort to do so, the initial column temperature was decreased to 65°C and held for three minutes to allow enough time for the SF<sub>6</sub> peak to elute before increasing the temperature. Following the three minute hold, the column temperature was ramped up at 100°C per minute to 175°C and the split ratio was adjusted from 10:1 to 50:1. The split ratio was modified to achieve better peak shape since both SF<sub>6</sub> and PMCH were highly sensitive on this column. As illustrated by Figure 4.16 below, baseline separation of oxygen and SF<sub>6</sub> was achieved.

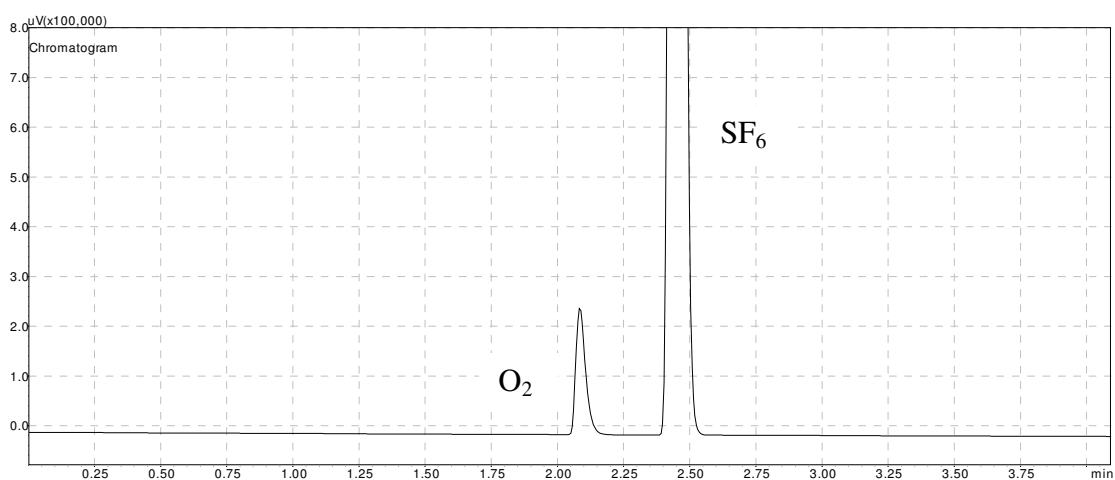


**Figure 4.16: 100ppm Sample of SF<sub>6</sub> in N<sub>2</sub> (65°C initial column temp, hold 3 minutes, ramp 100°C to 175°C)**

After establishing baseline separation of SF<sub>6</sub> and oxygen, a 100ppm mixture of SF<sub>6</sub> and PMCH in nitrogen was made to see if the two could be separated on the column. As seen in Figure 4.17 below, there is significant baseline separation between the two tracers.

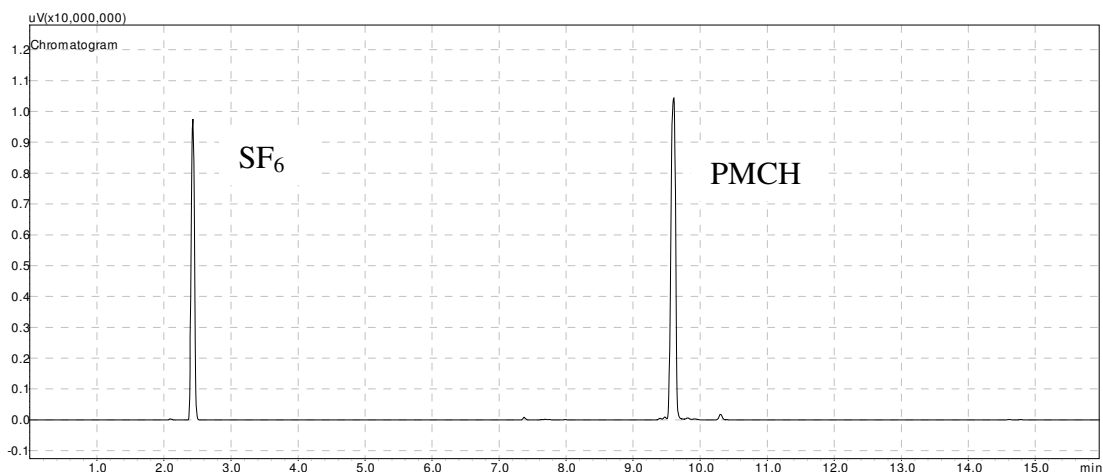


**Figure 4.17: 1mL Injection of a Sample of 100ppm SF<sub>6</sub> & PMCH in N<sub>2</sub>**

To establish a final protocol for separation of oxygen, SF<sub>6</sub>, and PMCH on this column, it was necessary to determine the optimal initial column temperature and the final hold time after the column temperature reached 180°C. This is important because various components of the PMCH have associated peaks as mentioned previously and shown in Figure 4.14. These peaks are small relative to the SF<sub>6</sub> and PMCH peaks as indicated by Figure 4.17 above, however, maintaining the high temperature for a set period of time will allow for all components to elute from the column. This ensures the column is clean before running another sample.

Three different initial column temperatures and three different hold times were tested to establish the final protocol. Initial column temperatures were set to 70°C, 65°C, and 67°C while hold times were set to 8:00, 15:00, and 12:30 minutes. The hold time was established first, by testing all three hold times at 70°C. It was determined that a 12 minute 30 second hold time was optimal to ensure all peaks eluted. Since PMCH has a high molecular weight, there are several trace impurities associated with this compound requiring a long hold time. Following this, initial column temperatures of 65°C and 67°C were tested. The average retention times and peak areas for the gases are shown below in Table XXXI and Table XXXII, respectively. It is apparent that oxygen, SF<sub>6</sub>, and PMCH each have their own unique retention time at each temperature and comparable sensitivity.

**Table XXXI: Average Retention Time of Gases on HP-AL/S Column**

Method		Average Retention Time ( $t_R$ )		
Name	Column Temperature	O <sub>2</sub>	SF <sub>6</sub>	PMCH
SF6 & PMCH protocol.gcm	70°C	2.09	2.43	9.61
SF6 & PMCH protocol.gcm	65°C	2.08	2.48	9.74
SF6 & PMCH protocol.gcm	67°C	2.07	2.44	9.69

**Table XXXII: Average Peak Area of Gases on HP-AL/S Column**

Method		Average Peak Area	
Name	Column Temperature	SF <sub>6</sub>	PMCH
SF6 & PMCH protocol.gcm	70°C	34,400,000	49,500,000
SF6 & PMCH protocol.gcm	65°C	61,800,000	79,700,000
SF6 & PMCH protocol.gcm	67°C	42,400,000	63,400,000

The k and alpha values are better indicators for which initial column temperature would be optimal. PMCH is well retained at every temperature. The primary concern is the alpha value indicated separation of SF<sub>6</sub> and O<sub>2</sub>. These values are given below in Table XXXIII and Table XXXIV.

**Table XXXIII: Capacity Factor Values for Gases on HP-AL/S Column**

Method		k-values		
Name	Column Temperature	O <sub>2</sub>	SF <sub>6</sub>	PMCH
SF6 & PMCH protocol.gcm	70°C	0.255	0.459	4.76
SF6 & PMCH protocol.gcm	65°C	0.248	0.491	4.84
SF6 & PMCH protocol.gcm	67°C	0.243	0.466	4.82

**Table XXXIV: Selectivity Values for Gases on HP-AL/S Column**

Method		$\alpha$ values		
Name	Column Temperature	SF <sub>6</sub> & O <sub>2</sub>	PMCH & O <sub>2</sub>	PMCH & SF <sub>6</sub>
SF6 & PMCH protocol.gcm	70°C	1.80	18.7	10.4
SF6 & PMCH protocol.gcm	65°C	1.98	19.5	9.86
SF6 & PMCH protocol.gcm	67°C	1.92	19.8	10.3

Though an initial column temperature of 65°C yields the highest alpha value, there are other important factors to consider. Equilibration time, or the time it takes for the gas chromatograph to cool down from 180°C to the initial column temperature, is necessary to note. Ideally, equilibration time should be minimized as it influences the total time necessary for one sample. Another sample cannot be injected until the machine equilibrates. Equilibration time for an initial column temperature of 65°C is longer than the equilibration time at 67°C and 70°C. Though an initial column temperature of 70°C has a shorter equilibration time than 67°C, the optimal initial column temperature is 67°C because it maximizes alpha while minimizing equilibration time. Equilibration time for an initial column temperature of 67°C is about 2 minutes. This brings the total run time per sample to 18 minutes. The final protocol, shown previously in Table XIV, produces the resulting chromatogram shown below in Figure 4.18.

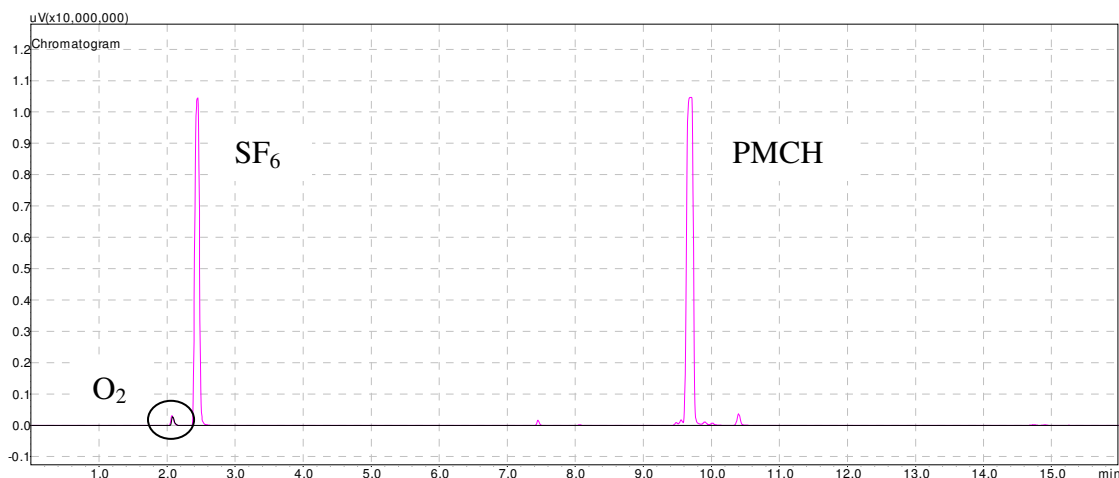


**Figure 4.18: 1mL Sample of 100ppm  $\text{SF}_6$  & PMCH in  $\text{N}_2$  Using Final GC Protocol**

This final protocol ensured adequate separation of  $\text{SF}_6$  from oxygen, and also allotted enough time for the column to clean out prior to the next sample run. This column is sufficient for separation of  $\text{SF}_6$  from the novel tracer, PMCH and the same protocol can be used for separating a mixture of the two tracers. Though total sample analysis time is around 18 minutes per sample, it is still practical because the two tracers can be separated on the same column following this protocol. This eliminates additional time that would be needed if each tracer required a varied protocol or a different column. Therefore, it has been determined that the HP-AL/S column is a good choice for separation of a mixture of  $\text{SF}_6$  and PMCH.

#### 4.7 Summary

CF<sub>4</sub> and C<sub>3</sub>F<sub>8</sub> were also tested on four different columns at various temperatures. Both tracers consistently produced poor results, if any. Additionally, these two tracers typically had close retention times to SF<sub>6</sub>, and therefore separation and quantification of peak area would be difficult. Furthermore, pure samples of 10μL of CF<sub>4</sub> and C<sub>3</sub>F<sub>8</sub> were far less sensitive with the ECD than pure samples of 1μL or even less of SF<sub>6</sub> which would make practical applications difficult especially when concentrations reach the ppb range in underground mines.

PMCH was tested on an HP-AL/S column under various conditions. PMCH has its own unique retention time from SF<sub>6</sub>, allowing for more experimentation for method development. Difficulties associated with this column and compound were achieving adequate separation of SF<sub>6</sub> from oxygen, and ensuring the contaminants of PMCH was removed from the column prior to the next sample run. A final protocol was established that produced baseline separation of SF<sub>6</sub> and oxygen. The runtime per sample is about 18 minutes including equilibration time. This long runtime is a weakness of the protocol when assessment of multiple samples containing a PMCH and SF<sub>6</sub> mixture is necessary. Additionally, PMCH is a liquid which will complicate fieldwork thus making establishing release methods and protocol important. It was determined that PMCH elutes when the column temperature reaches a temperature around 180°C, however, this particular column has a maximum temperature of 200°C. In order to ensure that the column remains intact, 180°C is the maximum temperature that should be set. Otherwise, increasing the temperature, could allow for a shorter hold time and a decreased sample runtime overall. This final protocol (Table XIV, pg. 38) is acceptable for running samples containing a mixture of SF<sub>6</sub> and PMCH.

## Chapter 5: Summary and Conclusion

Overall, initial steps to establishing best sampling methods have been completed. Currently, plastic syringes remain the optimal sampling method because they are sensitive, inexpensive, and easy to use. Further studies need to be conducted to determine the robustness of various sampling methods and if there is significant sample leakage during transportation and while waiting for samples to be analyzed. Though SPME fibers demonstrate low sensitivity to both SF<sub>6</sub> and PMCH, SPME fibers are still a relatively new technology. Additional studies can be conducted to determine an appropriate SPME fiber coating that will absorb SF<sub>6</sub> and PMCH. Not only can various coating types be evaluated, but various coating thicknesses can be tested as well. As there are more applications of SPME fibers in tracer gas studies, other fibers could be developed that are more sensitive to the aforementioned tracers. SPME could greatly enhance the ease and speed of the method making it more accessible to mining operations, but also to other industries including earth atmospheric sciences and indoor air quality control. SPME, in particular, is highly portable and accurate, if appropriate protocols and fiber coatings can be determined.

Furthermore, practicality of tracer gas analysis techniques is of utmost importance. Therefore, determining novel tracer gases that can be separated from SF<sub>6</sub> using the same gas chromatograph, detector, column, and protocol is vital. It is important to maintain accuracy and precision while reducing sample run time. Determining a column and establishing a GC protocol is time consuming and often is a result of trial and error. To establish one robust, user friendly analytical method two chromatographic parameters to consider are the capacity factor ( $k$ ) and separation factor ( $\alpha$ ). These values indicate how well an analyte is retained on the column and the degree of separation of two or more substances, respectively.

It has been determined that perfluoromethylcyclohexane (PMCH) can be used with sulfur hexafluoride (SF<sub>6</sub>) and experiments have shown that mixtures of PMCH and SF<sub>6</sub> can be separated by gas chromatography easily since  $\alpha$  is greater than two. A final protocol was established that has a sample run time of 16 minutes and an equilibration time of 2 minutes. It was necessary to establish a protocol for a SF<sub>6</sub> and PMCH mixture so that when the multiple tracer gas technique is applied to the characterization of ventilation controls, the retention times of these two tracers are known. This baseline will help to identify both tracers among the other peaks that might elute from mine air samples. Additionally, since the current protocol has a long hold time at a high temperature, it is already well suited for sample analysis via SPME fibers. SPME fibers typically need

column temperature programming and holding at a high temperature for quantitative analyte desorption.

Since there is limited literature comparing sampling techniques in the mining industry, the findings and conclusions gained from the sampling comparison study provide a benchmark for establishing optimal sampling practices for tracer gas techniques. This work also introduces SPME, a unique sampling technique to the mining industry, as a viable technique if an optimal fiber coating can be determined.

Additionally, the determination of a novel tracer gas that can be used with and separated from SF<sub>6</sub> using the same analytical method increases the practicality and robustness of multiple mine tracer gas techniques. There is limited work on multiple mine tracer gases, and the practicality of previous multiple mine tracer gases is limited due to background mine concentrations and specialized detectors. However, multiple mine tracer gases will increase the flexibility and speed of tracer gas surveys by eliminating the time needed for one tracer to flush out of the mine system and allowing for simultaneous injection of tracers at different points. Therefore, this robust, analytical method is well suited for the analysis of one sample containing a mixture of PMCH and SF<sub>6</sub>.

This initial work on sampling techniques and determination of a novel tracer will contribute to the larger project scope of determining a methodology for the remote characterization of mine ventilation systems through utilizing multiple mine tracer gases and CFD. This will be completed through several phases including initial laboratory testing of novel tracer gases in a model mine apparatus to develop a methodology for releasing, sampling, and modeling a mine ventilation plan and tracer gas dispersion in CFD, completing field trials to validate and enhance the multiple tracer gas methodology, and finally information dissemination for the wide scale application of multiple mine tracer gas techniques.

Future work includes developing a release or injection methodology for both tracers. Mass flow controllers designed and calibrated for SF<sub>6</sub>, can accurately release a known quantity of SF<sub>6</sub>. Also, permeation tubes can be another release mechanism utilized to accurately release a known quantity of gas or vapor. Permeation tubes are small devices that, when held at a constant temperature, can ensure a constant rate of sample diffusion through its membrane. These devices can be easily calibrated to release both SF<sub>6</sub> and PMCH. This methodology can first be developed by utilizing the model mine apparatus and validating it through gas chromatography and CFD modeling.

Perfluoromethylcyclopentane (PMCP) could be another viable tracer for multiple tracer gas applications as it has similar properties to PMCH, but has a lower molecular weight and therefore, theoretically, would elute between SF<sub>6</sub> and PMCH. The compounds with a lower molecular weight would also have fewer trace impurities which could reduce the hold time necessary for column and SPME fiber cleaning. This would provide an opportunity to achieve a shorter sample analysis time. Perfluorodimethylcyclohexane (PDCH) could also be tested as a fourth tracer, if needed, but would theoretically have a longer analysis time than PMCH and more trace impurities since it has a higher molecular weight.

Finally, tracer gas techniques will continually improve in the future. As mass flow controllers and remote sensing techniques become more precise and affordable, instrumentation of a mine for automatic remote tracer gas surveys will be possible. This will allow engineers to evaluate the state of the ventilation system quickly, and without cumbersome sampling and analysis techniques.



## References

- [1] J.F. Brune, K.L. Cashdollar, and R.K. Zipf, "Explosion Prevention in United States Coal Mines," *Explosion*.
- [2] R.S. Suglo and S. Frimpong, "Accuracy of tracer gas surveys in auxiliary ventilation systems in coal mines," *Mine Ventilation*, 2002, pp. 168-175.
- [3] Z.B. Alfassi, *Determination of Trace Elements*, Rehovot: Balaban Publishers, 1994.
- [4] O. Huhn, W. Roether, P. Beining, and H. Rose, "Validity limits of carbon tetrachloride as an ocean tracer," *Deep Sea Research Part I: Oceanographic Research Papers*, vol. 48, Aug. 2001, pp. 2025-2049.
- [5] A. Machmuller and R. Hegarty, "Alternative tracer gases for the ERUCT technique to estimate methane emission from grazing animals," *International Congress Series*, vol. 1293, Jul. 2006, pp. 50-53.
- [6] N. Salhani, "A comparative study of the gas exchange potential between three wetland species using sulfur hexafluoride as a tracer," *Ecological Engineering*, vol. 18, Oct. 2001, pp. 15-22.
- [7] B. Han, B. Jafarpour, V.N. Gallagher, P.T. Imhoff, P.C. Chiu, and D. a Fluman, "Measuring seasonal variations of moisture in a landfill with the partitioning gas tracer test.," *Waste management (New York, N.Y.)*, vol. 26, Jan. 2006, pp. 344-55.
- [8] R.J. Wilcock, "Methyl chloride as a gas-tracer for measuring stream reaeration coefficients-II," *Soil Science*, vol. 18, 1984, pp. 53-57.
- [9] M. Adams, "Hydrofluorocarbons as geothermal vapor-phase tracers," *Geothermics*, vol. 30, Dec. 2001, pp. 747-775.
- [10] J. Clark, M. Davisson, G. Hudson, and P. Macfarlane, "Noble gases, stable isotopes, and radiocarbon as tracers of flow in the Dakota aquifer, Colorado and Kansas," *Journal of Hydrology*, vol. 211, Nov. 1998, pp. 151-167.
- [11] N.D. Malcosky and G. Koziar, "Gas Tracer Composition and Method," , 1985.
- [12] R. Kleven, O. Hovring, S.T. Opdal, S. Norway, T. Bjornstad, O. Dugstad, and I.A. Hundere, "Non-Radioactive Tracing Of Injection Gas In Reservoirs," *Gas Technology Conference*, Calgary: 1996.
- [13] S.D. McCallum, D.E. Riestenberg, D.R. Cole, B.M. Freifeld, R.C. Trautz, S.D. Hovorka, and T.J. Phelps, "Monitoring Geologically Sequestered CO<sub>2</sub> during the

- Frio Brine Pilot Test using Perfluorocarbon Tracers,” *Fourth Annual Conference On Carbon Capture And Sequestration DOE/NETL*, Alexandria: 2005.
- [14] S. Laporte, “A comparative study of two tracer gases: SF<sub>6</sub> and N<sub>2</sub>O,” *Building and Environment*, vol. 36, Apr. 2001, pp. 313-320.
- [15] M. Sandberg and C. Blomqvist, “A quantitative estimate of the accuracy of tracer gas methods for the determination of the ventilation flow rate in buildings,” *Building and Environment*, vol. 20, 1985, pp. 139-150.
- [16] S. Fanson, “Air flow measurement using three tracer gases,” *Building and Environment*, vol. 17, 1982, pp. 245-252.
- [17] H. Okuyama, Y. Onishi, S. Tanabe, and S. Kashihara, “Statistical data analysis method for multi-zonal airflow measurement using multiple kinds of perfluorocarbon tracer gas,” *Building and Environment*, vol. 44, Mar. 2009, pp. 546-557.
- [18] T. Lim, J. Cho, and B.S. Kim, “The predictions of infection risk of indoor airborne transmission of diseases in high-rise hospitals: Tracer gas simulation,” *Energy and Buildings*, vol. 42, Aug. 2010, pp. 1172-1181.
- [19] M.J. McPherson, “Subsurface Ventilation Engineering,” *Organization*, 1993.
- [20] J. Higgins and E.H. Shuttleworth, “A tracer gas technique for the measurement of airflow in headings,” *Colliery Engineering*, vol. 35, 1958, pp. 413-418.
- [21] E.D. Thimons, R.J. Bielicki, and F.N. Kissell, *Using sulfur hexafluoride as a gaseous tracer to study ventilation systems in mines*, Pittsburgh, PA: BM-RI-7916, Bureau of Mines, Washington, DC (USA), 1974.
- [22] D.J. Kennedy, A.W. Stokes, and W.G. Klinowski, “Resolving Complex Mine Ventilation Problems with Multiple Tracer Gases,” *3rd Mine Ventilation Symposium*, 1987.
- [23] R.P. Vinson, F.N. Kissell, and B.O. Mines, “Report of Investigations 8142: Three Coal Mine Ventilation Studies Using Sulfur Hexafluoride Tracer Gas,” 1976, p. 19.
- [24] R.J. Timko, F.N. Kissell, and E.D. Thimons, “Evaluating ventilation parameters of three coal mine gobs,” 1986.
- [25] W.G. Klinowski and D.J. Kennedy, “Tracer gas techniques used in mine ventilation,” *Proc. of the 5th US Mine Ventilation Symposium*, Morgantown: 1991, pp. 1-5.

- [26] G. Arpa, K. Sasaki, and Y. Sugai, "Narrow vein shrinkage stope ventilation measurement using tracer gas and numerical simulation," *12th U.S./North American Mine Ventilation Symposium*, K. Wallace, ed., Reno: 2008, pp. 261-266.
- [27] A. Stokes, D. Kennedy, and S. Hardcastle, "A real-time tracer gas analyzer—an investigational tool for mine ventilation studies," *Mining Science and Technology*, vol. 5, Jul. 1987, pp. 187-196.
- [28] J.E. Matta, E.D. Thimons, and F.N. Kissell, *Jet Fan Effectiveness as Measured With SF6 Tracer Gas*, Washington, DC (USA): 1978.
- [29] F. Kissell, R. Jurani, R. Dresel, and C. Parker, "Silica dust control in hard rock tunnels," *Rapid Excavation and Tunneling Conference*, Las Vegas: Society for Mining, Metallurgy, and Exploration, 1999, pp. 241-247.
- [30] A.B. Cecala, G.W. Klinowski, and E.D. Thimons, *Reducing Respirable Dust Concentrations at Mineral Processing Facilities Using Total Mill Ventilation Systems*, Washington, DC (USA): 1993.
- [31] V.K. Singh, "Air leakage through underground ventilation stoppings and in situ assessment of air leakage characteristics of remote filled cement concrete plug by tracer gas technique," 2004, pp. 101-106.
- [32] F.N. Kissell and R.J. Bielicki, *Ventilation Eddy Zones at a Model Coal Mine Working Face*, Washington, DC (USA): 1974.
- [33] E.D. Thimons and C.E. Brechtel, "Measurement and Simulation of Face Ventilation Effectiveness for Large Diesel Powered Equipment," *3rd Mine Ventilation Symposium*, 1987.
- [34] J.E. Matta, S.D. Maksimovic, and F.N. Kissell, *Tracer Gas Method for Measuring Leakage Through Mine Stoppings*, Washington, DC (USA): 1978.
- [35] R.E.J. Ray, J.W. Stevenson, J.A. Berry, and R.J. Timko, "Design of permanent block stopping to resist strata convergence," *AIME Transactions*, vol. 278, 1985, pp. 1308-1312.
- [36] J.F.T. Thimons, Edward D.; Brechtel, Carl E.; Adam, Marvin E.; Agapito, *Leakage and Performance Characteristics of Large Stoppings for Room-and-Pillar Mining*, Sp: 1988.
- [37] E.D. Adam, M.E.; Brechtel, C.E.; Agapito, J.F.T.; Thimons, "Leakage Testing of Large Ventilation Control Structures for Room and Pillar Oil Shale Mining," *3rd Mine Ventilation Symposium*, J.M. Mutmanky, ed., University Park: Society Of

- Mining Engineers Of AIME Underground Ventilation Committee, 1987, pp. 365-370.
- [38] P. Buchwald and Z. Jaskólski, "Application of the SF<sub>6</sub> tracer gas in identifying mine air flows through abandoned workings sealed from the ventilation system," *Group*, 2004, pp. 169-178.
- [39] R.J. Timko and R.L. Derick, "Evaluating gas exchange from sealed areas in underground coal mines," *5th US Mine Ventilation Symposium*, Y.J. Wang, ed., Morgantown: 1991, pp. 168-176.
- [40] T.P. Mucho, W.P. Diamond, F. Garcia, J.D. Byars, and S.L. Cario, "Implications of Recent NIOSH Tracer Gas Studies on Bleeder and Gob Gas Ventilation Design."
- [41] R. Balusu, S. Kue, M. Wendt, C. Mallett, B. Robertson, R. Holland, R. Moreby, D. Mclean, and G. Deguchi, "An investigation of the gas flow mechanics in longwall goafs," Kingston: Taylor & Francis, 2002.
- [42] A.M. Wala, J.D. Robertson, and B. Ni, "Development of a radioactive tracer method for mine ventilation study," *Society for Mining , Metallurgy, and Exploration*, vol. 302, 1998, pp. 87-93.
- [43] B.F.N. Kissell and R.J. Bielicki, *Methane Buildup Hazards Caused by Dust Scrubber Recirculation at Coal Mine Working Faces , A Preliminary Estimate*, Washington, DC (USA): 1975.
- [44] E.D. Vinson, Robert P.; Kissell, Fred N.; LaScola, John C.; Thimons, *Face Ventilation Measurement With Sulfur Hexafluoride (SF<sub>6</sub>)*, Pittsburgh, PA: 1980.
- [45] G.V.R. Goodman, C.D. Taylor, and E.D. Thimons, *Jet Fan Ventilation in Very Deep Cuts-A Preliminary Analysis*, Spokane: 1992.
- [46] J.C. Volkwein, S.K. Ruggieri, C. Mcglathlin, and F.N. Kissell, *Exhaust ventilation of deep cuts using a continuous-mining machine*, 1985.
- [47] J. Organiscak and T. Beck, "Continuous miner spray considerations for optimizing scrubber performance in exhaust ventilation systems," *SME Annual Meeting*, Phoenix: 2010.
- [48] J.C. Lascola, J.E. Matta, and F.N. Kissell, *Assessing the methane hazard of gassy coals in storage silos*, 1981.
- [49] R.J. Timko and R.L. Derick, "Determining the integrity of escapeways during a simulated fire in an underground coal mine," *4th US Mine Ventilation Symposium*, M.J. McPherson, ed., Berkeley: 1989, pp. 48-56.

- [50] J.E. Urosek and T.R. Watkins, "Gob Ventilation and Bleeder Systems in US Coal Mines," *the 7th US Mine Ventilation Symposium*, 1995.
- [51] S.J. Page and S.D. Maksimovic, "Transport of respirable dust from overburden drilling at surface coal mines," *3rd Mine Ventilation Symposium*, J.M. Mutmanskiy, ed., University Park: Society Of Mining Engineers Of AIME Underground Ventilation Committee, 1987, pp. 625-629.
- [52] R.J. Timko and E.D. Thimons, *Sulfur hexafluoride as a mine ventilation research tool-Recent field applications*, Washington, DC (USA): 1982.
- [53] G.W. Klinowski and D.J. Kennedy, "Tracer Gas Based Evaluation of the Auxiliary Ventilation System," *4th Mine Ventilation Symposium*, Berkeley: 1989, pp. 123-127.
- [54] W.P. Diamond, S.J. Schatzel, F. Garcia, J.C. LaScola, F.E. McCall, P.W. Jeran, and T.P. Mucho, "Characterization of gas flow in longwall gobs: Pittsburgh coalbed, PA," *Safety And Health*, pp. 1-12.
- [55] W.H. Freedman, Robert W.; Ferber, Benjamin I.; Duerr, *Gas-Sampling Capability of Vacutainers*, Washington, DC (USA): 1978.
- [56] B.R.P. Vinson, F.N. Kissell, and R. P, *A Spiral Sequential Sampler for Air and Liquids Preliminary Results*, Washington, DC (USA): 1976.
- [57] S. Van Buggenhout, a Van Brecht, S. Eren Özcan, E. Vranken, W. Van Malcot, and D. Berckmans, "Influence of sampling positions on accuracy of tracer gas measurements in ventilated spaces," *Biosystems Engineering*, vol. 104, Oct. 2009, pp. 216-223.
- [58] M. Chai and J. Pawliszyn, "Analysis of Environmental Air Samples by Solid-Phase Microextraction and Gas Chromatography/Ion Trap Mass Spectrometry," *Environmental Science & Technology*, vol. 29, Mar. 1995, pp. 693-701.
- [59] J. Song, B.D. Gardner, J.F. Holland, and R.M. Beaudry, "Rapid Analysis of Volatile Flavor Compounds in Apple Fruit Using SPME and GC/Time-of-Flight Mass Spectrometry," *Journal of Agricultural and Food Chemistry*, vol. 45, May. 1997, pp. 1801-1807.
- [60] J. a Koziel, J. Noah, and J. Pawliszyn, "Field sampling and determination of formaldehyde in indoor air with solid-phase microextraction and on-fiber derivatization.," *Environmental science & technology*, vol. 35, Apr. 2001, pp. 1481-6.

- [61] M. Hippelein, "Analysing selected VVOCs in indoor air with solid phase microextraction (SPME): a case study.," *Chemosphere*, vol. 65, Oct. 2006, pp. 271-7.
- [62] J.A. Koziel and I. Novak, "Sampling and sample-preparation strategies based on solid-phase microextraction for analysis of indoor air," *Trends in Analytical Chemistry*, vol. 21, 2002, pp. 840-850.
- [63] F. Augusto, J. Koziel, and J. Pawliszyn, "Design and validation of portable SPME devices for rapid field air sampling and diffusion-based calibration.," *Analytical chemistry*, vol. 73, Feb. 2001, pp. 481-6.
- [64] R. Patterson, K. Jackson, K. Luxbacher, H. McNair, and R. Boggess, "A Comparison Of Well-Accepted Tracer Gas Sampling Methods Utilized In Underground Mines With Solid-Phase Microextraction (SPME) Fibers Through Laboratory Testing Of Sulfur Hexafluoride," *Society for Mining , Metallurgy, and Exploration*, Denver, CO: 2011.
- [65] H.M. McNair and E.J. Bonelli, *Basic Gas Chromatography*, Berkeley: Consolidated Printers, 1969.
- [66] A. Dietrich, "Dietrich, CEE 5184 Class Notes."
- [67] I. Ferrante and M. Bergna, "Ultra Trace Detection of Perfluorocarbon Tracers by Means of a Thermal Desorption-Gas Chromatography-Electron Capture Detector (TD-GC-ECD) System," 2010.

## Appendix A: Chromatograms of Sampling Technique Comparison

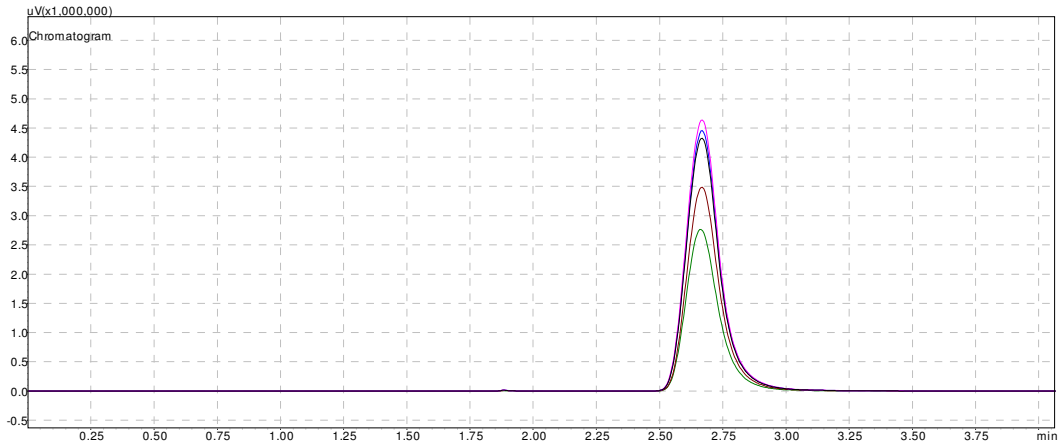


Figure A. 1: Overlay of 5 Glass Syringe Sample Runs

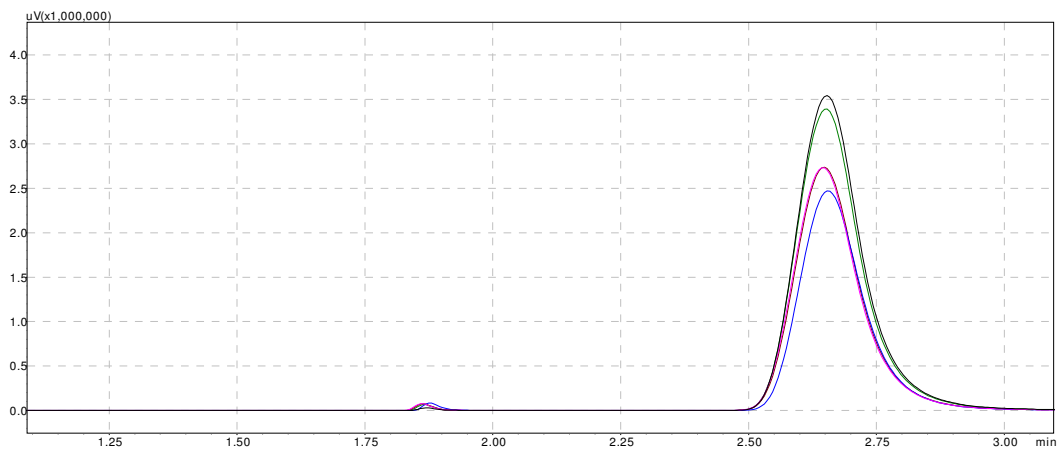


Figure A. 2: Overlay of 5 Plastic Syringe Sample Runs

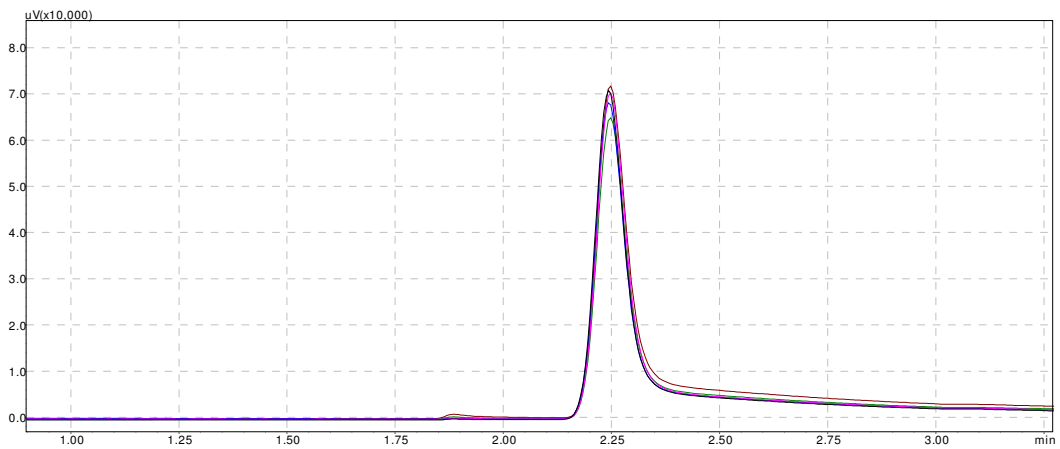
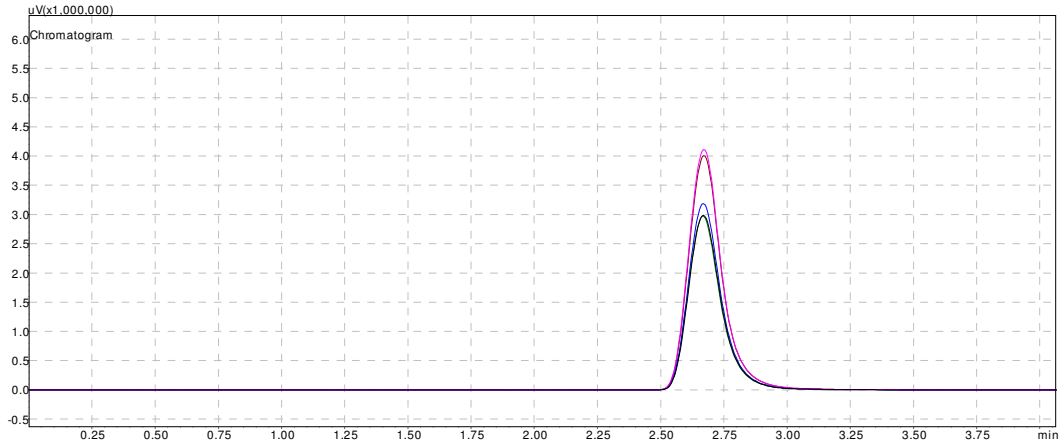
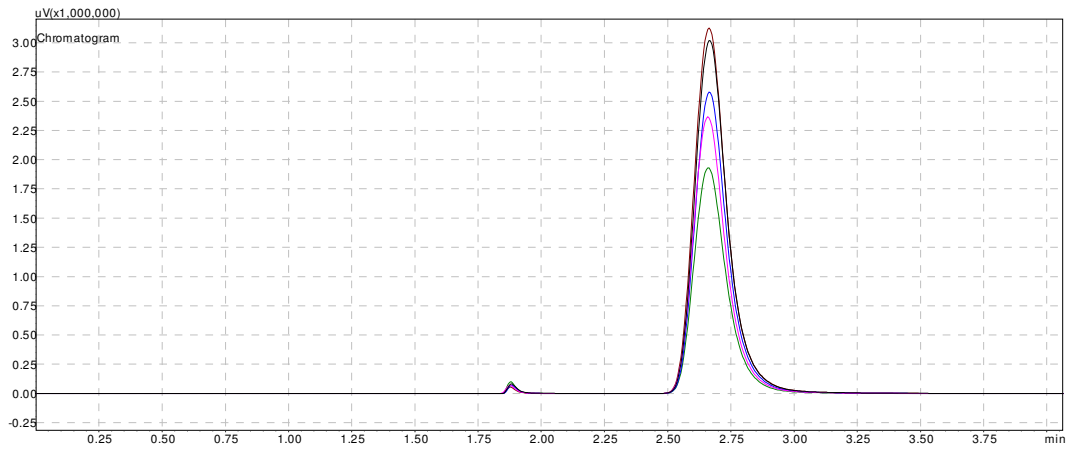


Figure A. 3: Overlay of 5 SPME Sample Runs



**Figure A. 4: Overlay of 5 Tedlar Bag/Glass Syringe Sample Runs**



**Figure A. 5: Overlay of 5 Tedlar Bag/Plastic Syringe Sample Runs**

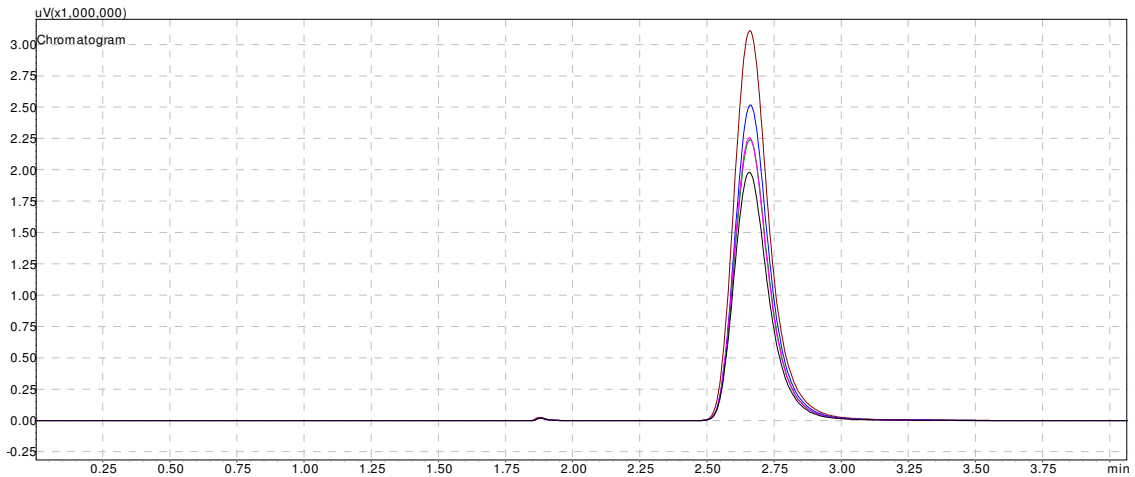


**Figure A. 6: Overlay of 5 Vacutainer/Glass Syringe Sample Runs**



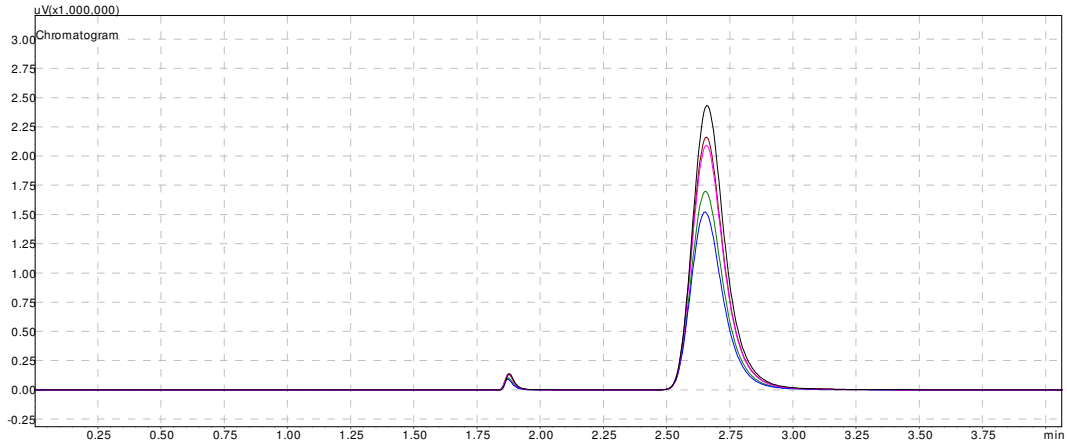


**Figure A. 7: Overlay of 5 Vacutainer/Plastic Syringe Sample Runs**

## Appendix B: Chromatograms of Novel Tracer Gas Testing

Chromatograms from samples run on the SBP-1 Sulfur column utilizing the gas\_sf6.gcm method with a 40°C column.

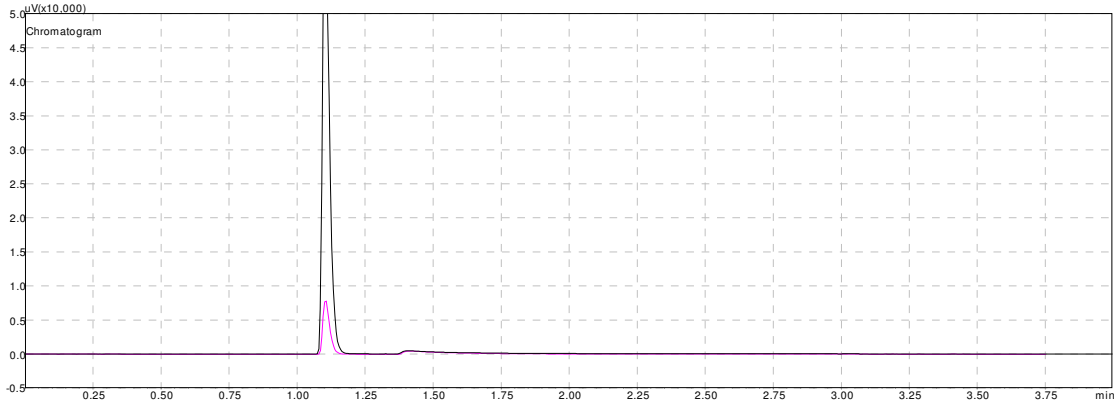


Figure B. 1: Comparison of Oxygen Peak (black line) with 10  $\mu\text{L}$  Pure Injection of  $\text{CF}_4$  (pink line)

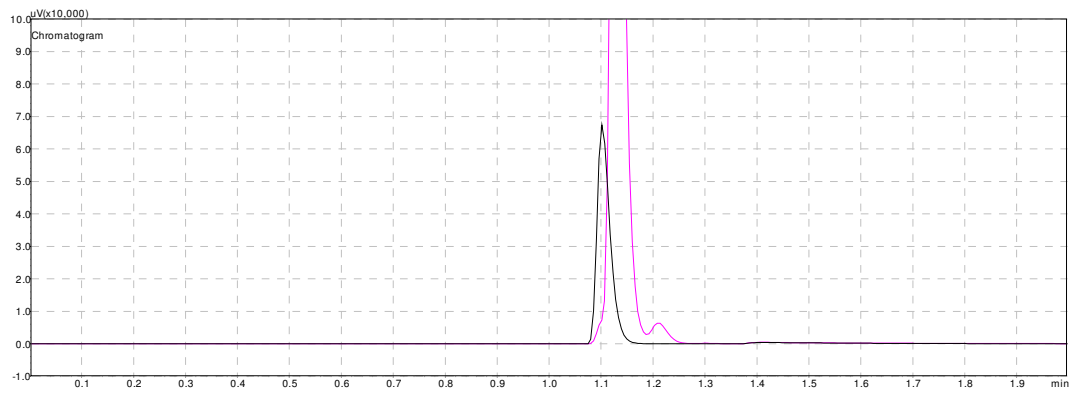


Figure B. 2: Comparison of Oxygen Peak (black line) with 10  $\mu\text{L}$  Pure Injection of  $\text{C}_3\text{F}_8$  (pink line)

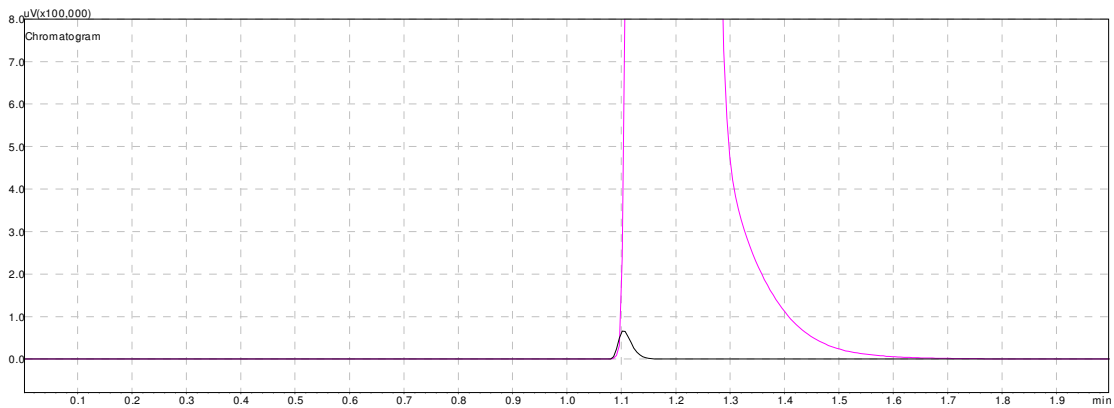
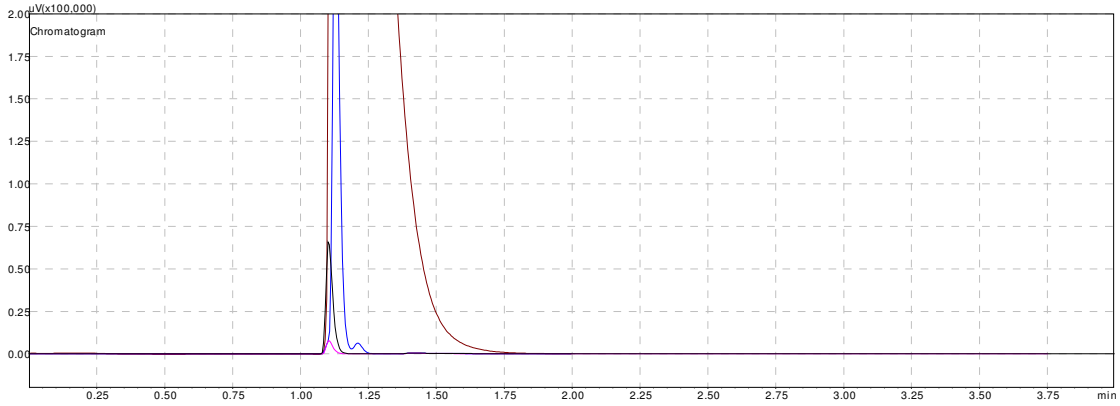
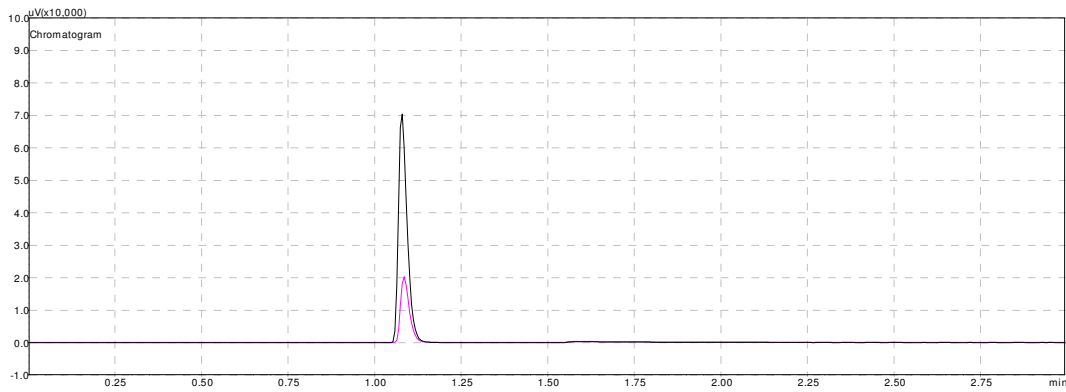


Figure B. 3: Comparison of Oxygen Peak (black line) with 5  $\mu\text{L}$  Pure Injection of  $\text{SF}_6$  (pink line)



**Figure B. 4: Overlay of All Tracer Gases-Black=Syringe Blank;Pink=CF<sub>4</sub>;Blue=C<sub>3</sub>F<sub>8</sub>; Brown=SF<sub>6</sub>**

Chromatograms from samples run on the SBP-1 Sulfur column utilizing the cyro\_method1.gcm method with a 20°C column.



**Figure B. 5: Comparison of Oxygen Peak (black line) with 10μL Pure Injection of CF<sub>4</sub> (pink line)**

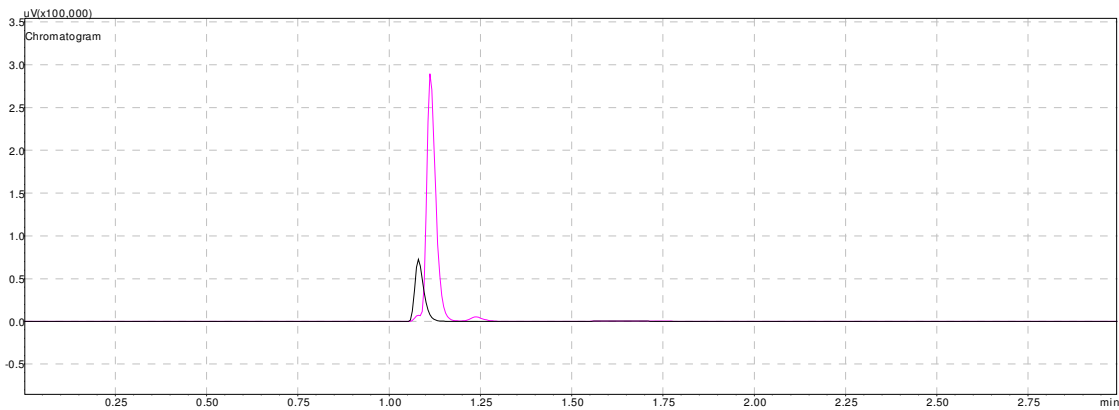


**Figure B. 6: Comparison of Oxygen Peak (black line) with 10μL Pure Injection of C<sub>3</sub>F<sub>8</sub> (pink line)**

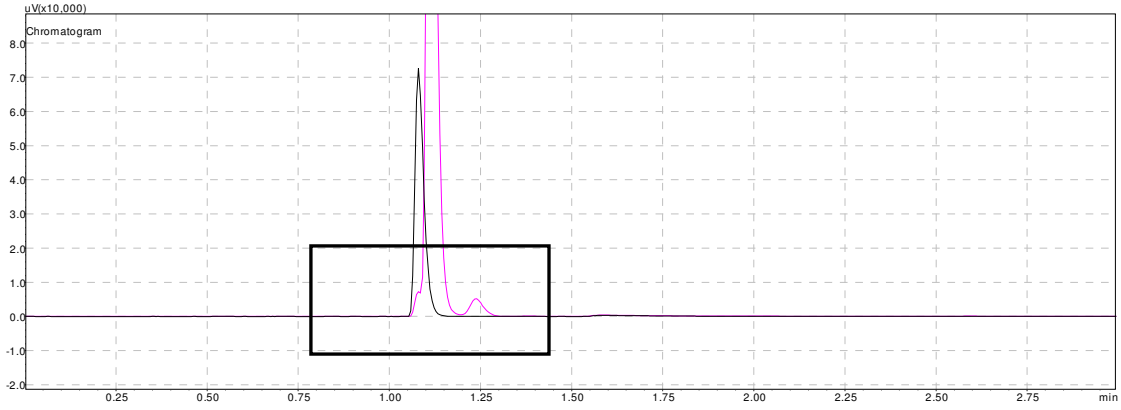


**Figure B. 7: Figure B.6 zoomed in uV x10,000**

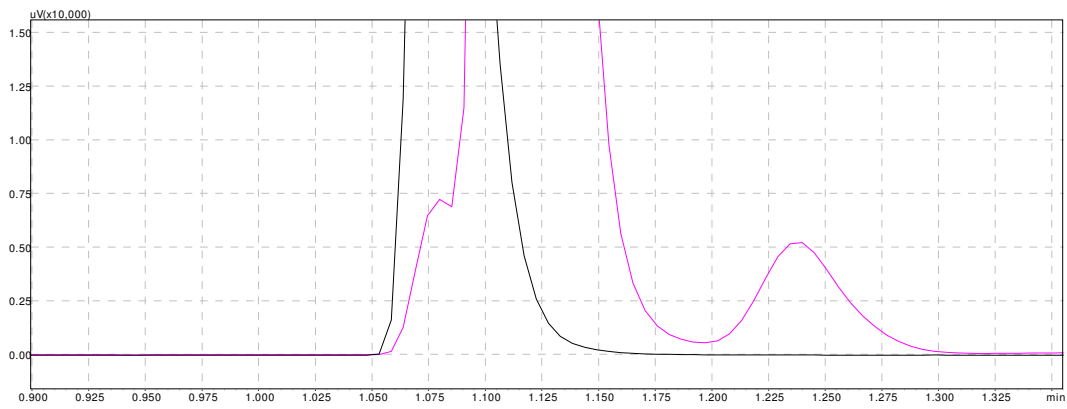


**Figure B. 8: Magnified area of box in Figure B.7**

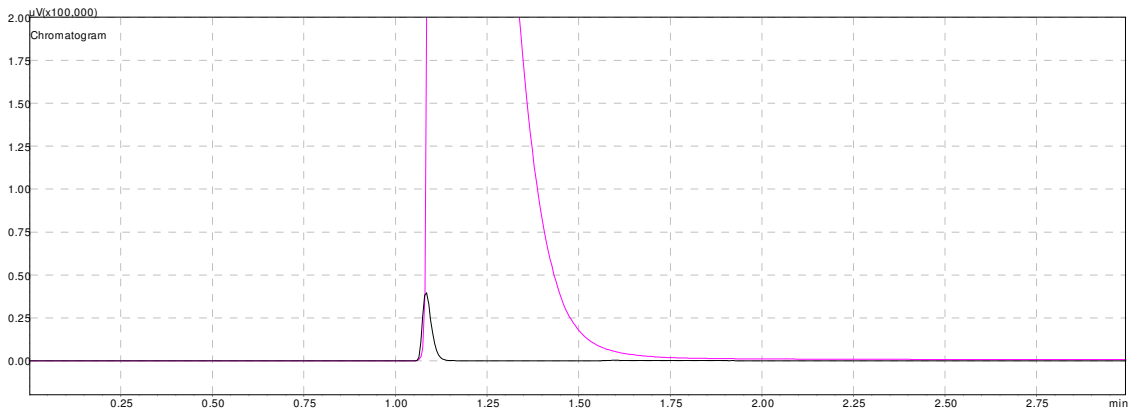


**Figure B. 9: Comparison of Oxygen Peak (black line) with 1µL Pure Injection of SF<sub>6</sub> (pink line)**

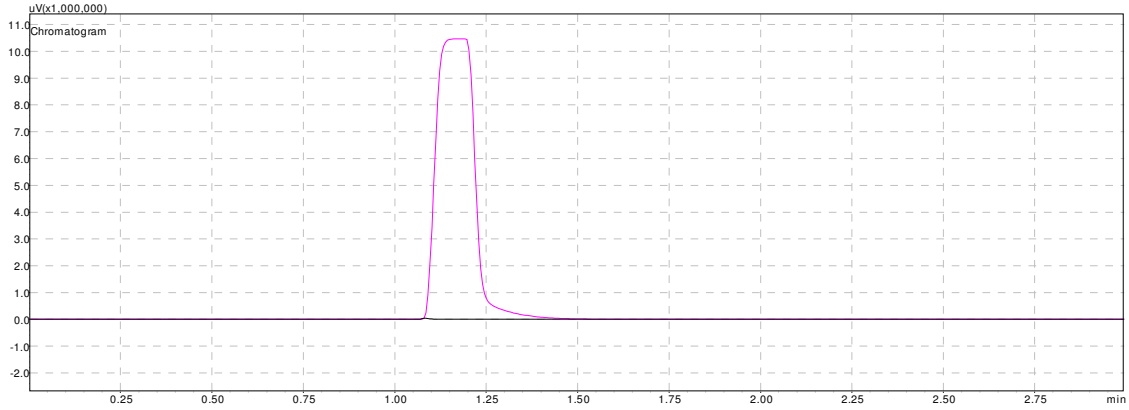


**Figure B. 10: Zoomed-Out Version of Figure B.9 (uVx1,000,000); Indicates SF<sub>6</sub> is overloading column**

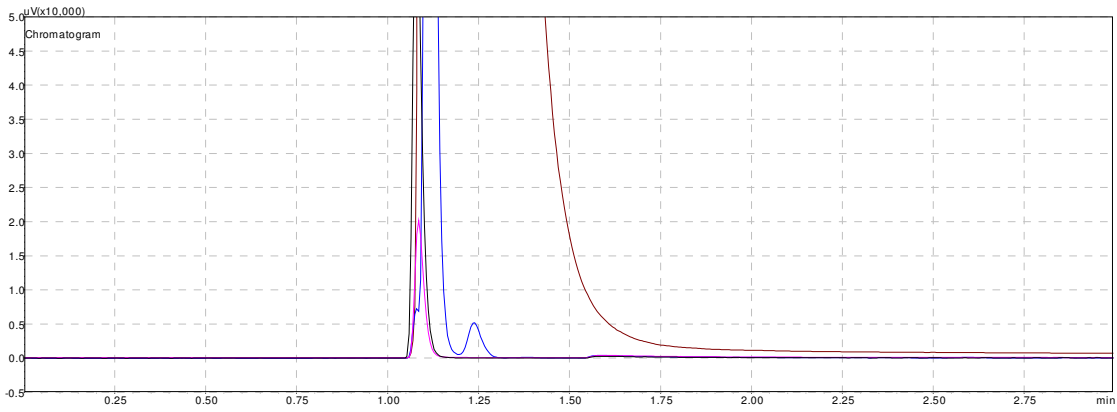


**Figure B. 11: Overlay of All Tracer Gases-Black=Syringe Blank;Pink=CF<sub>4</sub>;Blue=C<sub>3</sub>F<sub>8</sub>; Brown=SF<sub>6</sub>**

Chromatograms from samples run on the ZB-624 column utilizing the gas\_sf6.gcm method with a 40°C column.



**Figure B. 12: Comparison of Oxygen Peak (black line) with 10µL Pure Injection of CF<sub>4</sub> (pink line)**



**Figure B. 13: Zoomed-in version of Figure B.12 (uVx1,000); Shows potential CF<sub>4</sub> peak-very broad**

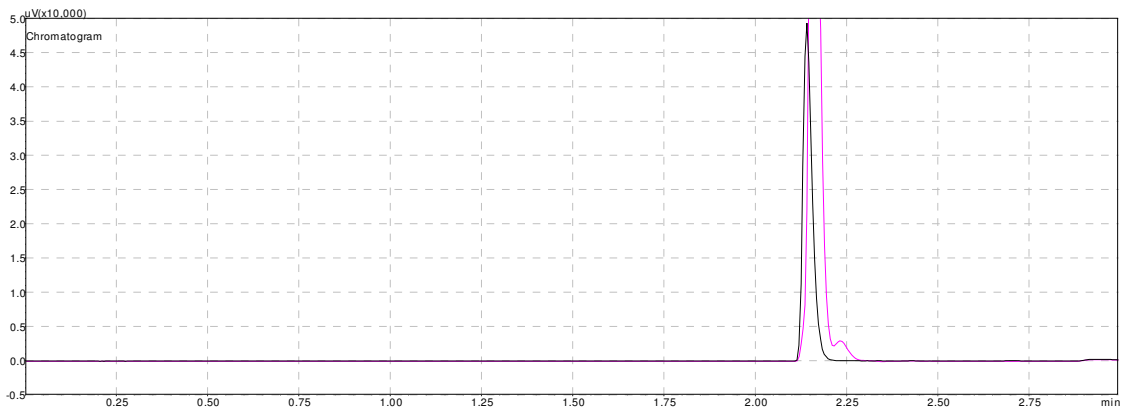


**Figure B. 14: Comparison of Oxygen Peak (black line) with 10µL Pure Injection of C<sub>3</sub>F<sub>8</sub> (pink line)**

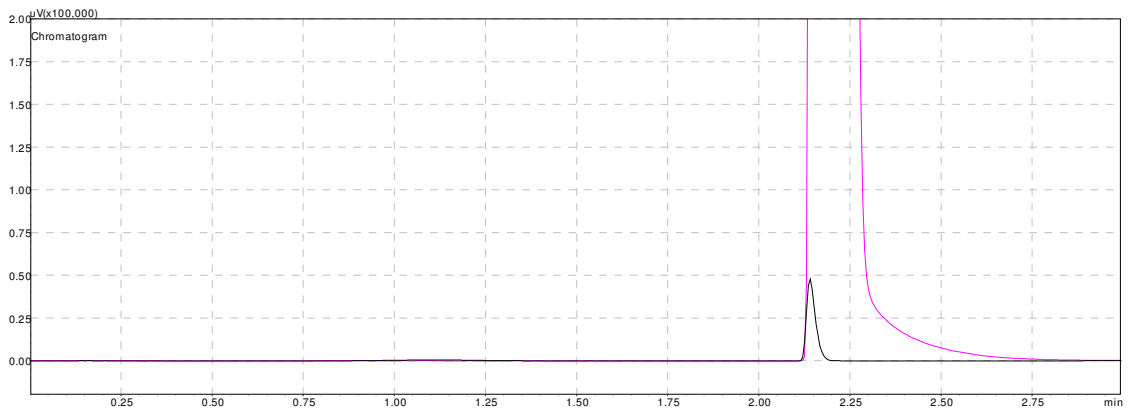


**Figure B. 15: Comparison of Oxygen Peak (black line) with 1µL Pure Injection of SF<sub>6</sub> (pink line)**

Chromatograms from samples run on the ZB-624 column utilizing the cyro\_method1.gcm method with a 20°C column.

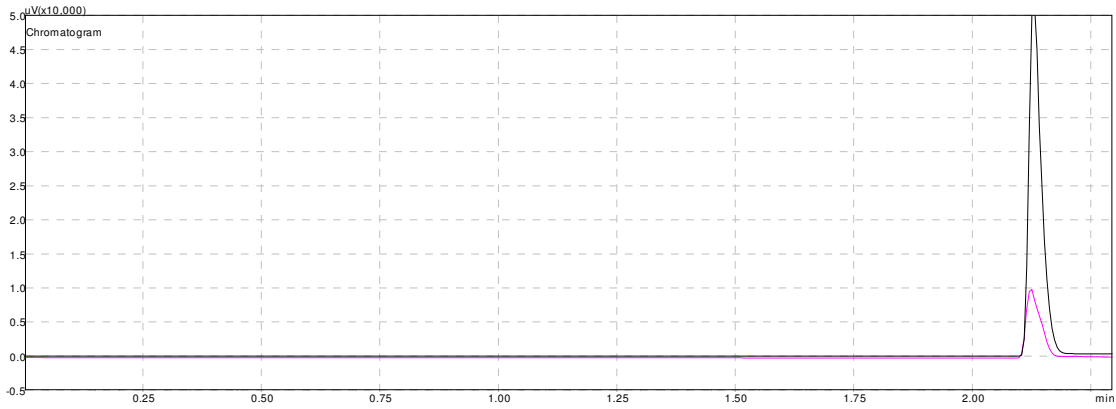


Figure B. 16: Comparison of Oxygen Peak (black line) with 10µL Pure Injection of CF<sub>4</sub> (pink line)

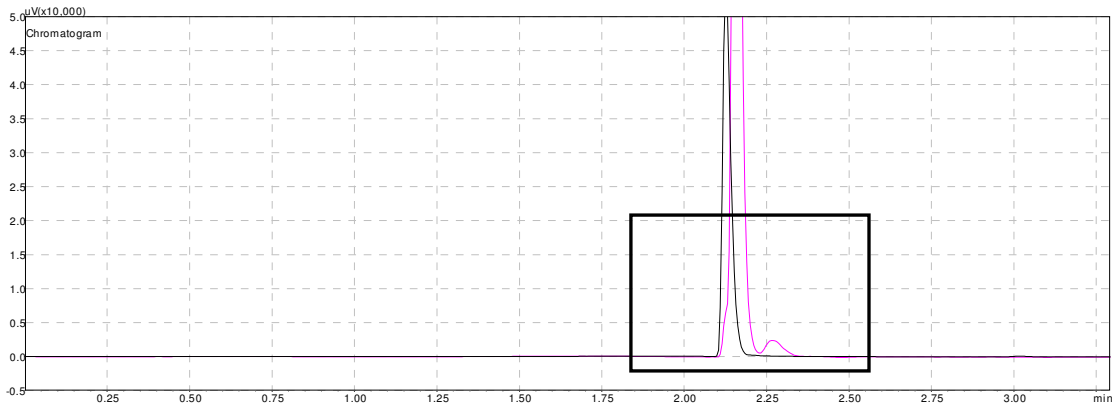


Figure B. 17: Comparison of Oxygen Peak (black line) with 10µL Pure Injection of C<sub>3</sub>F<sub>8</sub> (pink line)

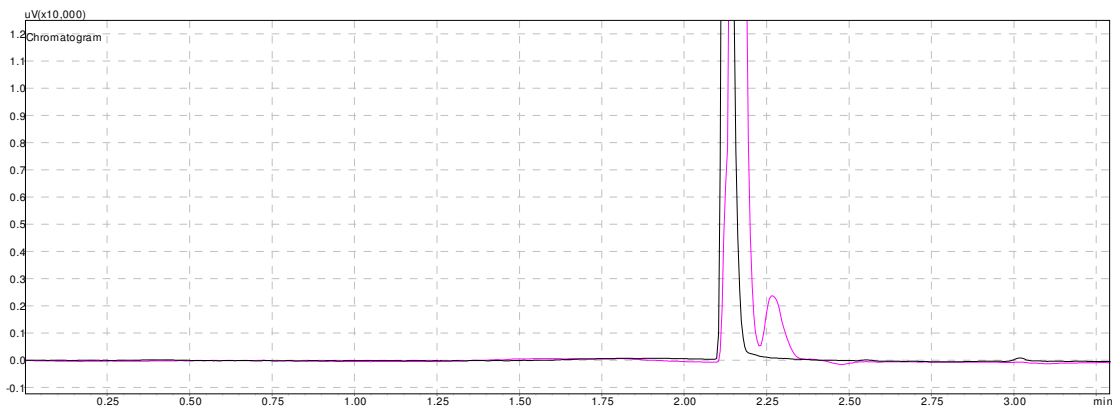
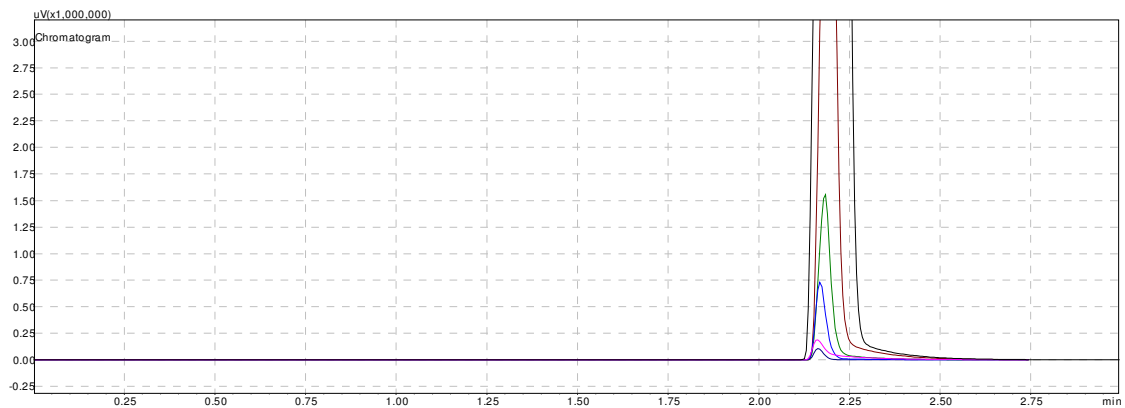
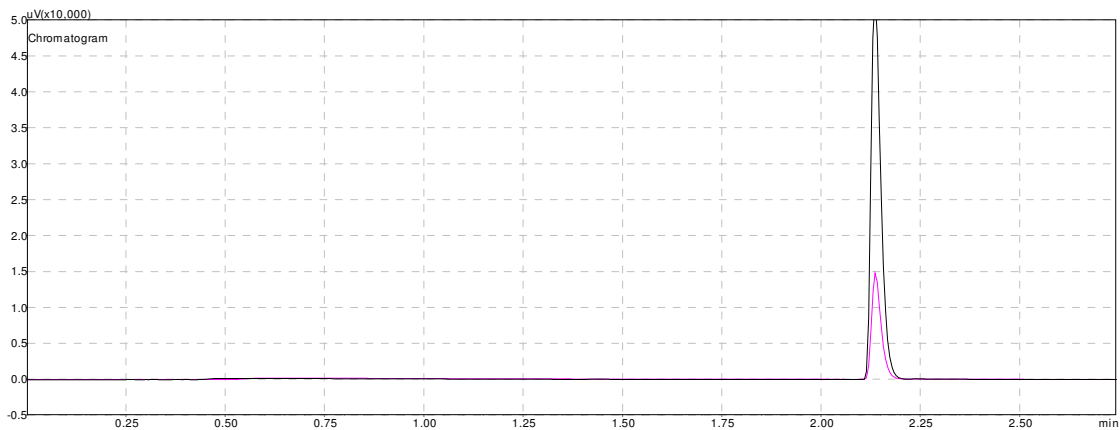


Figure B. 18: Magnified Area of Box in Figure B.17



**Figure B. 19: 1 $\mu$ L injections of pure SF<sub>6</sub>; Variance demonstrates clogging of plastic syringe needle**

Chromatograms from samples run on the ZB-624 column utilizing the cyro\_method1.gcm method with a 0°C column.



**Figure B. 20: Comparison of Oxygen Peak (black line) with 10 $\mu$ L Pure Injection of CF<sub>4</sub> (pink line)**

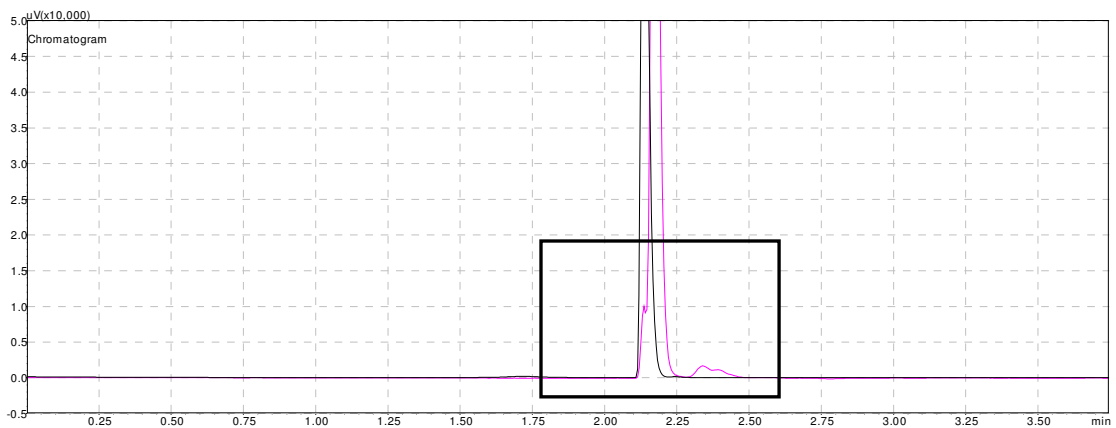


**Figure B. 21: Comparison of Oxygen Peak (black line) with 10 $\mu$ L Pure Injection of C<sub>3</sub>F<sub>8</sub> (pink line)**



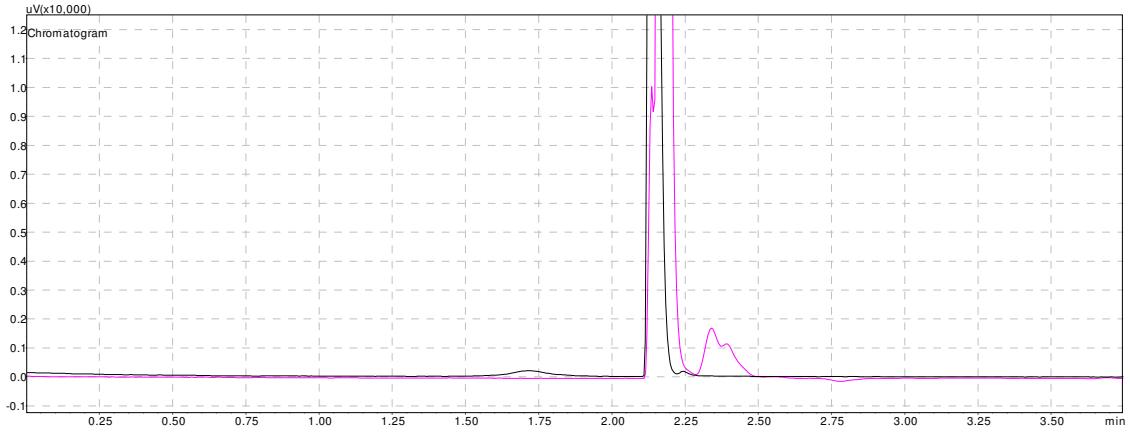


**Figure B. 22: Magnified Area of Box in Figure B.21**

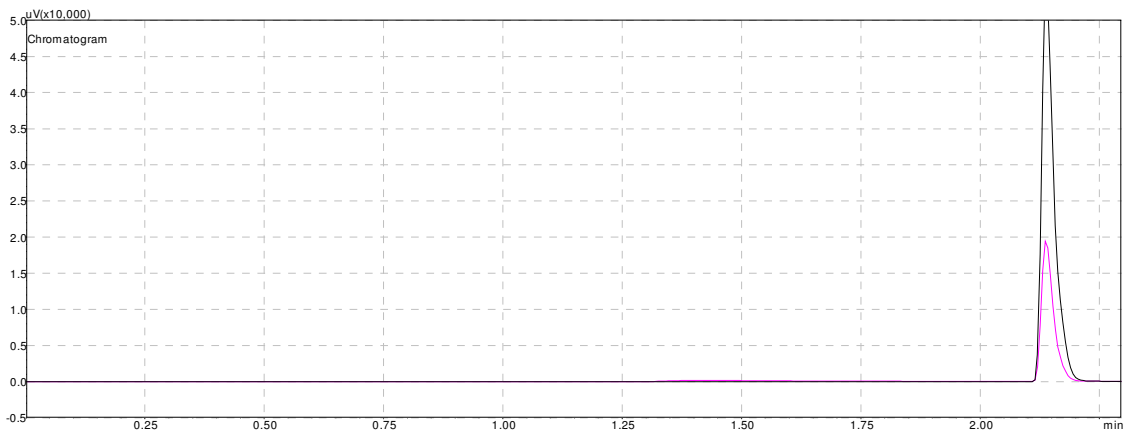


**Figure B. 23: Comparison of Oxygen Peak (black line) with 10 $\mu$ L Pure Injection of CF<sub>4</sub> (pink line)- Repeat run**

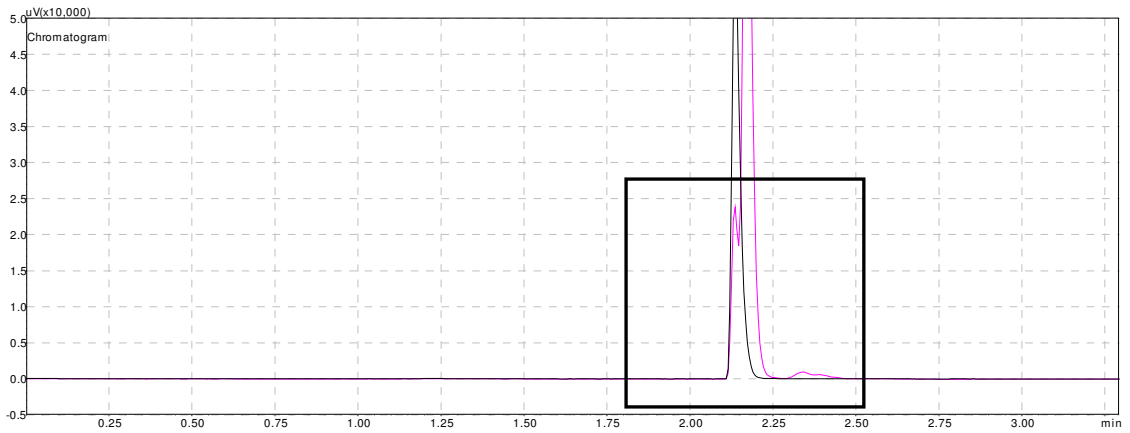


**Figure B. 24: Comparison of Oxygen Peak (black line) with 10 $\mu$ L Pure Injection of C<sub>3</sub>F<sub>8</sub> (pink line)- Repeat run**

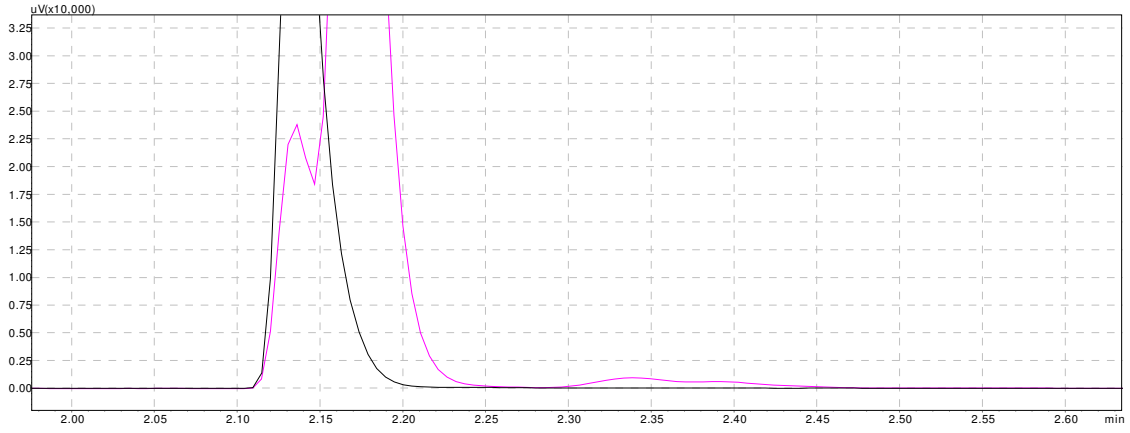


**Figure B. 25: Magnified Area of Box in Figure B.24**

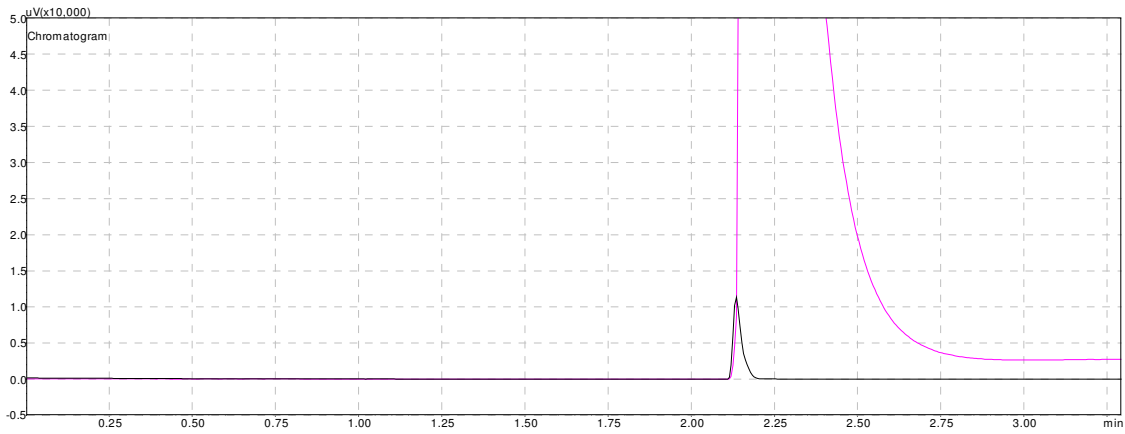


**Figure B. 26: Comparison of Oxygen Peak (black line) with 1 $\mu$ L Pure Injection of SF<sub>6</sub> (pink line)**

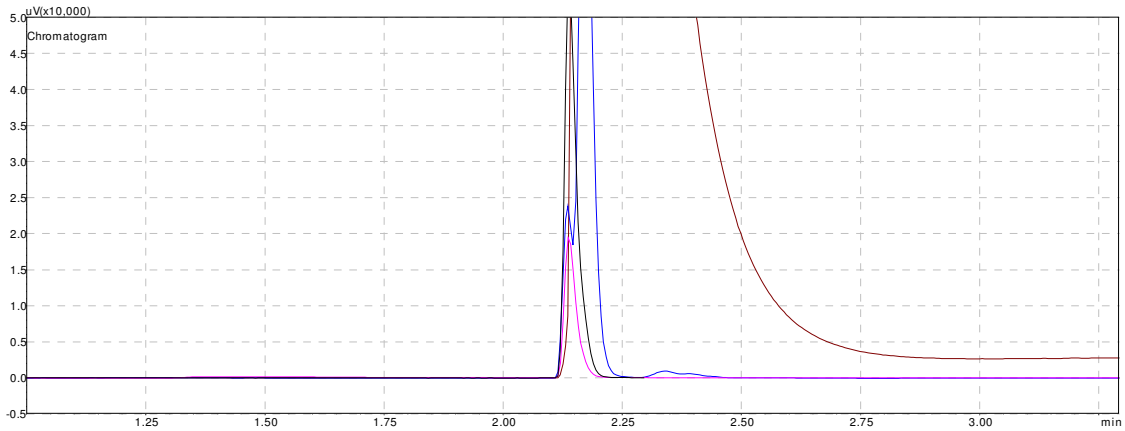


**Figure B. 27: Overlay of All Tracer Gases-Black=Syringe Blank;Pink=CF<sub>4</sub>;Blue=C<sub>3</sub>F<sub>8</sub>; Brown=SF<sub>6</sub>**

Chromatograms from samples run on the TG Bond Q+ column utilizing the gas\_sf6.gcm method with a 40°C column.

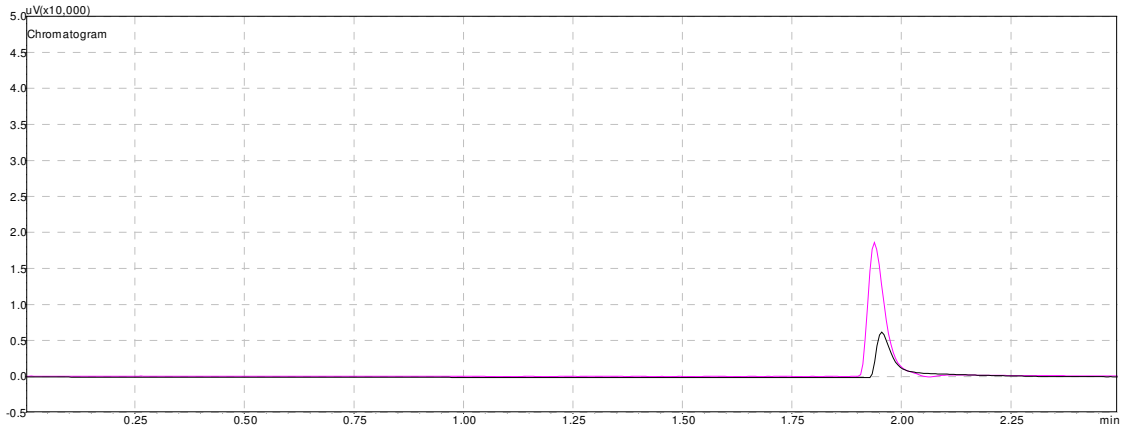


**Figure B. 28: Comparison of Oxygen Peak (black line) with 10µL Pure Injection of CF<sub>4</sub> (pink line)**

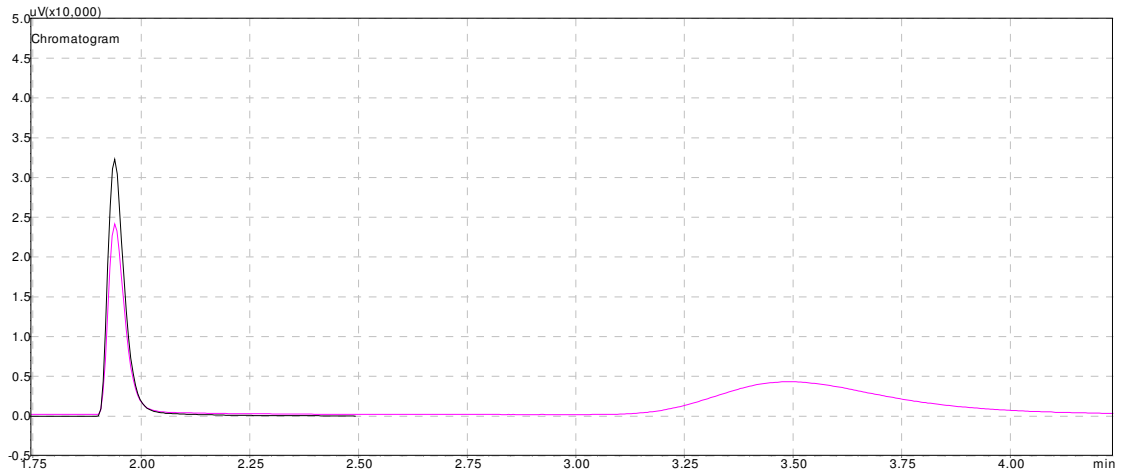


**Figure B. 29: Comparison of Oxygen Peak (black line) with 10µL Pure Injection of C<sub>3</sub>F<sub>8</sub> (pink line)**

Chromatograms from samples run on the TG Bond Q+ column utilizing the cyro\_method1.gcm method with a 20°C column.

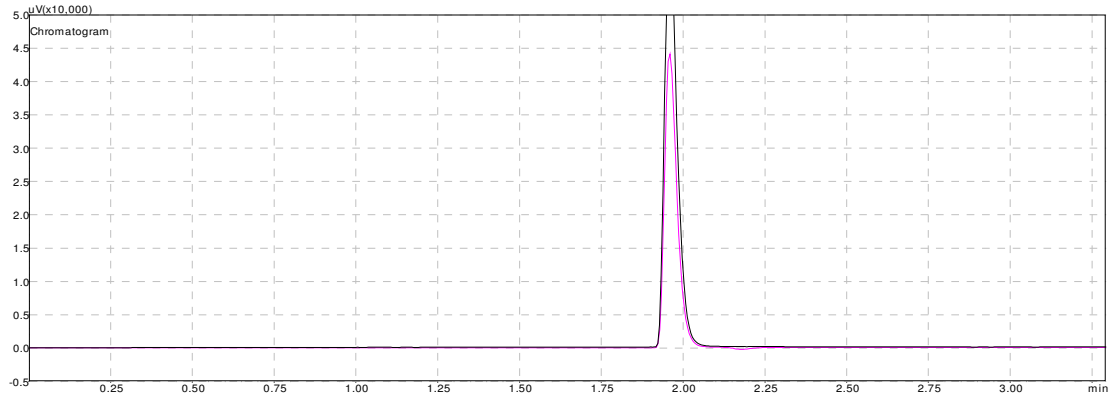


Figure B. 30: Comparison of Oxygen Peak (black line) with 10 $\mu\text{L}$  Pure Injection of  $\text{CF}_4$  (pink line)

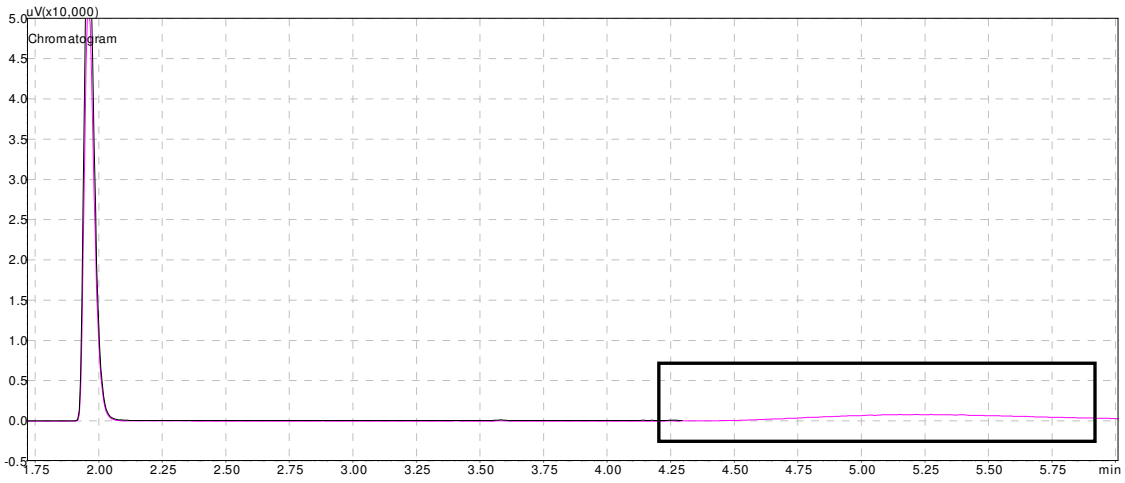


Figure B. 31: Comparison of Oxygen Peak (black line) with 10 $\mu\text{L}$  Pure Injection of  $\text{C}_3\text{F}_8$  (pink line)

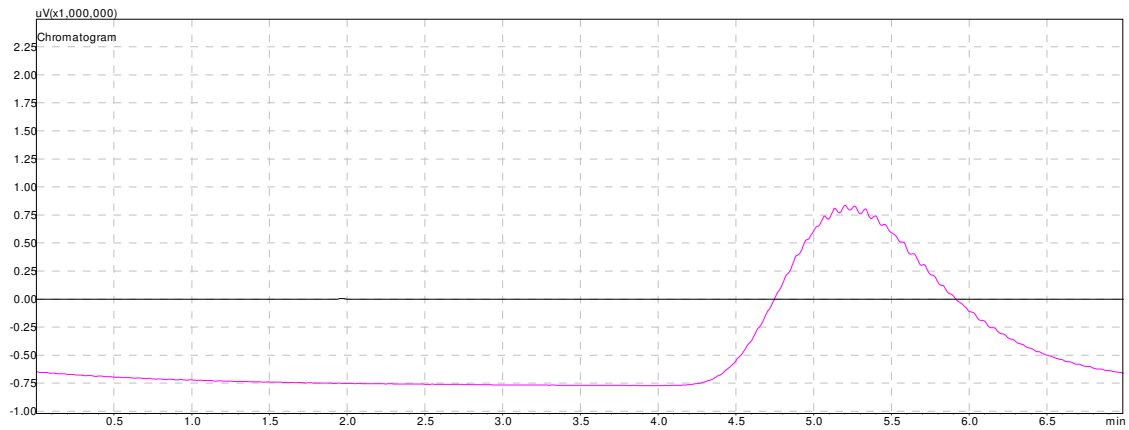
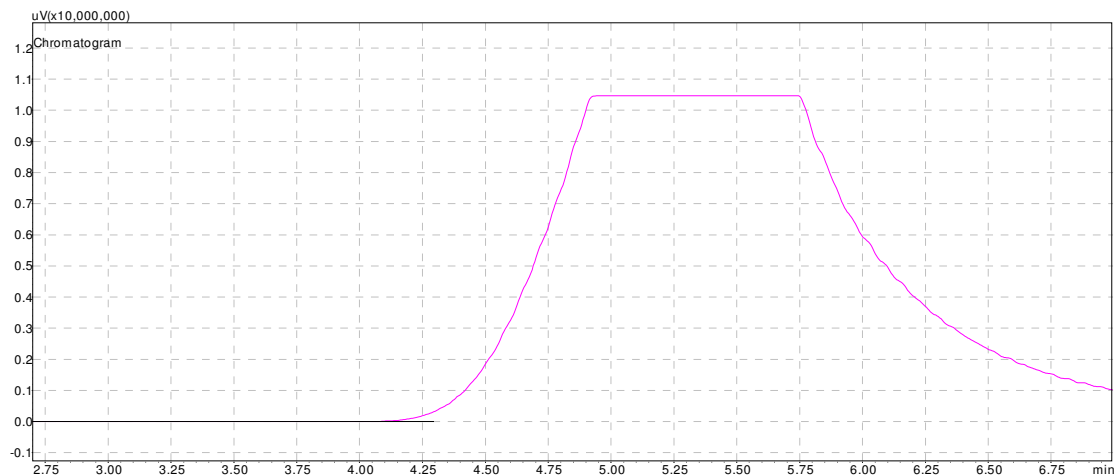
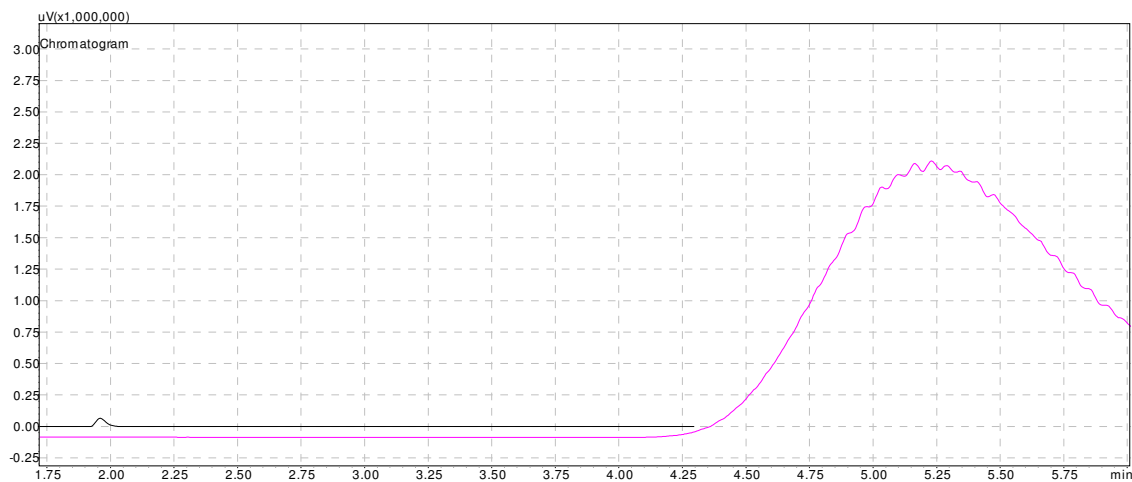


Figure B. 32: Zoomed-in version of Figure B.31 Showing Broad  $\text{C}_3\text{F}_8$  Peak Eluting Around 5.2 Minutes



**Figure B. 33: Comparison of Oxygen Peak (black line) with 1 $\mu\text{L}$  Pure Injection of SF<sub>6</sub> (pink line)-- Flat Line Due to Column & Detector Overloaded with Sample**



**Figure B. 34: Comparison of Oxygen Peak (black line) with 0.5 $\mu\text{L}$  Pure Injection of SF<sub>6</sub> (pink line)-- Very Broad Peak & Peak Tailing on Right Side until 7 Minutes**

Chromatograms from samples run on the TG Bond Q+ column utilizing the cyro\_method1.gcm method with a 0°C column.

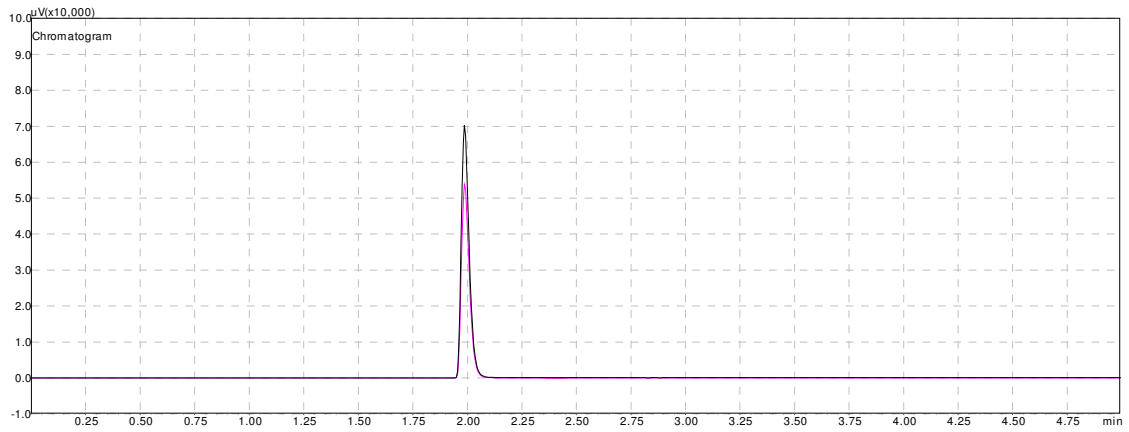


Figure B. 35: Comparison of Oxygen Peak (black line) with 10 $\mu\text{L}$  Pure Injection of  $\text{CF}_4$  (pink line)

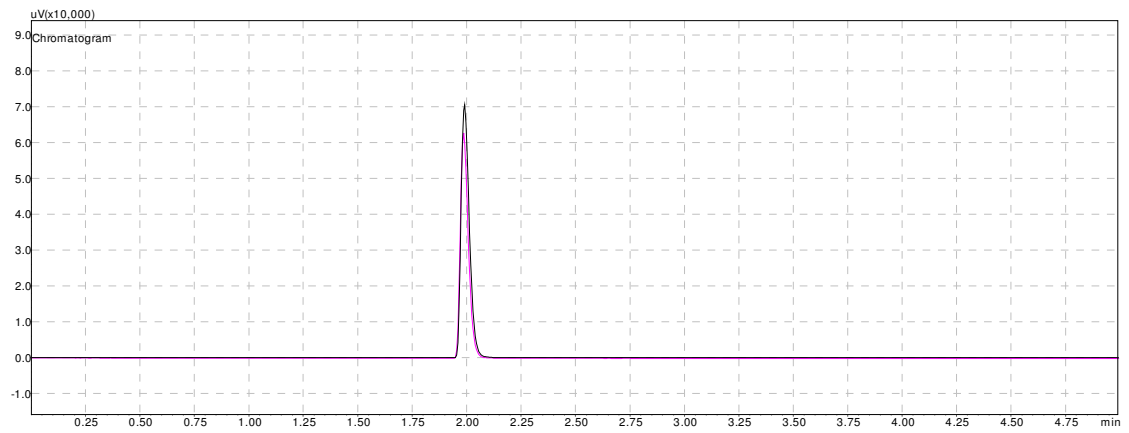


Figure B. 36: Comparison of Oxygen Peak (black line) with 10 $\mu\text{L}$  Pure Injection of  $\text{C}_3\text{F}_8$  (pink line)

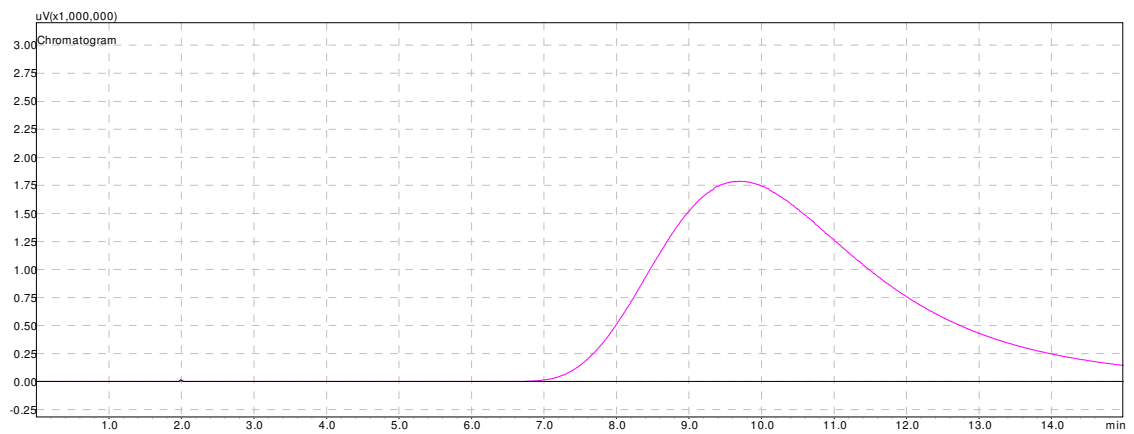
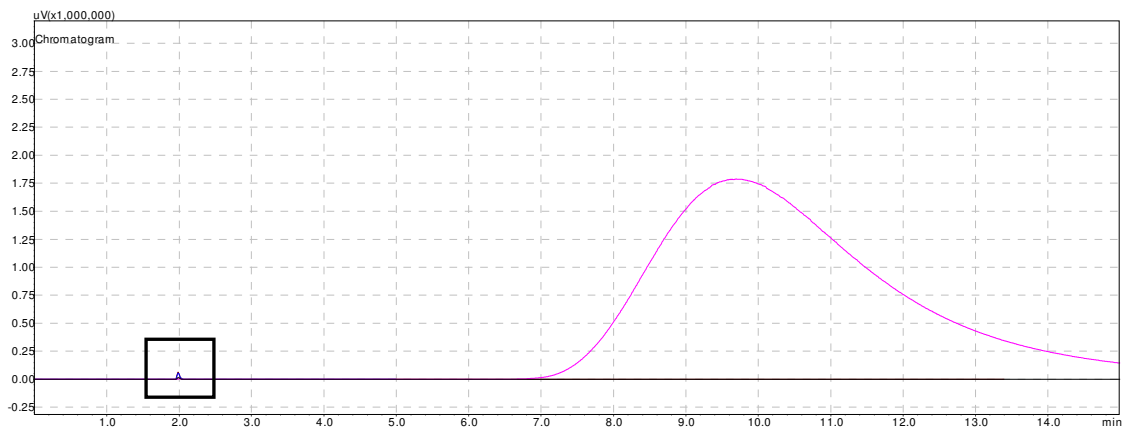
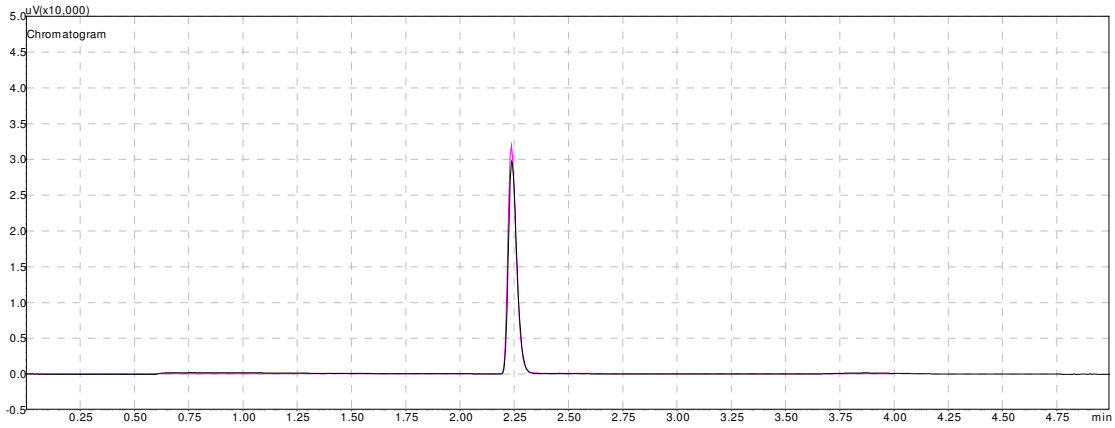


Figure B. 37: Comparison of Oxygen Peak (black line) with 0.5 $\mu\text{L}$  Pure Injection of  $\text{SF}_6$  (pink line)



**Figure B. 38: Overlay of all Gases ( $O_2$ ,  $CF_4$  in box;  $C_3F_8$  too small on scale-under pink  $SF_6$  peak), pink= $SF_6$**

Chromatograms from samples run on the TG Bond Q column utilizing the gas\_sf6.gcm method with a 40°C column.



**Figure B. 39: Comparison of Oxygen Peak (black line) with 10µL Pure Injection of CF<sub>4</sub> (pink line)**

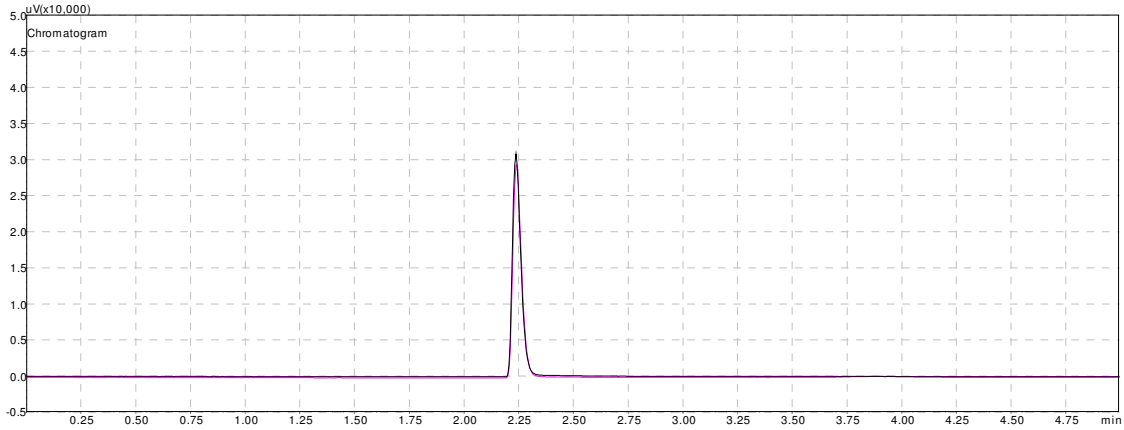


**Figure B. 40: Comparison of Oxygen Peak (black line) with 10µL Pure Injection of C<sub>3</sub>F<sub>8</sub> (pink line)**

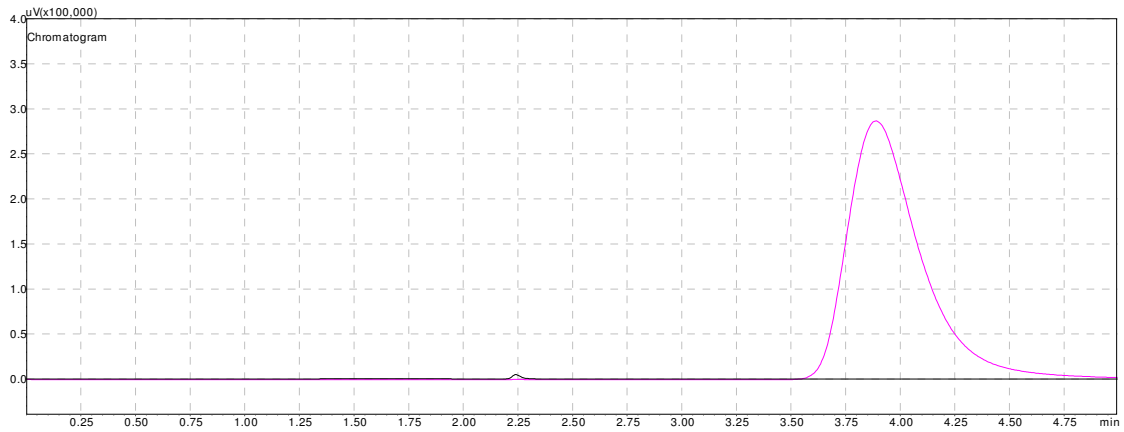


**Figure B. 41: Comparison of Oxygen Peak (black line) with 1µL Injection of 1% standard SF<sub>6</sub> & N<sub>2</sub> (pink line)**



Chromatograms from samples run on the TG Bond Q column utilizing the cyro\_method1.gcm method with a 20°C column.

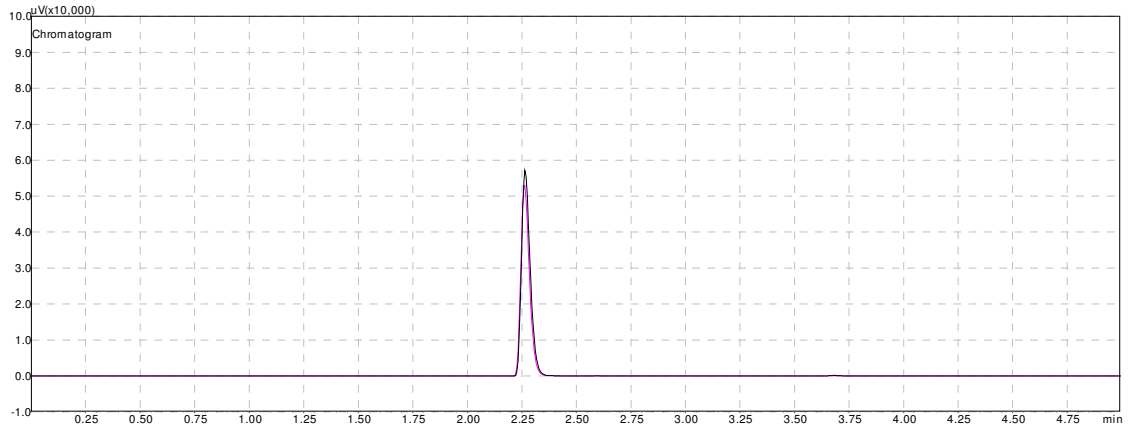


Figure B. 42: Comparison of Oxygen Peak (black line) with 10 $\mu$ L Pure Injection of CF<sub>4</sub> (pink line)

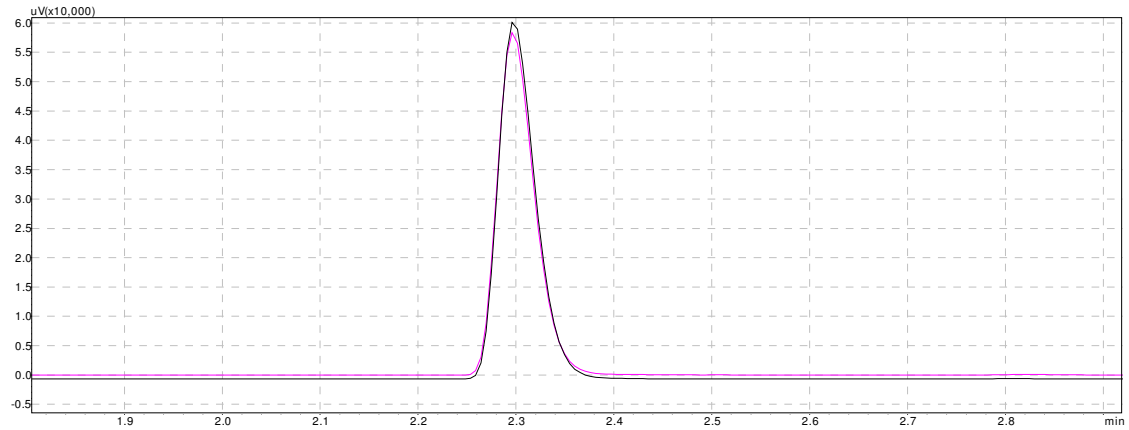


Figure B. 43: Comparison of Oxygen Peak (black line) with 10 $\mu$ L Pure Injection of C<sub>3</sub>F<sub>8</sub> (pink line)

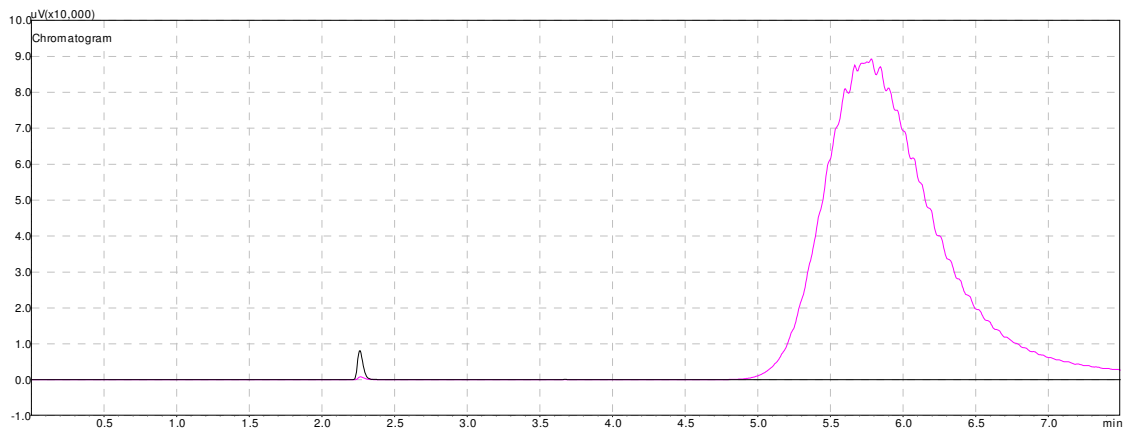
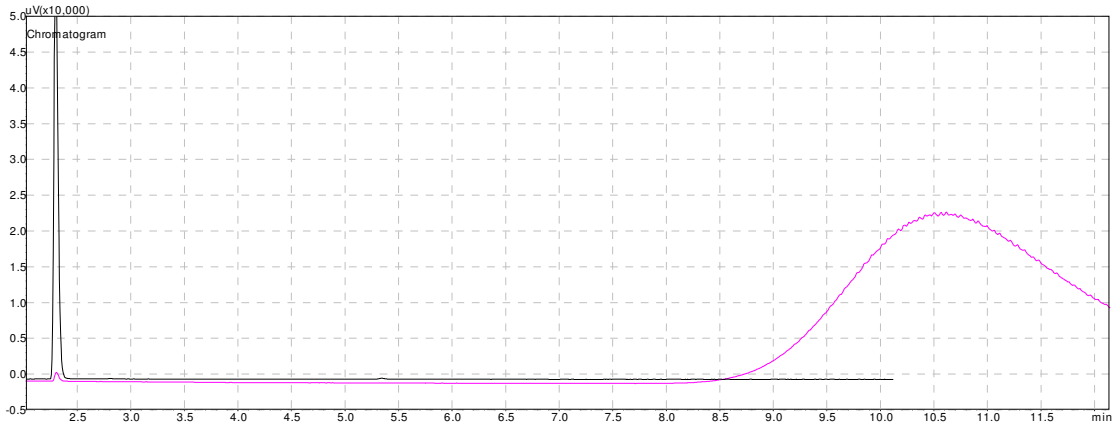
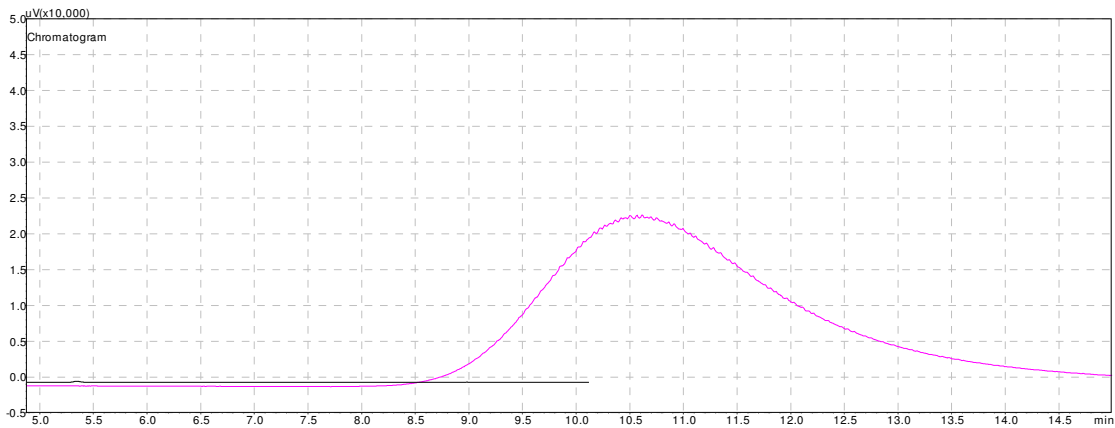


Figure B. 44: Comparison of Oxygen Peak (black line) with 1 $\mu$ L Injection of 1% standard SF<sub>6</sub> & N<sub>2</sub> (pink line)

Chromatograms from samples run on the TG Bond Q column utilizing the cyro\_method1.gcm method with a 0°C column.



**Figure B. 45: Comparison of Oxygen Peak (black line) with 1μL Injection of 1% standard SF<sub>6</sub> & N<sub>2</sub> (pink line)**



**Figure B. 46: Extended view of Figure B.43 Showing Entire SF<sub>6</sub> Peak**

Chromatograms from samples run on the TG Bond Q column utilizing the gas\_sf6.gcm method with a 60°C column.

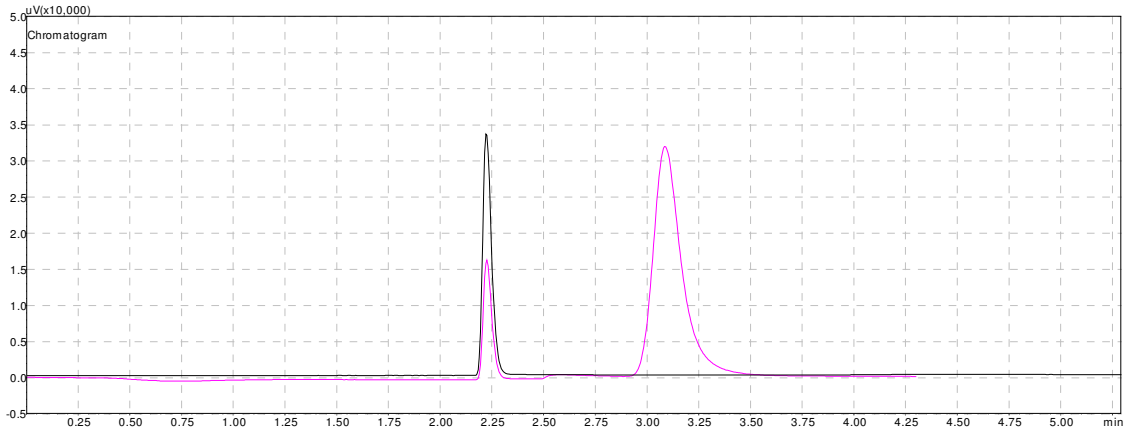


Figure B. 47: Comparison of Oxygen Peak (black line) with 10μL Pure Injection of C<sub>3</sub>F<sub>8</sub> (pink line)

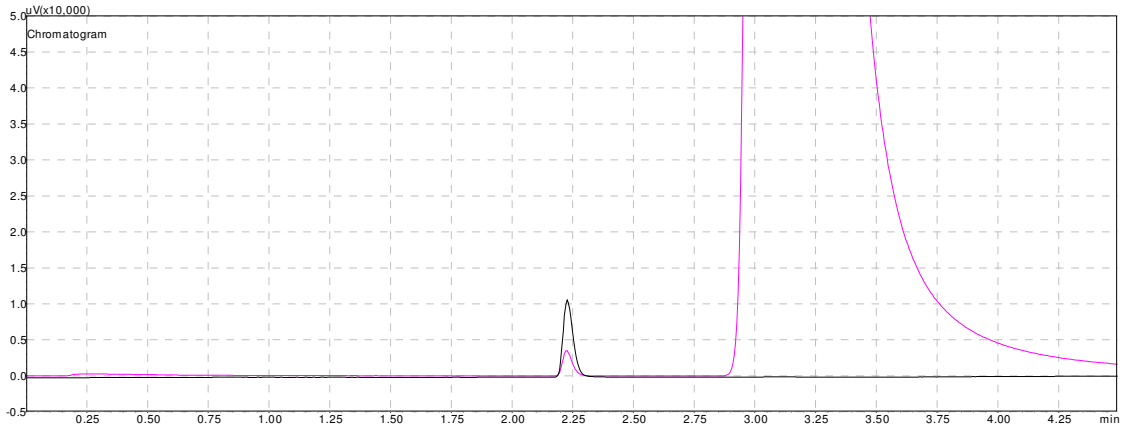


Figure B. 48: Comparison of Oxygen Peak (black line) with 1μL Injection of 1% standard SF<sub>6</sub> & N<sub>2</sub> (pink line)

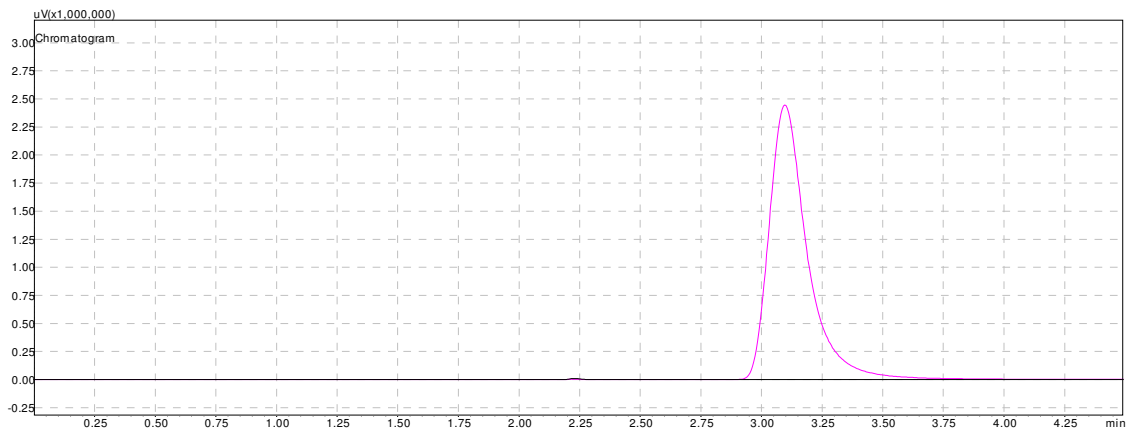
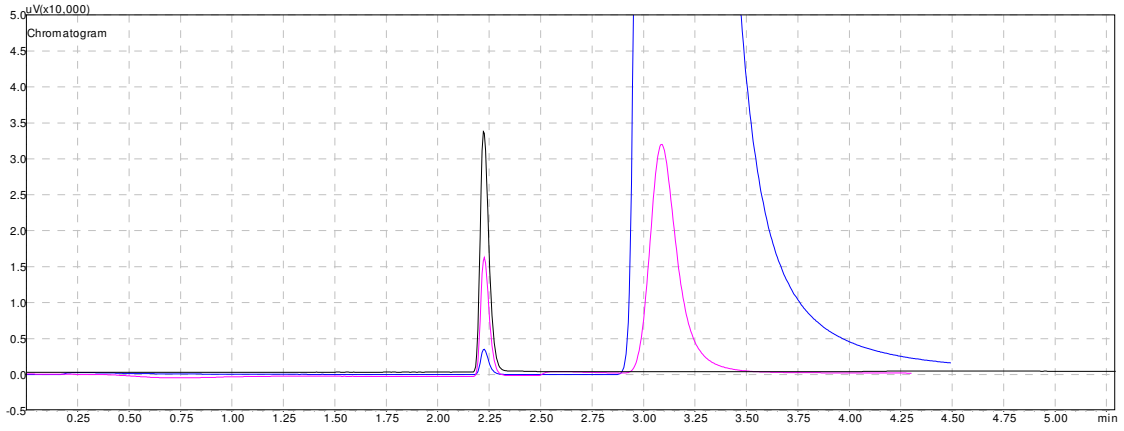
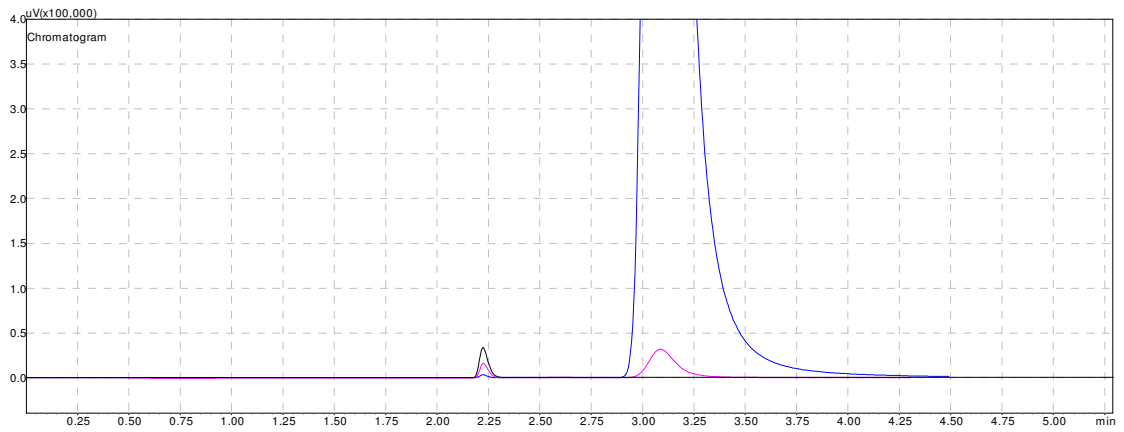


Figure B. 49: Zoomed-out View of Figure B.46 Showing Entire SF<sub>6</sub> Peak



**Figure B. 50: Overlay of All Tracer Gases-Black=Syringe Blank; Pink=C<sub>3</sub>F<sub>8</sub>; Blue=SF<sub>6</sub>**



**Figure B. 51: Zoomed-out version of Figure B.48 (uV 1,000,000)**

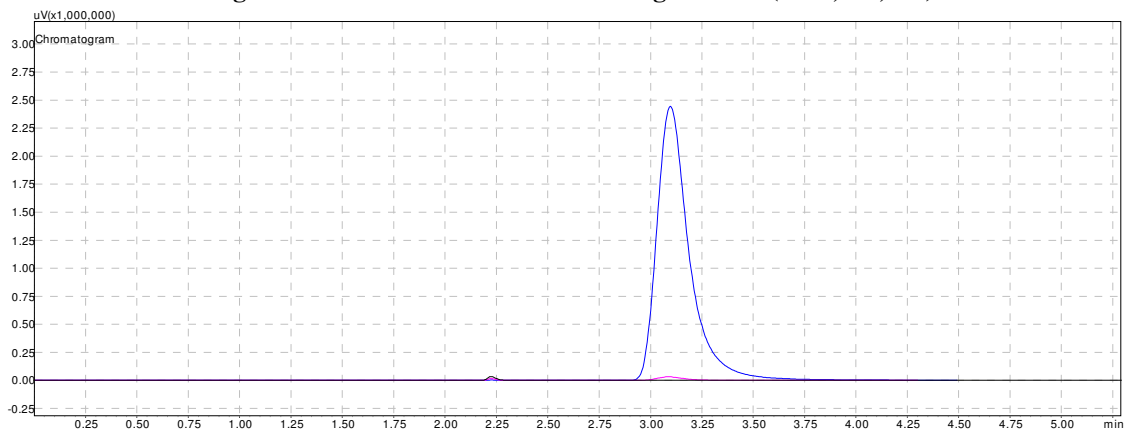


**Figure B. 52: Zoomed-out version showing entire SF<sub>6</sub> peak**

Chromatograms from samples run on the TG Bond Q column utilizing the gas\_sf6.gcm method with a 50°C column.

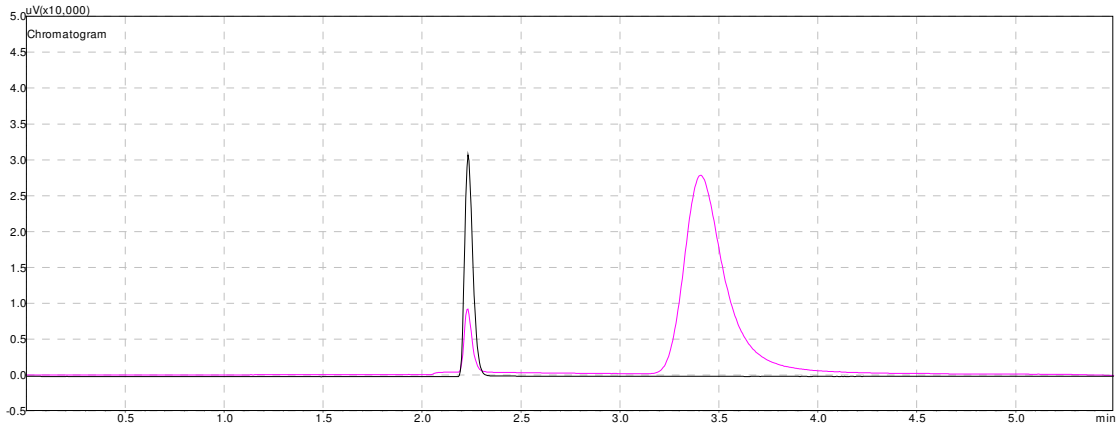


**Figure B. 53: Comparison of Oxygen Peak (black line) with 10μL Pure Injection of C<sub>3</sub>F<sub>8</sub> (pink line)**

Chromatograms from samples run on the HP-AL/S column utilizing the HP-AL/S Column method with an initial column temperature of 80°C and temperature programming at 30°C per minute to 190°C.

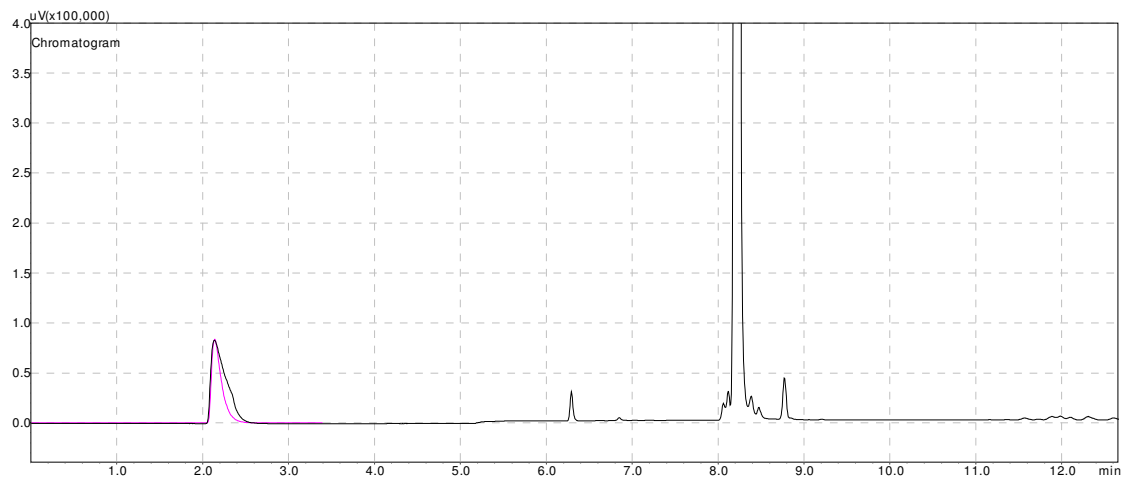


**Figure B. 54: Comparison of Syringe Blank (pink) with 1mL Injection of 100ppm PMCH in N<sub>2</sub> (black)**

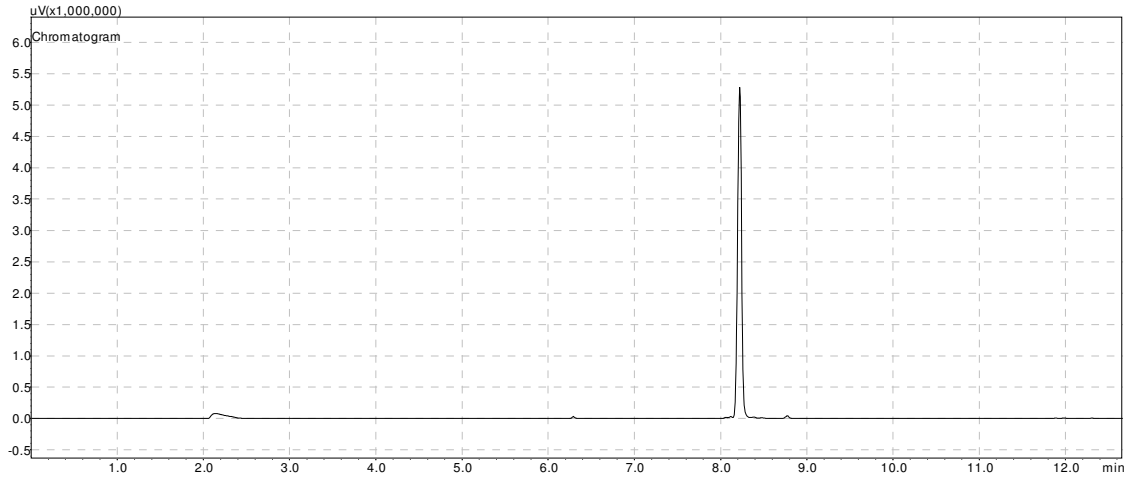


**Figure B. 55: Zoomed-out version of Figure B. 54 above**

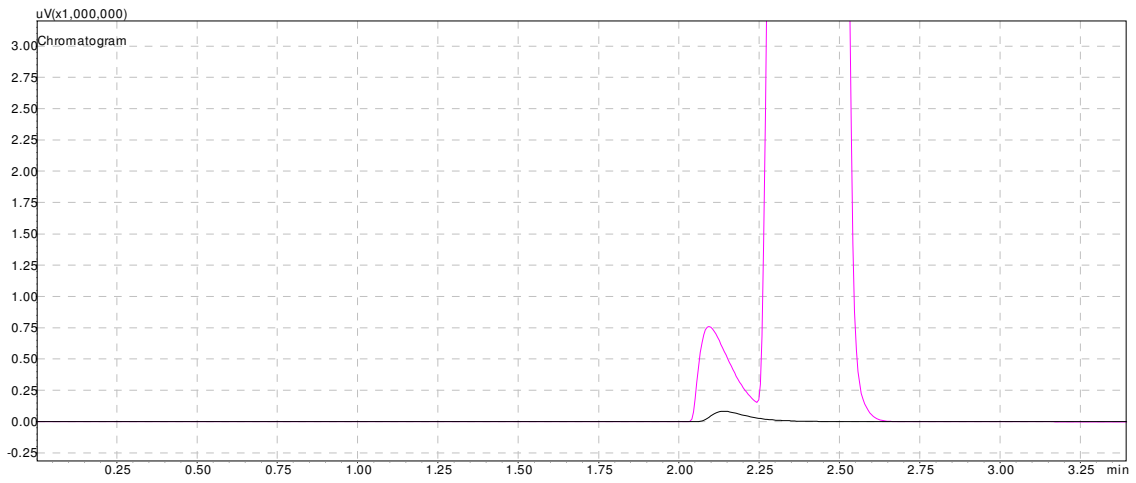


**Figure B. 56: Comparison of Syringe Blank (Black) with 1mL Injection of 100ppm SF<sub>6</sub> in N<sub>2</sub> (pink)**

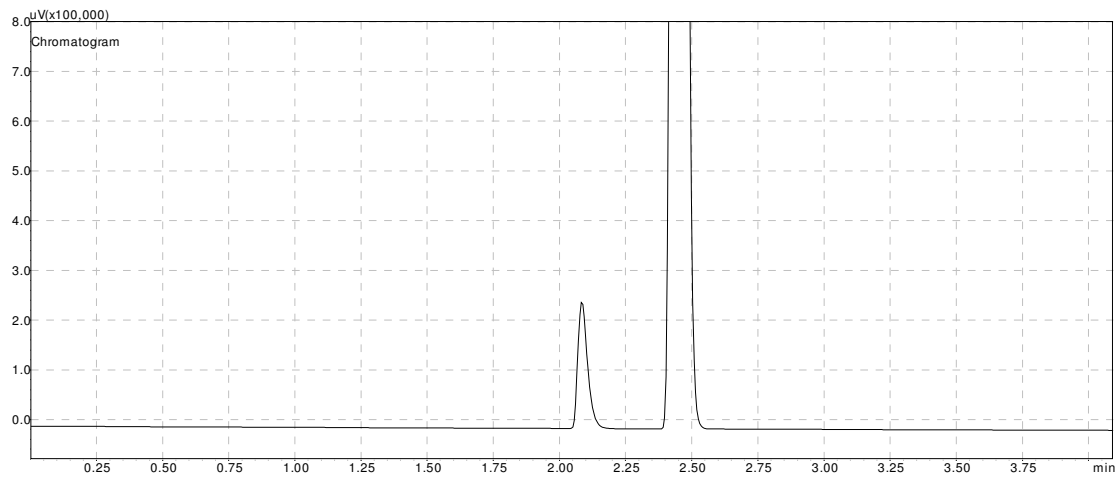


**Figure B. 57: 100ppm Sample of SF<sub>6</sub> in N<sub>2</sub> (65°C initial column temp, hold 3 minutes, ramp 100°C to 175°C)**

Chromatogram from samples run on the HP-AL/S column utilizing the SF<sub>6</sub> & PMCH Protocol method with an initial column temperature of 70°C, 2.75 minute hold time and temperature programming at 120°C per minute to 180°C and holding for 8 minutes.

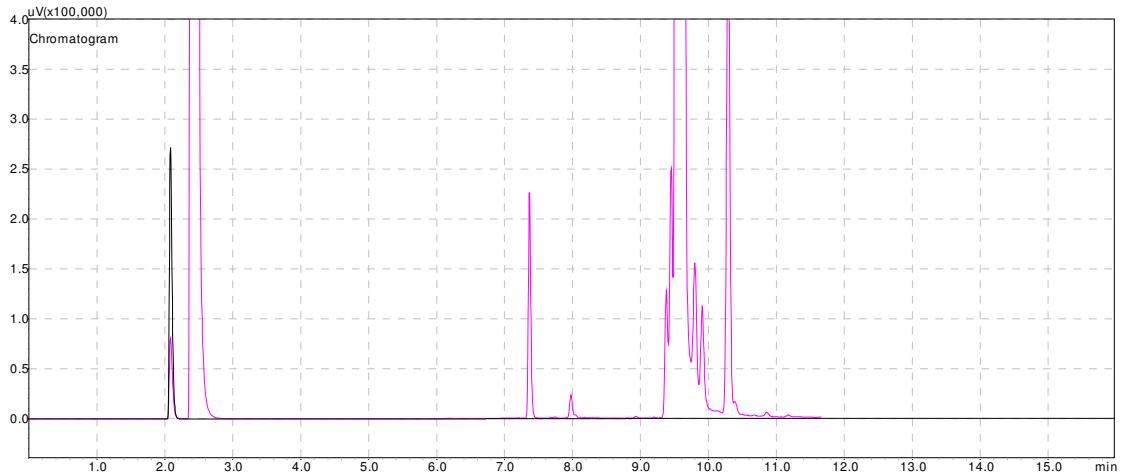


**Figure B. 58: Establishing Protocol for Separation of SF<sub>6</sub> & PMCH; Initial Column Temperature of 70°C, Hold Time 8 Minutes**

Chromatogram from samples run on the HP-AL/S column utilizing the SF<sub>6</sub> & PMCH Protocol method with an initial column temperature of 70°C, 2.75 minute hold time and temperature programming at 120°C per minute to 180°C and holding for 15 minutes.

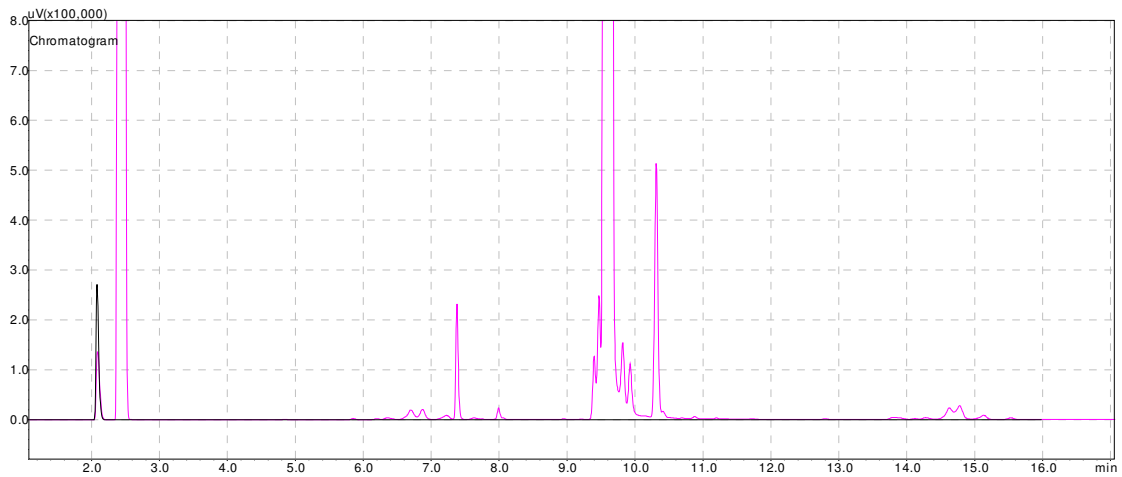


**Figure B. 59: Establishing Protocol for Separation of SF<sub>6</sub> & PMCH; Initial Column Temperature of 70°C, Hold Time 15 Minutes**

Chromatograms from samples run on the HP-AL/S column utilizing the SF<sub>6</sub> & PMCH Protocol method with an initial column temperature of 70°C, 2.75 minute hold time and temperature programming at 120°C per minute to 180°C and holding for 12 minutes, 30 seconds.

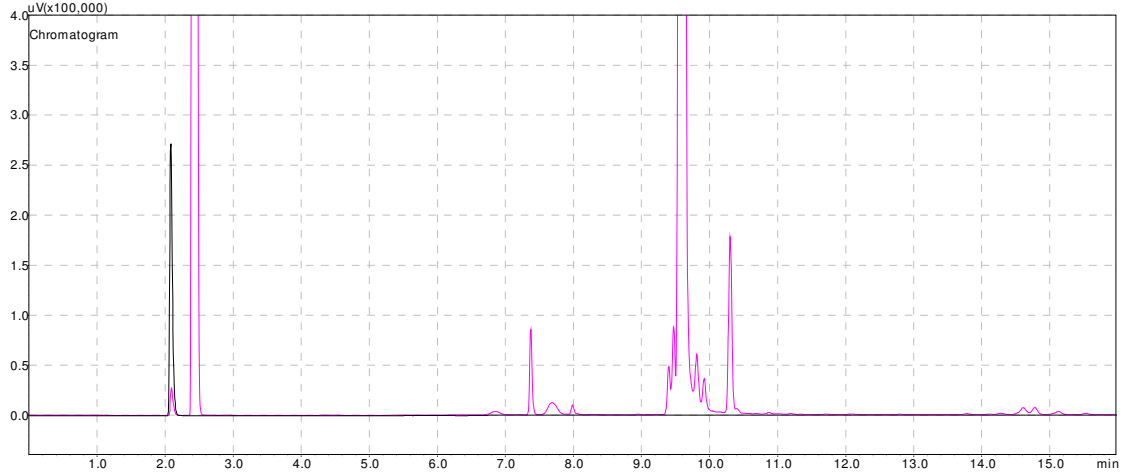


**Figure B. 60: Separation of SF<sub>6</sub> & PMCH; Initial Column Temperature of 70°C, Hold Time 12:30 Minutes (Black=Syringe Blank; Pink=100ppm mix SF<sub>6</sub> & PMCH in N<sub>2</sub>)**

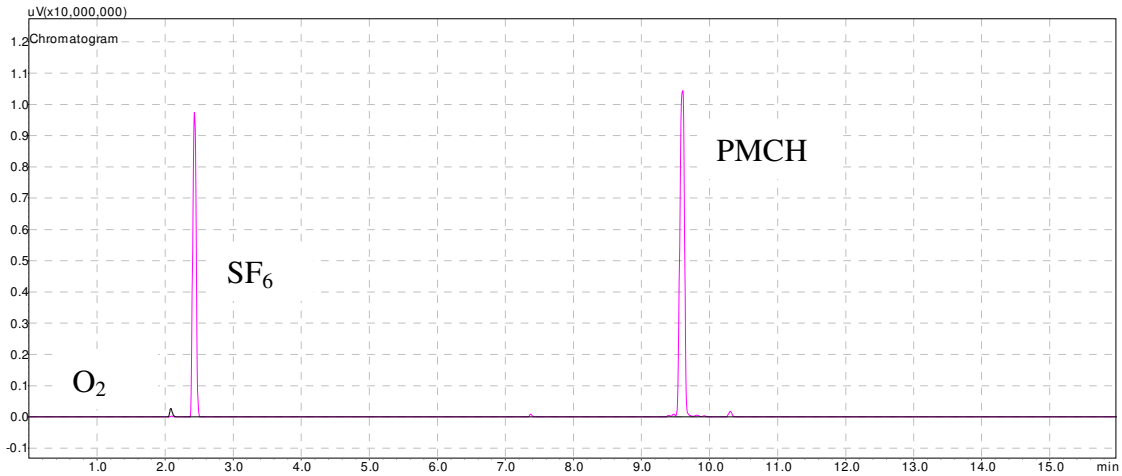


**Figure B. 61: Zoomed-out version of Figure B. 60 showing entire SF<sub>6</sub> and PMCH peak**



Chromatogram from samples run on the HP-AL/S column utilizing the SF<sub>6</sub> & PMCH Protocol method with an initial column temperature of 65°C, 2.75 minute hold time and temperature programming at 120°C per minute to 180°C and holding for 12 minutes, 30 seconds.

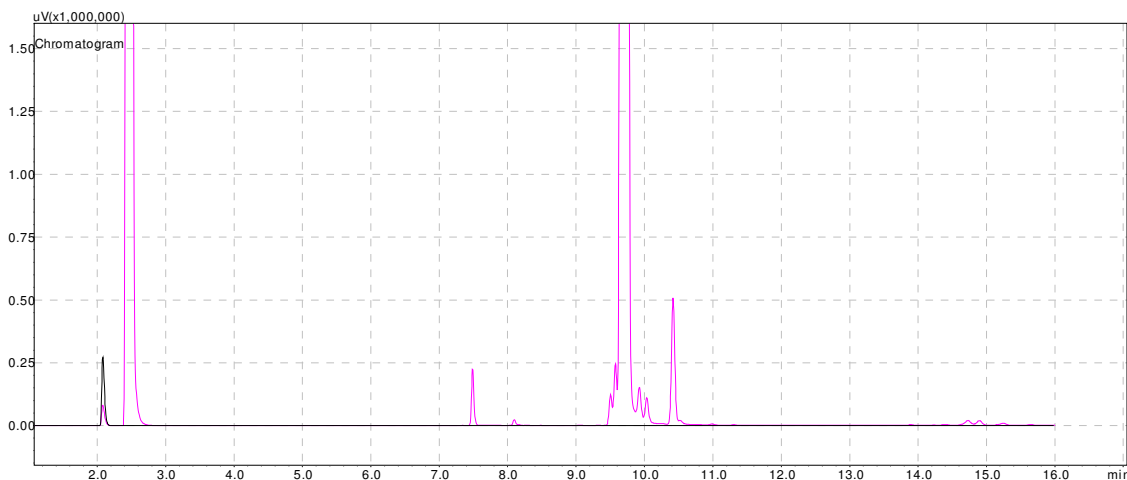


**Figure B. 62: Separation of SF<sub>6</sub> & PMCH; Initial Column Temperature of 65°C, Hold Time 12:30 Minutes (Black=Syringe Blank; Pink=100ppm mix SF<sub>6</sub> & PMCH in N<sub>2</sub>)**

Chromatograms from samples run on the HP-AL/S column utilizing the SF<sub>6</sub> & PMCH Protocol method with an initial column temperature of 67°C, 2.75 minute hold time and temperature programming at 120°C per minute to 180°C and holding for 12 minutes, 30 seconds.

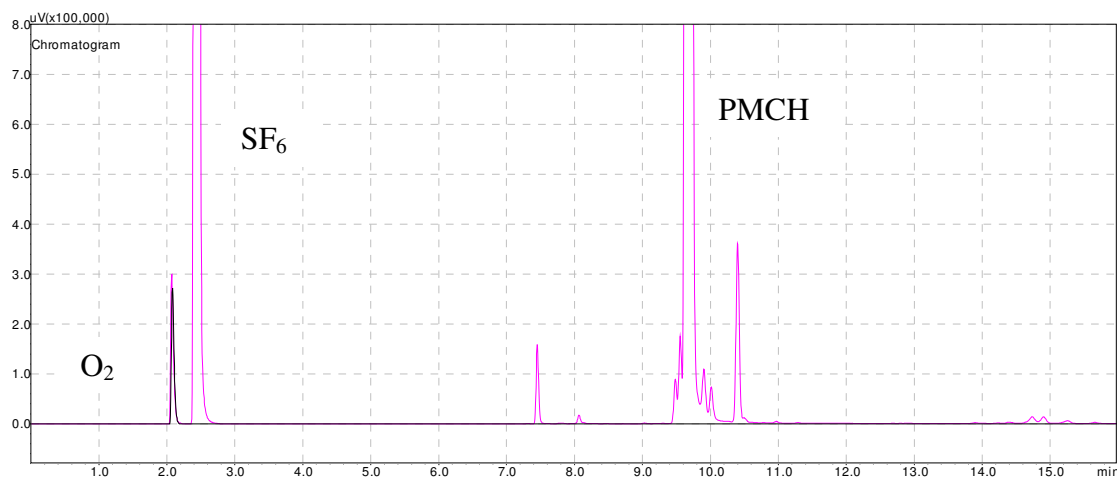


**Figure B. 63: Separation of SF<sub>6</sub> & PMCH; Initial Column Temperature of 67°C, Hold Time 12:30 Minutes (Black=Syringe Blank; Pink=100ppm mix SF<sub>6</sub> & PMCH in N<sub>2</sub>)**

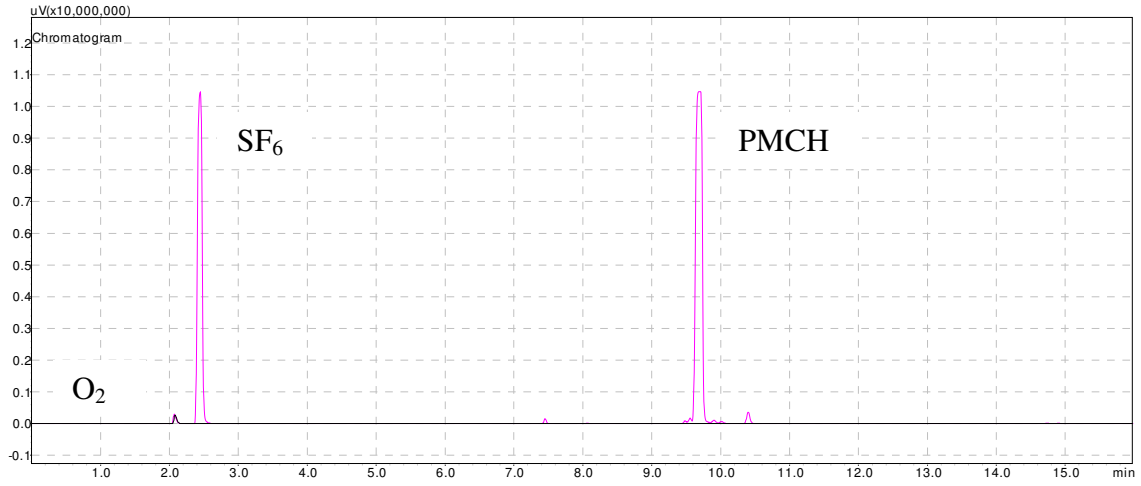


**Figure B. 64: Zoomed-out version of Figure B. 63 showing entire SF6 & PMCH peaks**